

Ecosystem Models of the Chesapeake Bay Relating Nutrient Loadings, Environmental Conditions, and Living Resources

FINAL REPORT
1 May 1998 - April 30 1999

PREPARED BY

W. Michael Kemp, Rick Bartleson and Steve Blumenshine
Horn Point Laboratory
Cambridge, MD 21613

J. D. Hagy and W. R. Boynton
Chesapeake Biological Laboratory
Solomons, MD 20688

University of Maryland
Center for Environmental Science

PREPARED FOR

Kent Mountford and Richard Batiuk
U.S. Environmental Protection Agency
Chesapeake Bay Program Liaison Office
Annapolis, MD 21403

January 2000
UMCES[HPL] Contribution # 3218

Executive Summary

During the 1998-1999 funding year, our ecosystem modeling activities have focused on several objectives which were established to identify strategies for enhancing Chesapeake Bay Program (CBP) modeling and monitoring activities. The goal of this report is to provide numerical and statistical analyses that will improve the CBP's ability to predict and assess living resource responses to nutrient loading reductions. Our results address three critical concerns of the CBP: (1) habitat and food resource issues relevant to benthic organisms; (2) factors affecting the planktonic food-webs; and (3) water quality effects on submerged aquatic vegetation (SAV). Each of the three areas of concern was addressed using both empirical analyses and numerical modeling approaches, yielding the six chapters that comprise this final report. Specifically, our activities include: 1) a modeling analysis of the relative importance of food requirements versus habitat quality (bottom oxygen) for production of benthic organisms in both deep and shallow water (Chapter I); 2) an empirical analysis of factors affecting the development of deep water hypoxia (Chapter IV); 3) a modeling analysis of the effects of nutrient enrichment and nutrient variability on the efficiency by which primary production is transferred to upper trophic levels of planktonic food-webs (Chapter II); 4) an empirical analysis of factors affecting the abundance and species composition of the mesozooplankton in relation to physical habitat and trophic relations (Chapter VI); 5) a mechanistic modeling analysis of SAV-water quality interactions (Chapter III); and 6) an empirical analysis of relationships between mid-channel water quality and SAV survival in adjacent littoral areas (Chapter IV).

Our analysis of food requirements and habitat limitations of the benthos in mesohaline regions of Chesapeake Bay revealed that even conservative estimates of the food resources available to the benthos are more than sufficient to support their nutritional needs. The benthic community was found to be limited primarily by the severity of the oxygen conditions to which it is subjected. This suggests that improvements in oxygen conditions that might be associated with reductions in nutrient loading, and associated organic matter supply, should lead to enhanced benthic production, and that the counter-effect due to food limitation will be of limited importance. By way extension, our analysis of factors affecting hypoxia concluded that while differences among tributaries in average vulnerability to hypoxia could be attributed to mean depth, significant interannual changes in the extent of hypoxia were positively correlated with total nitrogen loading. The precision of this relationship, which has been noted before, has been improved by accounting for nutrient inputs from all sources above and below the fall line, and by accounting for inter-basin differences in size and bathymetry. One caveat is that while hypoxia will decrease with reductions in TN loading within the present ecosystem regime, realistic reductions in the TN loading rates would not be expected to eliminate hypoxia, or even substantially reduce it in some estuaries (e.g. Mainstem and Potomac River). This introduces an important implication of several aspects of this report: incremental changes in nutrient loading will improve water quality conditions, but more dramatic changes could result from structural changes in the ecosystem that might occur if modest but persistent reductions in nutrient loading are achieved.

In support of this analysis, our modeling study of nutrient enrichment, habitat variability, and trophic transfer efficiency found that a dramatic decrease in trophic transfer efficiency accompanied the transition from mesotrophic to moderately eutrophic conditions. Associated with this decline in trophic efficiency, there was an increase in organic matter transfer to microbial decomposition pathways. This dramatic shift was attributable to the saturation of the ability of consumer organisms to utilize the increased primary production associated with higher nutrient inputs. This finding was supported by our empirical analysis of variations in zooplankton abundance, which were independent of changes in phytoplankton chlorophyll-a concentrations. This inability to find any correlation between phytoplankton and zooplankton abundances persists, despite our aggressive and robust statistical analyses designed to detect responses in any context, with any functional form, and with any error distribution. Instead, we concluded that the juxtaposition of salinity and temperature requirements, in combination with an effect of predator control by ctenophores under some circumstances were the best predictors of zooplankton abundances. While there is ample opportunity for additional empirical analysis of these data, we did not find evidence to support an assertion that decreases in primary production will have any adverse effect on the secondary productivity of pelagic food webs.

Our analysis of SAV interactions with water quality paints a complex picture of SAV habitat requirements, but also one that nonetheless largely supports the previously established SAV habitat requirements for water quality and light availability. An important result of the simulation modeling analysis is that the responses to nutrient concentrations are not independent of the initial SAV biomass. Specifically, where SAV is more abundant, it is better able to survive higher nutrient concentrations because SAV competes with algae and epiphytes for available nutrients. This results underscores again the point that incremental restoration efforts in the form of nutrient loading reductions may be met with structural changes in the SAV community that could elicit additional positive developments in ecosystem restoration. The results of the empirical analysis of SAV pointed to a down-bay change in the relative importance of different water quality factors for regulating SAV. In the oligohaline regions of the Bay, high nutrient and sediment concentrations in mid-channel waters were not an effective predictor of SAV absence, although extreme levels of TSS were associated with unvegetated areas. Toward the higher salinity regions of the Bay, where water is generally less turbid, there was a shift toward DIN concentration as the most important factor predicting SAV presence.

Table of Contents

Executive Summary	2
Table of Contents	4
List of Figures	7
List of Tables	11
Chapter I. Food versus habitat limitations for benthic macrofauna in mesohaline regions of Chesapeake Bay	13
Abstract	13
Introduction	13
Study Site and Data	15
Methods	15
Results and Discussion	19
References	23
Tables	26
Figures	29
Chapter II. Nutrient Enrichment, Habitat Variability and Trophic Transfer Efficiency in Food Webs of Estuarine Ecosystems	30
Abstract	30
Introduction	30
Methods	32
Results and Discussion	34
Concluding Comments	38
References	39
Tables	42
Figures	44

Chapter III. Effects of Nutrients and Other Water Quality Variables on Submerged Aquatic Vegetation in Chesapeake Bay: Ecosystem Modeling Analyses	45
Abstract	45
Introduction	46
Methods	47
Results and Discussion	50
Appendix III-A: Documentation for SAV Model	56
Appendix III-B: Theoretical Basis for SAV Nutrient Interactions in Space	63
References	65
Figures	74
Chapter IV. Tree-Structured Models of Water Quality and Submersed Aquatic Vegetation in Chesapeake Bay	
Abstract	76
Introduction	76
Methods	77
Results and Discussion	78
Appendix IV-A: Introduction to Tree Structured Data Analysis	83
References	86
Tables	87
Figures	90
Chapter V. Controls on Hypoxia in Chesapeake Bay and its Major Tributaries	91
Abstract	91
Introduction	91
Methods	92
Results and Discussion	95
References	99
Tables	100
Figures	101

Chapter VI. Empirical Analysis of Mesozooplankton and Gelatinous Zooplankton Abundance in Maryland Chesapeake Bay and Patuxent River	102
Abstract	102
Introduction	102
Methods	103
Results and Discussion	104
References	112
Tables	113
Figures	114

List of Figures

Chapter I.

- Fig. I-1. Map of Chesapeake Bay mesohaline macrobenthos monitoring stations used in this study.
- Fig. I-2. Water column data from selected mesohaline macrobenthos sampling sites illustrated in Fig. I-1.
- Fig. I-3. Variability of macrofaunal biomass within years for selected spatially-adjacent pairs of stations (identified in Fig. I-1) within the mesohaline region of Chesapeake Bay.
- Fig. I-4. Mean annual summer biomass at deep stations (n=5) from 1985-1988 versus hypoxia index.
- Fig I-5. Seasonal patterns in taxonomic composition of total macrobenthos biomass. Smoothed data among 1985-1989.
- Fig I-6. Seasonal variation in C demand (ration) by macrobenthos in shallow and deep communities in mesohaline mainstem stations.
- Fig. I-7. Composite data of NEM, POC deposition, and macrobenthic food ration for Chesapeake Bay mainstem.

Chapter II.

- Fig. II-1. Schematic sketches for five versions pelagic ecosystem model, with state variables indicated with boxes and trophic pathways and nutrient fluxes and indicated with arrows. State variables defined as: P = phytoplankton (L indicates large cells and S indicates small cells); Z = herbivorous zooplankton; N = dissolved inorganic nitrogen; D = detrital organic nitrogen (dissolved and particulate); F = zooplanktivorous fish. Arrows with double lines under them indicate respiration and imply N recycling.
- Fig. II-2. Time-course simulation of five-compartment pelagic ecosystem model (Fig. 1d) under conditions of: a) high; b) intermediate; c) low nutrient inputs.
- Fig. II-3. Variations in phytoplankton, zooplankton and detritus biomass (a) and production (b) with changes in nutrient loading to five-compartment pelagic ecosystem model (Fig. 1d). Note the phase shift at $N \approx 7 \mu\text{M}$.
- Fig. II-4. Variations in the biomass ratios of zooplankton/phytoplankton and zooplankton/detritus (a) and phytoplankton/detritus biomass and production (b) with changes in nutrient loading to five-compartment pelagic ecosystem model (Fig. 1d). Note the phase shift at $N \approx 7 \mu\text{M}$.
- Fig. II-5. Variations in the ratio of external N-input to total flux of nitrogen input (external input + recycling) to N state variable with changes in nutrient loading

from external sources to five-compartment pelagic ecosystem model (Fig. 1d). Note the phase shift at $N \approx 7 \mu\text{M}$.

Fig. II-6. Variations in trophic transfer efficiency TTE with changes in nutrient loading to five-compartment pelagic ecosystem model (Fig. 1d). Note the phase shift at $N \approx 7 \mu\text{M}$.

Fig. II-7. Effects of model complexity (Fig. 1 a-d) on the relationship between trophic transfer efficiency (TTE) and nitrogen loading. Relationships are scaled to respective maximum TTE in each case for comparison; note that the phase shift point changes with model complexity.

Fig. II-8. Effects of alternative zooplankton grazing equations (a) and alternative zooplankton mortality functions (b) on the relationship between trophic transfer efficiency (TTE) and nitrogen loading to two-compartment pelagic ecosystem model (Fig. 1a). Note that the phase-shift disappears with linear grazing and hyperbolic mortality.

Fig. II-9. Effects of changing half-saturation coefficients for phytoplankton uptake of N (a) and zooplankton grazing on phytoplankton (b) for two-compartment pelagic ecosystem model (Fig. 1a). Note that the phase-shift point changes with variations in half-saturation coefficients.

Fig. II-10. Time-course simulation of five-compartment pelagic ecosystem model (Fig. 1d) under variable input conditions at: a) high; b) intermediate; c) low nutrient loading rates.

Fig. II-11. Variations in trophic transfer efficiency TTE with changes in nutrient loading to five-compartment pelagic ecosystem model (Fig. 1d) for conditions of no variance in N and low and high variance.

Fig. II-12. Effects of changes in frequency distributions of phytoplankton (normal distributions with different mean and variances) on zooplankton growth using a Hollings Type III feeding function.

Fig. II-13. Summary of effects of variance in frequency distribution of phytoplankton food on trophic efficiency at which zooplankton grow on phytoplankton, considering interacting changes in mean and standard deviation of phytoplankton distributions.

Chapter III.

- Fig. III-1 General structure of SAV model is shown. Some material flows are left out for simplicity. N is modeled in stoichiometry with C except in SAV where structural and nonstructural N and C are modeled separately.
- Fig. III-2. Model results are shown with data from the 1995 mesocosm experiment. The system behavior is in the right range, but the biomasses aren't exactly what the model predicts.
- Fig. III-3 Sensitivity analysis showing percent change in SAV leaf biomass after 23 weeks for a 50% increase in the variable.
- Fig. III-4 Effect of interaction of exchange rate, nutrients and grazers on SAV biomass.
- Fig. III-5. Effects of initial conditions on model state variables over the course of an experiment.
- Fig. III-6. Model runs showing the results of mesocosm nutrient addition to SAV mesocosms containing no grazers (first column), grazers (second column), and grazers with fish (third column).
- Fig. III-7. Effect of treatment on SAV growth in mesocosm experiments and in simulations.
- Fig. III-8. Upper Panel--Simulated seasonal cycle of mean SAV biomass and nutrient (dissolved inorganic nitrogen, DIN) concentrations outside and within (mid-day and late-night) the plant bed. Lower Panel--Relationship between difference in DIN inside to outside SAV bed (delta DIN) in daytime and night time versus plant leaf biomass in a model of a mesocosm.
- Fig. III-9. Results of spreadsheet calculation showing nutrient concentrations over space as a result of uptake in patchy and continuous SAV.
- Fig. III-10. Effect of TSS and DIN on SAV and epiphyte biomass over the course of a season in a simulation model run.
- Fig. III-11. Seasonal run showing modeled SAV biomass using data from two York River sites: Guinea Marsh (GM) and Clay Banks (CBanks).

Chapter IV

- Fig. IV-1. CART Classification tree for Chesapeake Bay and Tributaries.
- Fig. IV-2. For areas with salinity < 5, equivalent classification (upper) and regression (lower) tree models relating median water quality at nearby Chesapeake Bay Monitoring Program stations to the presence and persistence of SAV in nearby shallow water areas.
- Fig. IV-3. For sites with salinity < 5, a logistic regression relating the percentage of years between 1986 and 1997 in which SAV was present in a quad to the median growing season TSS concentration in a mid-channel water quality monitoring station nearest to the quad
- Fig. IV-4. For areas with salinity 5-12 ppt, classification tree models relating median water quality at nearby Chesapeake Bay Monitoring Program stations to the presence and persistence of SAV in nearby shallow water areas.

Fig. IV-5. CART Classification tree for high salinity (>12 ppt).

Fig. IV-6. The percentage of years from 1986-1996 in which SAV was present in quads with salinity > 12 ppt related to dissolved inorganic nitrogen concentration by a CART model

Chapter V

Fig. V-1. Long-term mean hypoxia in Chesapeake Bay and selected tributaries as a function of the mean depth of the estuary.

Fig. V-2. Observed and predicted hypoxia in Chesapeake Bay and each of 5 tributaries between 1986 and 1996.

Fig. V-3. The predicted effect of total nitrogen loading rates in estuaries of varying depths according to a bi-variate sigmoidal model.

Chapter VI

Fig. VI-1. Major trophic relationships relevant to mesozooplankton illustrating, for mesozooplankton, the potential for resource limitation, predatory control, and release from predation due to trophic cascade effects.

Fig. VI-2. Annual mean Susquehanna River discharge at Conowingo, MD from 1984-1997 with the 1984-1997 mean and standard deviation as reference lines.

Fig. VI-3. Monthly means and standard errors for abundances of *Acartia* spp. and *Eurytemora affinis* adults and copepodites and total zooplankton abundance at 4 stations in the Maryland Chesapeake Bay and 3 stations in Patuxent River.

Fig. VI-4. Annual mean abundances of *Acartia* spp. and *Eurytemora affinis* adults and copepodites, *Bosmina* spp. and total mesozooplankton at 4 stations in the Maryland Chesapeake Bay and 3 stations in Patuxent River from 1984-1998.

Fig. VI-5. Contour plots showing the distribution of *Acartia* spp., *Eurytemora affinis*, and *Bosmina* spp. abundance over a range of water temperature and salinity in Maryland Chesapeake Bay and Patuxent River.

Fig. VI-6. Tree-structured regression models predicting median abundances of *Acartia* spp. and *Eurytemora affinis* adults and copepodites in Maryland Chesapeake Bay and Patuxent River.

Fig. VI-7. Contour plots showing the proportion of the total mesozooplankton abundance contributed by *Acartia* spp., *Eurytemora affinis*, or *Bosmina* spp. predicted as a function of water temperature and salinity by a bi-variate logistic regression model.

Fig. VI-8. Contour plots showing the biovolume of ctenophores (*Mnemiopsis leidyii* and *Beroe ovata*) and Scyphomedusae (*Chrysaora quinquecirrha* and *Cyanea capillata*) as a function of average salinity and water temperature.

Fig. VI-9. Annual mean gelatinous zooplankton biovolume at four stations in Chesapeake Bay (CB2.2, CB3.3C, CB4.3C, CB5.2) and two stations in Patuxent River (TF1.7, LE1.1). Annual mean gelatinous zooplankton abundances at TF1.5 were all zero.

List of Tables

Chapter I.

Table I-1. Correlations of surface chlorophyll biomass and macrobenthos biomass at shallow and deep stations.

Table I-2. Correlation parameters of biomass vs. hypoxic index for taxonomic groups of macrobenthos from samples defined in Fig. I-4.

Table I-3. Comparison of estimates of total macrobenthic production ($\text{g}\cdot\text{m}^{-2}\cdot\text{yr}^{-1}$) by station for 1985-1986.

Chapter II

Table II-1. Finite difference equations for five-compartment model of plankton trophic dynamics

Table II-2: Definition of coefficients and values used in base run for five-compartment plankton model.

Chapter III

No Tables.

Chapter IV

Table IV-1. Averages of growing season median water quality in each of the terminal nodes established in the CART model in Figure IV-1.

Table IV-2. Averages of growing season median water quality in each of the terminal nodes established in the CART models in Figure IV-2.

Table IV-3. Averages of growing season median water quality in each of the terminal nodes established in the CART classification model for the mesohaline (salinity 5-12 ppt) region.

Table IV-4. Locations of quads with $\text{DIN} \leq 0.11 \text{ mg l}^{-1}$ but with no SAV in some or all years and hypotheses suggesting an alternative explanation or hypothesis to a water quality based classification.

Table IV-5. CART model performance data (confusion matrices) for the composite model (top group) and for each of the salinity-zone specific models.

Chapter V

Table V-1. Mean depth, freshwater residence time, TN loading rates, TP loading rates, and average hypoxia for 6 sub-estuaries of Chesapeake Bay and for the mainstem of Chesapeake Bay. All averages are for the water year which begins in October.

Chapter VI

Table VI-3. ANCOVA model equations for each station where salinity > 10 ppt expressing the decline in *Acartia* spp. abundance with increasing ctenophore biovolume.

Table VI-2. Terminal Nodes of a CART regression model relating June-August *Acartia* spp. abundances to ctenophore biovolumes in waters of salinity > 10 ppt.

Table VI-1. Mean salinity and water temperature over the entire water column, averaged by month for 1984-1996 (Chesapeake Bay stations) and 1986-1997 (Patuxent River station).

Chapter 1

Food versus habitat limitations for benthic macrofauna in mesohaline regions of Chesapeake Bay

S.C. Blumenshine and W.M. Kemp

Abstract

This study examines the relative importance of food versus hypoxia and other factors as limitations on biomass and production of benthic macrofaunal communities in shallow (2 m) and deep (>12 m) stations of the mesohaline regions of Chesapeake Bay. Significant negative correlations were observed between benthic biomass and an index of bottom water hypoxia over four years (1986-1989) for five deep stations in the mainstem Bay, and the Patuxent and Potomac River estuaries. Crustaceans and mollusk species appeared to be more sensitive to low oxygen stress than did annelid worms. Benthic communities at shallow stations adjacent to these deep sites did not experience extended hypoxic conditions, and consequently, their variations in animal abundance were unrelated to hypoxia. We investigated the potential for food limitation in the benthic communities by calculating the rates of food delivery (as organic carbon) to the sediments and comparing this to the estimated food ration (as C) needed to support existing benthic biomass. Composite annual cycles of rates were computed from multiple years and stations. Even using highly conservative estimates, we found that for shallow stations food available exceeded benthic demand by a factor of 2-10. In fact, the net production of food in shallow regions greatly exceeds consumption by the integrated communities (macrofauna plus microbes), strongly suggesting a net lateral transport from shallow to deep regions of the Bay. Over the annual cycle, food available for benthic macrofauna at deep sites also greatly exceeded demands for all months but June. However, taking into account organic carbon potentially transported from adjacent shallows, suggests that there would be more than enough food to support benthic macrofaunal requirements for all months in both deep and shallow areas of the Bay's mesohaline regions. These results indicate that improvements in summertime bottom water oxygen conditions associated with reductions in nutrient loading should result in increased production of benthic macrofaunal assemblages in the mid-salinity regions of the Bay.

Introduction

In relatively shallow coastal systems such as Chesapeake Bay, benthic macrofauna represent potentially important energetic conduits between water column primary production and fisheries yields (Möller et al. 1985, Baird and Ulanowicz 1989). Macrobenthic production, however, can be limited on regional or estuary-wide scales by many factors, including food availability, predation pressure and habitat condition. At least two of these factors, food and habitat, are related to levels of nutrient loading and

phytoplankton production in many estuarine environments. Whereas ample food may be available to benthic macrofauna under nutrient-rich high productivity conditions, associated depletion of oxygen from bottom waters tends to limit the size and quality of macrobenthic habitat. Evidence suggests that in eutrophic coastal systems, high rates of primary production and bottom water consumption of dissolved oxygen (DO) can cause trophic shifts from pathways involving many large metazoans to those dominated by microbes (Diaz and Rosenberg 1995).

Nutrient loading in conjunction with naturally occurring water column stratification in the mesohaline regions of Chesapeake Bay affects the vertical distributions and concentration of DO and phytoplankton. Annual areal nitrogen loading rates are positively related to the extent and duration of hypoxia within and among Chesapeake Bay and its tributaries (Hagy and Boynton, this report). Establishment of water column stratification in summer retards exchange of oxygen-rich surface waters with below-pycnocline habitats, and sinking particulate organic matter fuels DO consumption in bottom layers of the water column.

The availability of DO and food resources are, thus, two proximal mechanisms linking nutrient loading with benthic macrofaunal community structure, biomass, and production. One complex question is, however, what is the nature of linkages among nutrient loading, primary, phytoplankton production, bottom-water DO depletion, and benthic macrofaunal abundance. For example, to what extent is benthic macrofaunal production limited by low DO concentration or by food supply, and how will it respond to reductions in nutrient loading?

A primary objective of this chapter is to explore the potential for limitation of benthic macrofaunal biomass and production by food or hypoxia in shallow and deep habitats in the mesohaline region of Chesapeake Bay. Our focus is on the mid-salinity regions, and we do not suggest extrapolation to other areas of the Bay, due differences in physical, chemical, and biological conditions among different salinity regions of estuary. The approaches used in this study include pattern analysis through correlation of variables, contrasts between macrobenthic community and environmental variables in shallow (above pycnocline) and deep (below pycnocline) habitats, and comparisons of the rates of particulate organic carbon (POC) deposition to benthic habitats versus carbon demand by macrobenthos and other aerobic heterotrophs.

Because water column processes tend to substantially alter the state of sinking particulate matter, zooplankton growth is often regarded as being limited by food quantity, whereas benthic production is more likely limited by food quality (Ahlgren et al. 1997). In the present paper, we assess food availability in a quantitative sense only, using budgets of organic carbon supply. In many cases, bulk measures of organic carbon are inadequate to characterize the utility of particulate organic material to support production by benthos or other consumer organisms (e.g., Marsh and Tenore 1990). Even simple measures of food quality such as carbon:nitrogen are highly variable in estuarine water columns (e.g., Malone et al. 1986). For this analysis, we take the view that, whereas food quality is of interest where supply and demand are nearly in balance, it is a

second-order concern when the two are far from balance (e.g., differing by a factor of 5 or more)..

The structure of our analyses and expectations were driven by seasonal water column stratification in the mesohaline region and its influence on the distribution of food and DO within and among years. Throughout the water column, spring phytoplankton blooms in conjunction with increasing water temperatures fuel pre-summer metabolic rates and thus the momentum for biomass production into summer. However, we expected summer hypoxia to suppress the biomass and food demand of macrobenthos in sub-pycnocline habitats, in contrast to expected homogeneous seasonal patterns in well-oxygenated shallow habitats above the pycnocline.

Study Area and Data

We examined macrobenthic community parameters from the Maryland portion of the Chesapeake Bay Program Benthic and Water Quality Monitoring databases. Specific methods for benthic sampling and data generation are described in Holland et al. (1988). Analyses of macrobenthic deposit feeder communities and habitat variables in this study focus on the period of regular sampling of 70 fixed sampling stations during July 1984-June 1990. Contemporaneous measurements of water temperature and dissolved oxygen concentrations ([DO]) were taken with a Hydrolab Surveyor II approximately 0.5m above the sediment surface during macrofaunal sampling events.

Eleven fixed stations within the mesohaline region of Chesapeake Bay were selected to examine spatial and inter-annual relationships of macrobenthic biomass, community structure, and food demand with environmental parameters. Of the 70 fixed stations regularly sampled, only these eleven included a continuous record of macrobenthos biomass data over the six year period. Macrobenthos and environmental parameters were measured 8-10 times per year, with a larger proportion of these sampling events occurring mid-year. We examine data from the eleven fixed stations (which were oriented in spatially adjacent clusters) and contrast them as shallow (<3m) and deep (>10m) habitats (Fig. I-1).

Methods

Benthos: sampling, enumeration, and biomass

The relevant variables produced from the benthic monitoring program for this exercise included species-specific biomass and mean individual size. Methods for sample collection and analysis are summarized here. Samples of benthic macrofauna in shallow stations (<3m) were obtained with a hand-operated box corer, samples from deep stations (>9m) were obtained with a WildCo box corer. Three replicate samples for macrobenthos were taken during each sampling event at each station. Sample replicates with a sediment penetration depth <0.2m were rejected and retaken.

Individual samples were sieved through 0.5 mm screens and preserved on board for later identification, enumeration, and measurement. The biomass of individual taxa in each sample was estimated through pre-determined length-weight relationships. Although biomass was estimated for individuals in samples, the database used in this analysis reported only species and sample-specific summed biomass of individuals. These biomass values were divided by densities to determine species-specific individual mean size in each replicate sample. From 1985-1989 density and biomass information was consistently available for 16 core species (Table I-1) which typically comprised at least 85% of total macrofaunal abundance.

Relationships of macrobenthos and water column parameters:

Hypoxia

We sought to capture annual duration and intensity of hypoxia for each station through a single integrative parameter. Thus, a simple index was devised to characterize variation in hypoxic conditions (<2.0 mg DO l^{-1}) among station-year combinations. An additional objective in calculating an index of hypoxia is to capture the spatial and interannual variation in a parameter that although fluctuates on diel cycles (D'Avanzo and Kremer 1994, Diaz et al. 1992, Breitburg 1990), may have chronic effects on benthic macrofauna which may not be predicted from laboratory tolerance trials.

We devised a hypoxic index value for each station-year combination through two steps. First, the number of days of hypoxia was defined as the interval between the first and last observations of hypoxic bottom water as estimated through linear interpolation between consecutive sampling events of normoxic and hypoxic bottom for each station and year. Second, the number of days of hypoxia was multiplied by the negative square of the mean dissolved oxygen concentration $[DO]^{-2}$ (mg l^{-1}) from measurements (n) during the hypoxic period, where n ranged from 0-4.

We used a correlative approach to assess the potential for the integrative measure of hypoxic duration and intensity (described above) to limit macrobenthos biomass among years and below-pycnocline stations. A wholesale shift in the benthic monitoring regime from fixed stations to a more spatially-intensive strategy in July 1989 precluded calculation of the hypoxic index for this year due to a reduced frequency of fixed station sampling visits after this date. Thus, this analysis included data from five stations and four years. Because the effects of hypoxia may include both long and short-term (<1 day) influences on macrobenthos on different levels of organization, the temporal variability of hypoxia and its effects on macrobenthos biomass and production is difficult to accurately discern with monitoring programs spanning broad spatial and temporal scales. Therefore, we focused on variation in 'summer' macrobenthos biomass against the index of hypoxia. Mean biomass for each station-year during average onset (late May) and waning of hypoxia (early-mid September) were calculated and correlated against the annual index of hypoxia for below-pycnocline stations. This temporal correspondence does not assume that effects of hypoxia are immediately detectable

through whole-community measures, but allows for that possibility of detecting differential susceptibilities to hypoxic conditions among taxa. For example, the utility of a flexible approach to considering responses of macrobenthos to hypoxia at different levels of organization would allow us to detect whether changes in community structure accompanied or were independent of changes in biomass.

If changes in macrobenthos biomass were independent of changes in community taxonomic structure, one possibility is that the biomass of specific taxonomic groups to vary with hypoxia in similar ways. The lack of uniform statistical significance in biomass-hypoxia correlations among taxa may reveal general clues as to hypoxia as a source of mortality, but the slopes of these relationships are more useful because they incorporate information about variation over parameter gradients.

Phytoplankton chlorophyll concentration

Relationships among macrobenthos and food supply from the water column were evaluated in two ways. First, the average biomass (mg l^{-1}) of phytoplankton chlorophyll *a* from near-surface (0.5m depth) samples was compared to time-lagged measures of macrobenthic biomass throughout years. Near-surface chlorophyll *a* biomass was determined via fluorometry from Chesapeake Bay Program Water Quality Monitoring sites, and compared with macrobenthos biomass at the nearest fixed benthic monitoring station (typically within 10 km). Both macrobenthos and chlorophyll *a* biomass were \log_{10} -transformed prior to correlations to reduce heteroscedacity. Data of both chlorophyll *a* and macrobenthos biomass were binned in 2 wk intervals to achieve temporal congruence. Data from binned time intervals of macrobenthos biomass were lagged by two 2 wk intervals relative to chlorophyll *a* data ensuring that measurements of resource biomass preceded those of consumer biomass. Further, this lag accounts for short-term delays of macrobenthic responses to availability of surface chlorophyll *a* through circulation or sedimentation, and for changes in food resources to be manifested as measurable changes in biomass through growth of individuals (Lehtonen and Andersin 1998).

POC deposition and benthic carbon demand

A comparison of POC deposition through the water column versus macrobenthos C demand was also used to address whether food or hypoxia was a factor limiting the biomass and production of macrobenthos in the study area. Monthly means of POC deposition in the mid-bay mainstem was calculated as areal gross primary production less areal planktonic respiration (Kemp et al. 1997, Smith and Kemp 1995). Volumetric respiration terms were multiplied by the depths of specific water column layers with respect to common depths of the above or below-pycnocline macrobenthic sampling stations. These calculations effectively vary respiration rates and thus POC deposition with depth. This accounting of POC includes fates such zooplankton grazing. Net ecosystem metabolism (NEM; see Kemp et al. 1997) corresponding with depths of shallow and deep macrobenthos sampling stations was estimated as POC deposition less benthic respiration. Benthic respiration measurements were taken using benthic

respiration chambers as described in Kemp and Boynton (1981). The macrobenthos fraction of total benthic respiration was estimated independently, yet linked to the production calculation described below. We applied a production to respiration (P:R) ratio of 0.436 for all suspension and deposit feeders (Bayne and Newall (1983). This ratio is similar to the P:R for aquatic detritivores (0.439)(Banse and Mosher 1980), and the P:R for *Macoma* spp. (0.409)(Hummel 1985).

Estimates of macrobenthos production (with estimation of food ration as an end goal) were generated from an equation based on a meta-analysis of annual secondary production of coastal benthic communities (Tumbiolo and Downing 1994). On the basis of per unit biomass, the equation coefficients emphasize allometric and environmental influence on production:

$$\log(\text{Production}) = 0.18 + 0.97 \log B - 0.22 \log W_m + 0.04 T_b - 0.014 T_b \log(Z+1)$$

Equation parameters are based on annual averages, where B = biomass (g AFDW m^{-2}), W_m = maximum individual body mass (mg dry mass), T_b = mean bottom water temperature ($^{\circ}C$), and Z = depth (m). The negative coefficient of the body mass term (W_m) allows for higher turnover rates in communities dominated by small organisms assuming other parameters held constant. Discrete production estimates were generated for each species ($n=16$) for which biomass was consistently determined in the CBP monitoring databases and summed as total macrobenthic production or across taxonomic groups as required for subsequent analyses. Resulting estimates of macrobenthic production for specific sampling events were converted to daily rates ($g\ m^{-2}\ d^{-1}$) by dividing output from the production equation by 365 after converting to base 10 units. Production was converted to carbon (C) units using the conversion $0.45\ g\ C = 1\ g\ AFDW$. A similar equation (Edgar 1990) to estimate macrobenthic production was applied to the data with less satisfactory results. This determination was based on comparison of production estimates against independently calculated production rates for the same samples through a cohort-based size-frequency approach in Holland et al. (1988).

Production estimates provide the basis for calculating food demand of macrobenthos and thus the ability to address food limitation when compared to POC deposition rates. Estimates of macrobenthos production were divided by the endpoints of a range (0.10-0.25) of production efficiencies (P:C) to provide a broad, conservative margin of food demand (Warwick et al. 1979, Schroeder 1981, Bayne and R.C. Newell 1983, Chardy and Dauvin 1992, R.I.E. Newell, pers. comm.). Food demand was also calculated with another approach to serve as check on the P:C assumptions above. The sums of daily production and respiration were divided by an assimilation efficiency term of 0.50 for shallow and deep station groupings (Warwick et al. 1979, Schroeder 1981, Bayne and Newell 1983, Hummel 1985). The resulting estimate of food demand lies within the range of food ration produced by using P:C = 0.10 and 0.25.

Results and Discussion

Covariance among individual physical, chemical, and biotic factors may confound univariate descriptors to explain variation in benthic community structure and dynamics over space and time. Thus, multivariate regression approaches are not appropriate to address the objectives of this study. Rather, our approach focused on integrative properties, hypoxia and POC deposition, with supporting evidence from patterns and relationships among other variables to address whether macrobenthos in the mesohaline portion of Chesapeake Bay are limited by seasonal hypoxia or food delivery. We also acknowledge a hierarchical approach to factors influencing benthic community structure and dynamics, such that physical factors set a template which modulates biotic interactions and community dynamics (Menge and Sutherland 1987, Zajac and Whitlack 1984). For example, hypoxia in Chesapeake Bay is a variable but recurring physical/chemical disturbance which decouples trophic linkages of consumers with their food sources and predators. Models of community assembly and dynamics taken in the example of this study would suggest that a decrease in environmental stress (hypoxia) would increase the importance of competition (e.g. as food limitation) or predation as influences on macrobenthos community structure and dynamics. A desired objective of an environmental and/or fisheries management perspective would be to ameliorate environmental stress where possible and maximize trophic efficiency of estuarine food webs. Closer coherence between macrobenthic biomass and food demand with hypoxia as opposed to POC deposition would suggest a weak potential for reductions in nutrient loading rates to exacerbate a decreased flow of energy through macrobenthos to upper trophic levels.

Water column parameters

Seasonality and depth of benthic habitats with respect to the pycnocline dictated the structure of our analyses of macrobenthos and environmental parameters. Although the magnitude and variation in water temperature were similar between shallow and deep benthic monitoring stations, patterns and concentrations of DO and chlorophyll *a* were quite different between shallow and deep habitats (Fig. I-2). DO and chlorophyll *a* concentrations declined considerably in deep habitats but were relatively constant among seasons at shallow stations. The average trend in below-pycnocline chlorophyll *a* concentrations among years declined ~10x over a six-week interval from late April to early June. There was no detectable change in chlorophyll *a* concentrations during this period in the upper mixed layer. The ratio of chlorophyll *a* as total POC below the pycnocline also declined sharply during this time period, indicating a decline in both food concentration and quality for consumers in deep habitats with the onset of summer. Significant positive correlations of near-surface chlorophyll *a* concentrations and macrobenthos biomass were observed for only two of six shallow stations, and two of five deep stations (Table I-2).

Macrobenthos biomass and hypoxia

Patterns of seasonal variation in macrobenthos biomass varied between spatially adjacent shallow and deep sites in consistent ways (Fig. I-3). Geometric mean annual biomass was ca. one order of magnitude greater across shallow compared to deep stations. Several key sediment parameters differ between shallow and deep stations, likely affecting or interacting with the water column parameters described above to dictate benthic community tolerances and responses to seasonal variation. Mean annual percent sediment organic C (mean \pm SD) among stations was quite low for shallow (0.297 ± 0.036) relative to deep habitats (3.426 ± 0.060), whereas the size fraction of sediment particles comprised of silts and clays was $2.05 \pm 1.79\%$ for shallow versus $90.68 \pm 5.85\%$ for deep stations. It is important to note that these inherent and persistent contrasts in key habitat parameters between shallow and deep benthic habitats likely influence the range of macrobenthic assemblage composition (Llansó 1992, Holland et al. 1977), and thus responses to variation in water column variables such as POC deposition and hypoxia.

Biomass at shallow sites varied little among seasons in contrast to biomass at deeper (below pycnocline) sites which typically demonstrated maximum and minimum points within short time intervals. The average onset of hypoxic conditions ($\text{DO} < 2.0 \text{ mg l}^{-1}$) among-stations and years at deep stations was 28 May, with an average return to normoxic conditions by 4 September (Fig. I-2). These dates approximately define the seasonal period with the greatest rate of change in macrobenthic biomass at deep stations (Fig. I-3). Within-year biomass maxima were observed in late spring, immediately prior to the onset of hypoxia in late May/early June. Biomass nadirs of deep assemblages were observed in late summer.

The mean date for the onset and wane of hypoxia given above represent a composite average among station and years. The application of a simple integrative measure of hypoxia duration and intensity (hypoxic index), is intended to capture long-term, seasonal variation in hypoxic stress on macrobenthos across stations and years. The presence of a gradient in this index facilitates a determination of the importance of hypoxia in explaining observed variation in macrobenthic summer biomass in below pycnocline (deep) habitats. The inclusion hypoxia duration is likely less important in systems that do not experience extended periods of hypoxia or where samples are infrequent. Ritter and Montagna (1999) applied a logistic model without a parameter for duration of hypoxic conditions which successfully characterized macrobenthic responses to and recovery from hypoxic conditions in Corpus Christi Bay, Texas.

Our analysis requires cautious interpretation of whether the observed gradients in the hypoxic index and macrobenthos biomass were due merely to site or year variations. Overall, station and year-specific measures of the hypoxic index and total macrobenthic summer biomass were negatively correlated in our study (Fig. I-4) ($r = -0.678$, $P = 0.001$, $n = 20$). However, a lack of within-station variation in the hypoxic index would not exclude the possibility that the overall biomass-hypoxia relationship is due to station differences due to factors other than hypoxia. A non-parametric ANOVA (Kruskal-

Wallis test) suggests that with the exception of the Patuxent River station, below pycnocline stations do not differ with respect to ranked values of the hypoxic index (Kruskal-Wallis test statistic = 6.971, $P=0.073$). This evidence for a lack of strong segregation of the hypoxic index based on spatial location (other than with respect to depth) along the gradient of hypoxia suggests that among-year variation in hypoxia influenced the overall relationship. The low number of years of consistent and frequent monitoring precludes a meaningful analysis of within-station variation in summer biomass and hypoxia.

Analysis of the residuals of the biomass-hypoxia relationship suggest that variation in community structure affects the influence of data from a given station-year to the overall relationship. For example, residuals of the correlation are positively related to log (mean individual body size) ($r=0.659$, $P=0.002$), and the proportion of total macrobenthic biomass comprised of mollusks ($r=0.502$, $P=0.024$). These variables are not independent, but are offered as links to respective analyses focusing on either taxonomic or size distribution aspects of community structure.

Taxa-specific biomass and hypoxia

The general biomass-hypoxia relationship is not consistent among broad taxonomic groups (Table I-3), suggesting differing tolerances for chronic hypoxia among taxa. The result is seasonal and intersite variation in community taxonomic and size-structure related to hypoxia in deep habitats (Holland et al. 1977, Dauer 1992, Llansó 1992). Among geographically diverse coastal areas, polychaetes are most tolerant of low DO conditions, followed by mollusks and crustaceans (Diaz and Rosenberg 1995). Indeed, a breakdown of correlation parameters relating taxa-specific biomass with the index of hypoxia in this study reveals a similar pattern (Table I-3). Slopes are more negative and correlation coefficients (r) are greater for arthropods (crustaceans) followed by mollusks and polychaetes. Based on these relationships, we would expect shifts in community structure related to the occurrence of hypoxic conditions. The within-year and station aggregate changes in community composition parallels seasonal and depth contrasts in benthic macrofauna biomass and water column parameters. Macrobenthos in deep habitats undergo dramatic shifts in taxonomic composition as measured by proportion of total biomass (Fig. I-5). Proportion of total biomass was comparatively more constant in shallow assemblages which do not experience sustained hypoxic conditions. Mollusks comprise the majority of macrobenthos biomass in shallow assemblages with a brief exception in the fall due to a spike in nemertean biomass.

Total biomass in deep assemblages were increasingly comprised of mollusks during spring phytoplankton blooms and increasing temperatures. However, the momentum for increases total community biomass and production through growth of potentially large and long lived mollusks is halted just following the onset of hypoxic conditions. Subsequent and dramatic shifts from mollusk to polychaete-dominated assemblages follow the onset of hypoxia in late May-early June until the end of the year. This pattern in community composition corresponds to seasonal changes in biomass and production of macrobenthos in deep habitats.

Macrobenthos production, food demand, and POC deposition

Total macrobenthos production estimates were compared to those generated with a cohort size-frequency approach by Holland et al. 1988 (Table I-4). Net differences between station-specific macrobenthos production rates estimated for 1985-1986 from the Tumbiolo and Downing equation and the cohort size-frequency approach in Holland et al. (1988) varied by only 18% on average; the absolute values of differences averaged 35% between the two methods. There was no systematic variation in error distribution between shallow or deep stations. Annual production:biomass (P:B) ratios were slightly higher in this study (mean P:B = 4.40) than for the same period and stations analyzed in Holland et al. (1988)(mean P:B = 3.84). If the turnover rates are slightly overestimated in this study relative to Holland et al. (1988), so will estimated ration, further suggesting that our determination of food limitation is conservative.

High levels of production (and thus food demand) are sustained for a greater portion of the year in shallow relative to deep macrobenthic assemblages (Fig. I-6). The shallow-deep contrast is conservative because our calculations of food demand did not account for non-lethal reductions in macrobenthic metabolic rates due to low DO stress. Macrobenthic respiration rates as a fraction of total benthic respiration ranged from 3-17% with values at the high end of this range observed from June-August. Kemp and Boynton (1981) estimated macrobenthic respiration as 1-39% of total benthic respiration in 3m and 6m deep benthic habitats in the Chesapeake Bay mesohaline.

Comparisons of seasonal variation in POC deposition versus carbon demand by macrofauna (and other heterotrophs) suggest a low potential for food limitation by benthic macrofauna in shallow or deep habitats (Fig. I-7). In fact, supply exceed macrobenthic demands by ca. 5-10x during most of the year, and is in excess of total demand of all benthic heterotrophs. This surplus above the pycnocline and the observed negative NEM for most of the year for below pycnocline benthic habitats suggests that the deficit of organic material balancing benthic metabolism is likely subsidized by lateral transport of material from shallow to deep habitats (Malone et al. 1986, Lehtonen and Andersin 1998). In fact, areal water column primary production in the shallow bay margins adjacent to the mesohaline mainstem is greater and likely focuses POC to deeper adjacent habitats. Thus, our method producing the observation of macrobenthic C demand exceeding supply via POC deposition to deep habitats in June is not likely to represent food limitation under these circumstances, because lateral transport of POC would not be fully accounted for. Limitation of production by food quality (and not quantity) would be expected if carbon-based measures typically failed to predict food limitation of consumers, or if parameters of food quality such as nitrogen or nitrogen-based compounds such as amino acids were largely independent of the carbon content of particulate organic material. Other studies have found that whether carbon is an adequate measure of food utility for consumers is variable with time and taxa (Marsh and Tenore 1990), or that compensatory feeding may overcome limitation strictly by food quality (Cruz-Rivera and Hay 2000).

Our findings suggest that increased nutrient limitation of water column primary production (and its subsequent deposition to benthic habitats) is unlikely to result in reduced macrofaunal production in mesohaline habitats. However, trophic linkages of producer-consumer production are strongly mediated by physical dynamics in the mesohaline region of Chesapeake Bay. Our analyses suggests the potential for greater mesohaline macrobenthic production based in observed patterns, but the extent to which this potential would be transferred to demersal upper trophic level populations has yet to be explored. Certainly, models attempting to predict these scenarios over multi-year time scales need to consider both community and ecosystem-based characteristics of macrobenthic communities to forecast dynamic links in Chesapeake Bay foodwebs.

References

- Ahlgren, G., W. Goedkoop, H. Markensten, L. Sonesten, and M. Boberg. 1997. Seasonal variation in food quality for pelagic and benthic invertebrates in Lake Erken – the role of fatty acids. *Freshw. Biol.* 38:555-570.
- Baird, D., and R.E. Ulanowicz. 1989. The seasonal dynamic of the Chesapeake Bay ecosystem. *Ecol. Monogr.* 59:329-364.
- Bayne, B.L., and R.C. Newell. 1983. Physiological energetics of marine mollusks. Chapter 9 in: A.S.M. Saleuddin and K.M. Wilbur (eds.) *The Molluska*, Volume 4 – Physiology, Part 1. Academic Press, New York.
- Breitburg, D.L. 1990. Near-shore hypoxia in the Chesapeake Bay: patterns and relationships among physical factors. *Est. Coastal Shelf Sci.* 30:593-609.
- Chardy P., and J.-C. Dauvin. 1992. Carbon flows in a subtidal fine sand community from the western English Channel: a simulation analysis. *Mar. Ecol. Progr. Ser.* 81:147-161.
- Cruz-Rivera, E., and M.E. Hay. 2000. Can quantity replace quality? Food choice, compensatory feeding, and fitness of marine mesograzers. *Ecology* 81:201-219.
- Dauer, D., Rodi, A.J. Jr., and J.A. Ransinghe. 1992. Effects of low dissolved oxygen events on the macrobenthos of the lower Chesapeake Bay. *Estuaries* 15:384-391.
- D'Avanzo, C., and J.N. Kremer. 1994. Diel oxygen dynamics and anoxic events in and eutrophic estuary in Waquoit Bay, Massachusetts. *Estuaries* 17:131-139.
- Diaz, R.J., R.J. Neubauer, L.C. Shaffner, L. Pihl, and S.P. Baden. 1992. Continuous monitoring of dissolved oxygen in an estuary experiencing periodic hypoxia and the effect of hypoxia on macrobenthos and fish. *Sci. Total Envir.* (Suppl. 1992) 1055-1068.

- Diaz, R.J., and R. Rosenberg. 1995. Marine benthic hypoxia: a review of its ecological effects and the behavioural responses of benthic macrofauna. *Ann. Rev. Oceanogr. Mar. Biol.* 33:245-303.
- Edgar, G.J. 1990. The use of the size structure of benthic macrofaunal communities to estimate faunal biomass and secondary production. *J. Exp. Mar. Biol. Ecol.* 137:195-214.
- Holland, A.F., N.K. Mountford, and J.A. Mihursky. 1977. Temporal variation in upper bay mesohaline benthic communities: I. The 9-m mud habitat. *Ches. Sci.* 18:370-378.
- Holland, A.F., A.T. Shaughnessy, L.C. Scott, V.A. Dickens, J. Gerritsen, and J.A. Ranasinghe 1988. Long-term benthic monitoring for the Maryland portion of Chesapeake Bay. Rep. to MD OEP, Baltimore. Versar Inc., Columbia Maryland.
- Hummel, H. 1985. An energy budget for a *Macoma balthica* (Molluska) population living on a tidal flat in the Dutch Wadden Sea. *Neth. J. Sea Res.* 19:84-92.
- Kemp, W.M., and W.R. Boynton. 1981. External and internal factors regulating metabolic rates of an estuarine benthic community. *Oecologia* 51:19-27.
- Kemp, W.M., E.M. Smith, M. Marvin-DiPasquale, and W.R. Boynton. 1997. Organic carbon balance and net ecosystem metabolism in Chesapeake Bay. *Mar. Ecol. Progr. Ser.* 150:229-248.
- Lehtonen, K.K., and A. B. Andersin. 1998. Population dynamics, response to sedimentation and role in benthic metabolism of the amphipod *Monoporeia affinis* in an open-sea area of the northern Baltic Sea. *Mar. Ecol. Progr. Ser.* 168:71-85.
- Llansó, R.J. 1992. Effects of hypoxia on estuarine benthos: the lower Rappahannock River (Chesapeake Bay), a case study. *Est. Coastal Shelf Sci.* 35:491-515.
- Malone, T.M., W.M. Kemp, H.W. Ducklow, W.R. Boynton, J.H. Tuttle, and R.B. Jonas. 1986. Lateral variation in the production and fate of phytoplankton in a partially stratified estuary. *Mar. Ecol. Progr. Ser.* 32:149-160.
- Marsh, A.G., and K.R. Tenore. 1990. The role of nutrition in regulating the population dynamics of opportunistic, surface deposit feeders in a mesohaline community. *Limnol. Oceanogr.* 35:710-724.
- Menge, B. A. and J. P. Sutherland. 1987. Community regulation: variation in disturbance, competition, and predation in relation to environmental stress and recruitment. *Am. Nat.* 130: 730-757.

- Möller, P., L. Pihl, and R. Rosenberg. 1985. Benthic faunal energy flow and biological interaction in some shallow marine soft bottom habitats. *Mar. Ecol. Progr. Ser.* 27:109-121.
- Nestlerode, J.A., and R.J. Diaz. 1998. Effects of periodic environmental hypoxia on predation of a tethered polychaete, *Glycera americana*: implications for trophic dynamics. *Mar. Ecol. Progr. Ser.* 172:185-195.
- Ritter, C., and P.A. Montagna. 1999. Seasonal hypoxia and models of benthic response in a Texas bay. *Estuaries* 22:7-20.
- Schroeder, L.A. 1981. Consumer growth efficiencies: their limits and relationships to ecological energetics. *J. Theor. Biol.* 93:805-828.
- Smith, E.M., and W.M. Kemp. 1995. Seasonal and regional variations in plankton community production and respiration for Chesapeake Bay. *Mar. Ecol. Progr. Ser.* 116:217-231.
- Tumbiolo, M.L., and J.A. Downing. 1994. An empirical model for the prediction of secondary production in marine benthic invertebrate populations. *Mar. Ecol. Progr. Ser.* 114:165-174
- Warwick, R.M., I.R. Joint, and P.J. Bradford. 1979. Secondary production of the benthos in an estuarine environment. In: R.L. Jeffries and A.J. Day (eds.), *Ecological Processes in Coastal Environments*. Blackwell Scientific Publications, Oxford.
- Zajac, R.N., R.B. Whitlatch. 1984. A hierarchical approach to modelling soft-bottom successional dynamics. In: P.E. Gibbs (ed.), *Proceedings of the Nineteenth European Marine Biology Symposium*, Plymouth, Devon, UK. Cambridge Univ. Press.

Table I-1. List of species used to estimate total macrofaunal community production and ration. These taxa typically comprise >85% of macrofaunal abundance for the sites and years of the current study.

Species	Major taxonomic group	Feeding Group
<i>Acteocina canaliculata</i>	Mollusca	Carnivore/Omnivore
<i>Carinoma tremaphoros</i>	Nemertea	Carnivore/Omnivore
<i>Cyathura polita</i>	Crustacea	Carnivore/Omnivore
<i>Gemma gemma</i>	Mollusca	Suspension
<i>Glycinde solitaria</i>	Polycheata	Carnivore/Omnivore
<i>Haminoea solitaria</i>	Mollusca	Carnivore/Omnivore
<i>Heteromastus filiformis</i>	Polycheata	Deep deposit
<i>Leptocheirus plumulosus</i>	Crustacea	Interface
<i>Macoma balthica</i>	Mollusca	Interface
<i>Macoma mitchelli</i>	Mollusca	Interface
<i>Micrura leidyi</i>	Nemertea	Carnivore/Omnivore
<i>Mulinia lateralis</i>	Mollusca	Suspension
<i>Mya arenaria</i>	Mollusca	Suspension
<i>Paraprionospio pinnata</i>	Polycheata	Interface
<i>Streblospio benedicti</i>	Polycheata	Interface
<i>Tagelus plebeius</i>	Mollusca	Suspension

Table I-2. Correlations of surface chlorophyll biomass and macrobenthos biomass at shallow and deep stations. Data from each parameter were binned in 2wk intervals for 1985-1989 to produce temporal correspondence and reduce variation in sample date differences. Macrobenthos biomass data was lagged by two 2wk intervals. Both variables were log-transformed to reduce heteroscedacity (Kolmogorov-Smirnoff test of distributions).

Station	Mean Depth (m)	r	P	n
<i>Shallow</i>				
1	2.4	0.370	0.026	36
5	3.1	0.326	0.069	32
6	1.1	0.043	0.803	36
15	1.9	0.112	0.534	33
18	1.9	0.250	0.191	29
51	2.9	0.573	<0.001	37
<i>Deep</i>				
3	13.8	0.324	0.066	33
8	12.5	0.241	0.170	34
17	26.9	0.430	0.010	35
52	10.8	0.297	0.093	33
71	15.2	0.032	0.874	27

Table I-3. Correlation parameters of biomass vs. hypoxic index for Taxonomic groups of macrobenthos from samples defined in Figure 4. N = 20 for all groups.

Taxonomic Group	r	P	slope	log exponent of y-intercept
Annelids	0.338	0.145	-0.003	2.31
Crustaceans	0.677	0.001	-0.008	1.74
Mollusks	0.629	0.003	-0.007	3.81

Table I-4. Comparison of estimates of total macrobenthic production ($\text{g m}^{-2} \text{y}^{-1}$) by station for 1985-1986. Mean proportional difference between station-specific estimates is 18%. Differences between methods were not systematically different between shallow and deep stations.

Station	Size-frequency (Holland et al. 1988) 1985-1986	<u>Production estimation approach</u>	
			Production equation in this study (Tumbiolo and Downing 1994) 1985-1986
<i>Shallow</i>			
1	4.2		7.1
5	8.0		12.3
6	14.6		6.2
15	14.8		15.9
18	58.4		36.1
51	13.3		19.4
<i>Deep</i>			
3	9.3		6.4
8	7.8		5.6
17	1.7		1.2
52	2.7		2.8
71	19.5		23.8

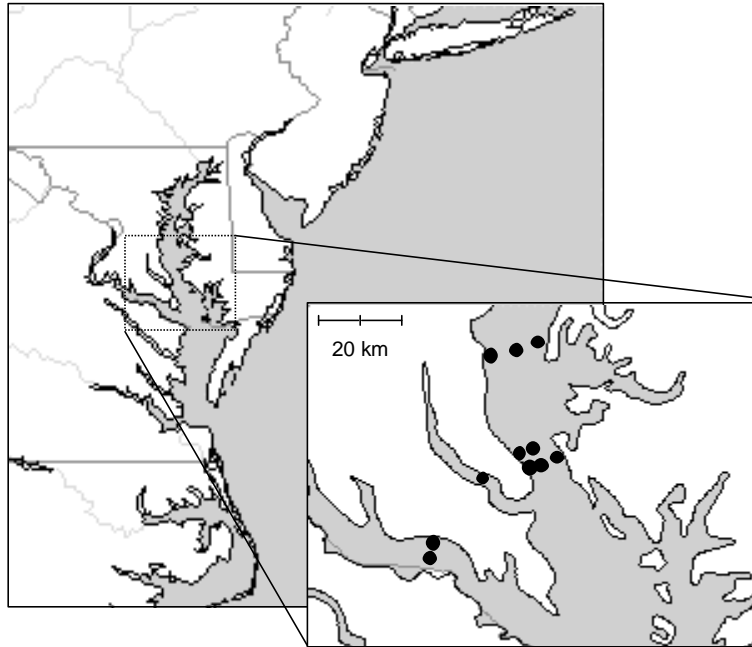


Fig I-1. Map of Chesapeake Bay mesohaline macrobenthos monitoring stations used in this study.

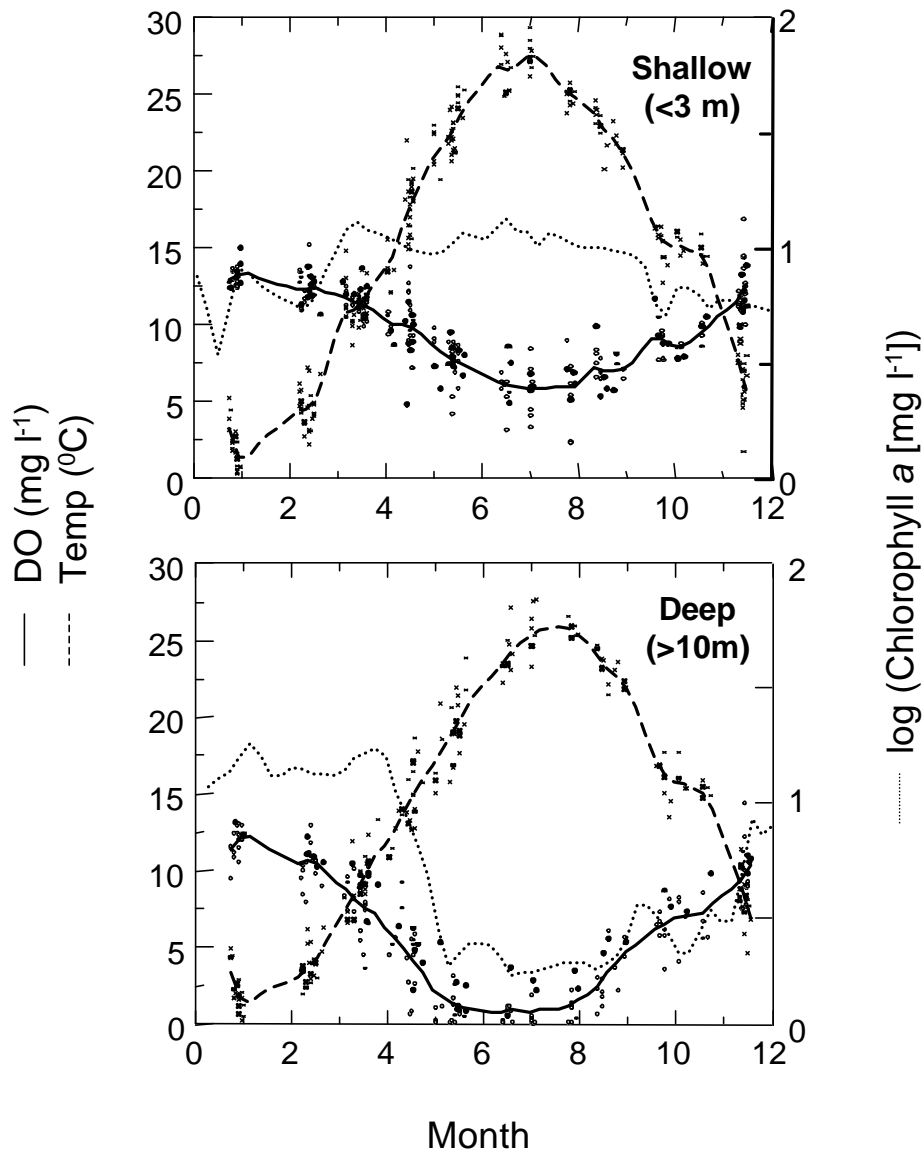


Fig. I-2. Water column data from selected mesohaline macrobenthos sampling sites illustrated in Fig. I-1. Chlorophyll a data is above and below-pycnocline data from Chesapeake Bay mainstem water quality sampling station (CB 4.4; Lat 38° 24', Long 76° 20'). Data in panels highlight patterns among stations and years (1985-1989) between shallow and deep macrofaunal habitats. Lines are generated from distance-weighted least squares.

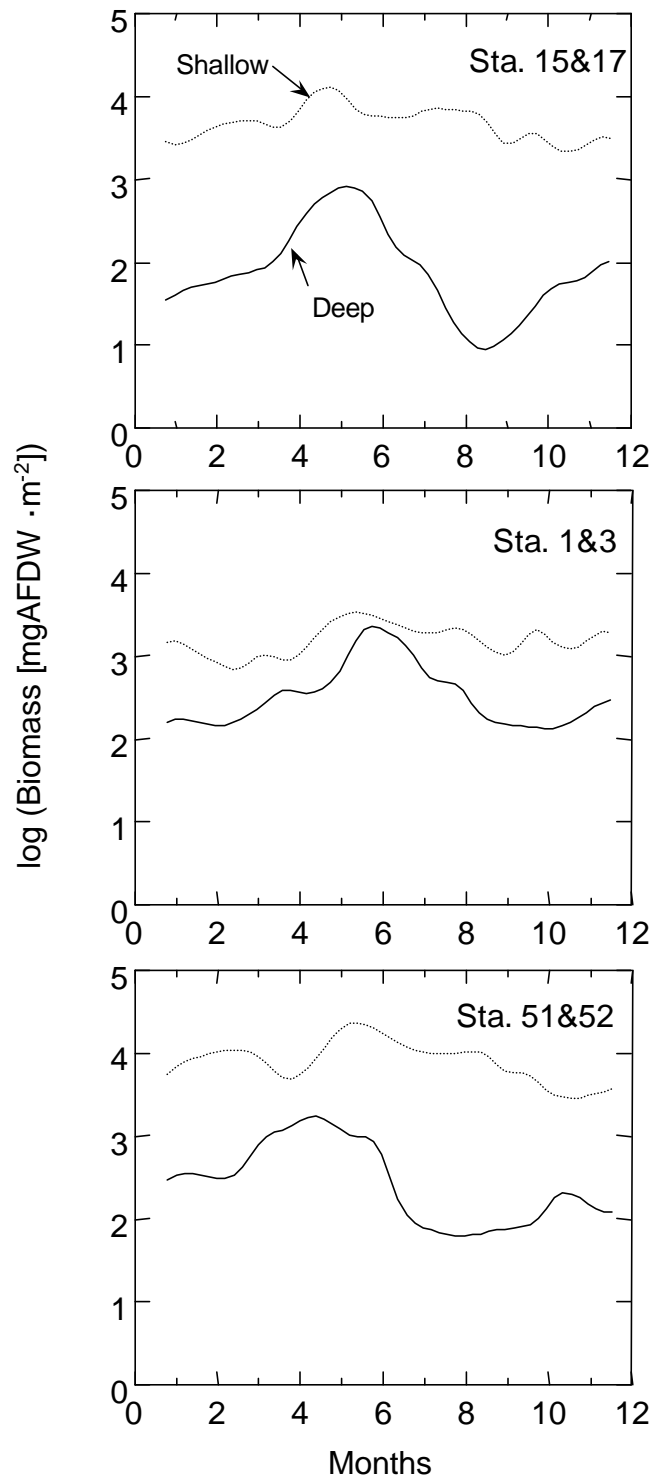


Fig. I-3. Variability of macrofaunal biomass within years for selected spatially-adjacent pairs of stations (identified in Fig. I-1) within the mesohaline region of Chesapeake Bay. Station-pair order is decreasing latitude from top panel to lower. Data years and smoothing method of seasonal patterns as in previous figure. Note the relative consistency of biomass within and among years at shallow relative to deep stations.

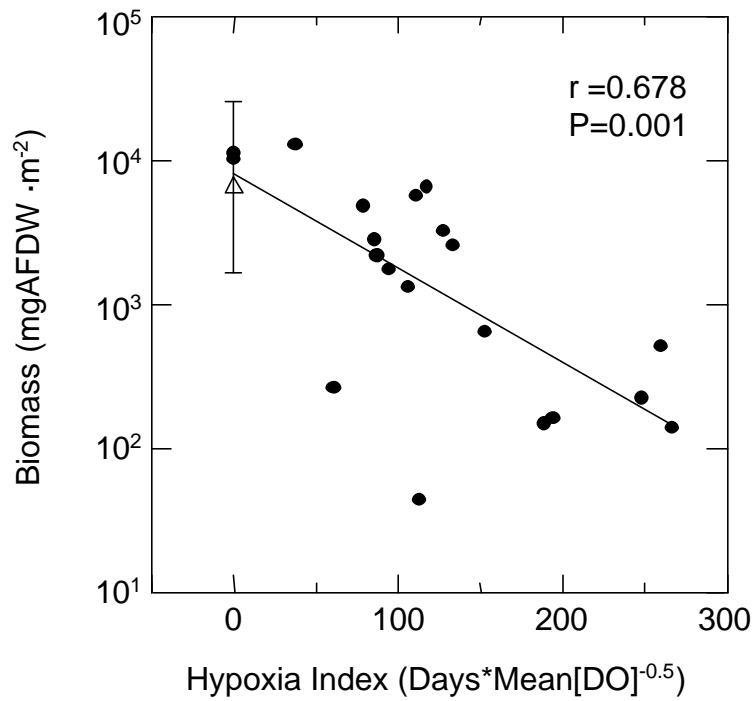


Fig. I-4. Mean annual summer biomass at deep stations (n=5) from 1985-1988 versus hypoxia index. Open triangle and error bar are the mean and standard deviation of biomass in shallow stations (n=6) for the same periods. Residuals of this regression are positively correlated with the proportion of total biomass comprised of molluscs ($r=0.502$, $P=0.024$).

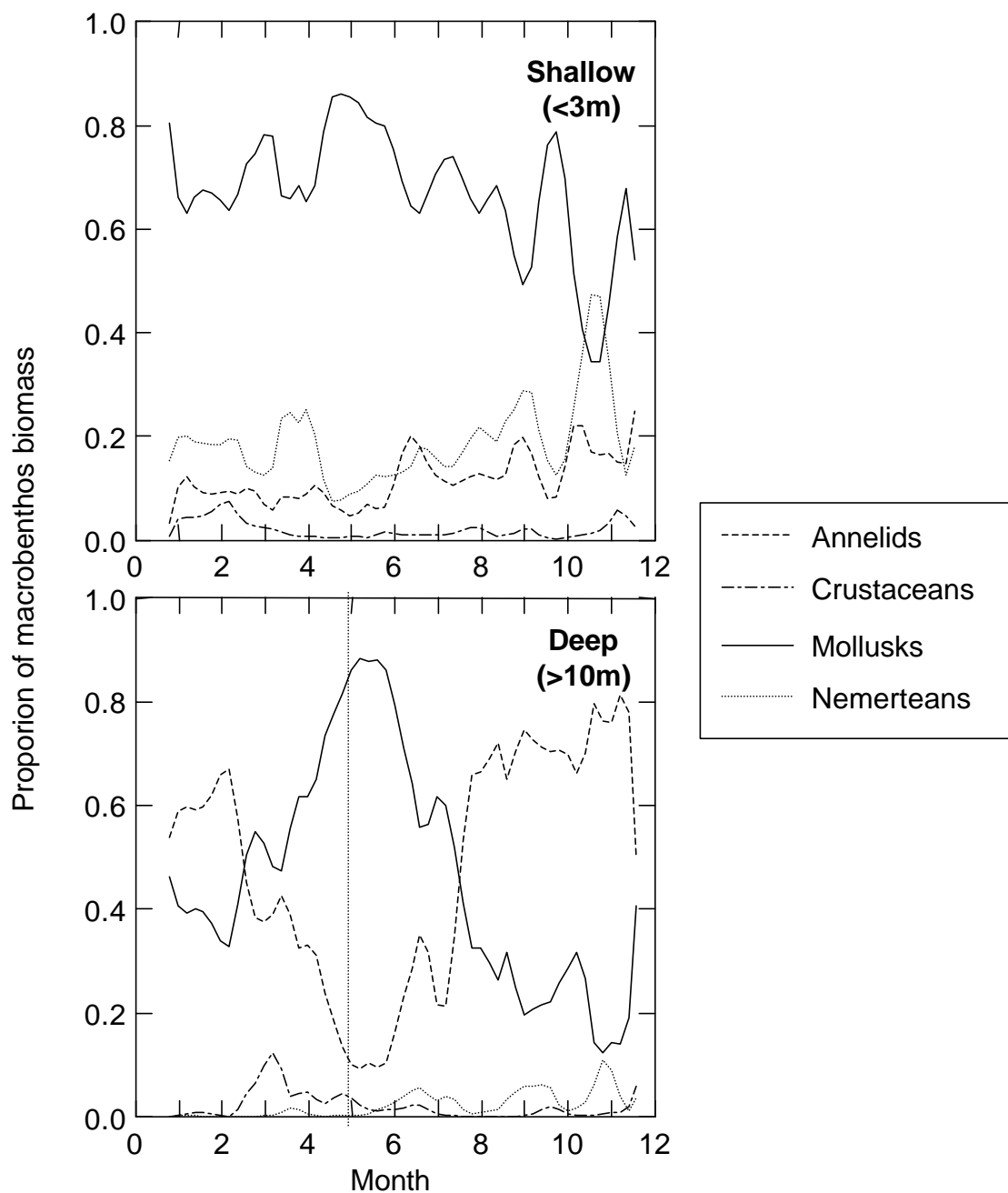


Fig I-5. Seasonal patterns in taxonomic composition of total macrobenthos biomass. Smoothed data among 1985-1989. Note relative consistency in shallow relative to deep communities. Dashed vertical line in lower panel represents the average date of first recorded hypoxia ($DO < 2 \text{ mg}\cdot\text{l}^{-1}$) at macrobenthos sampling sites.

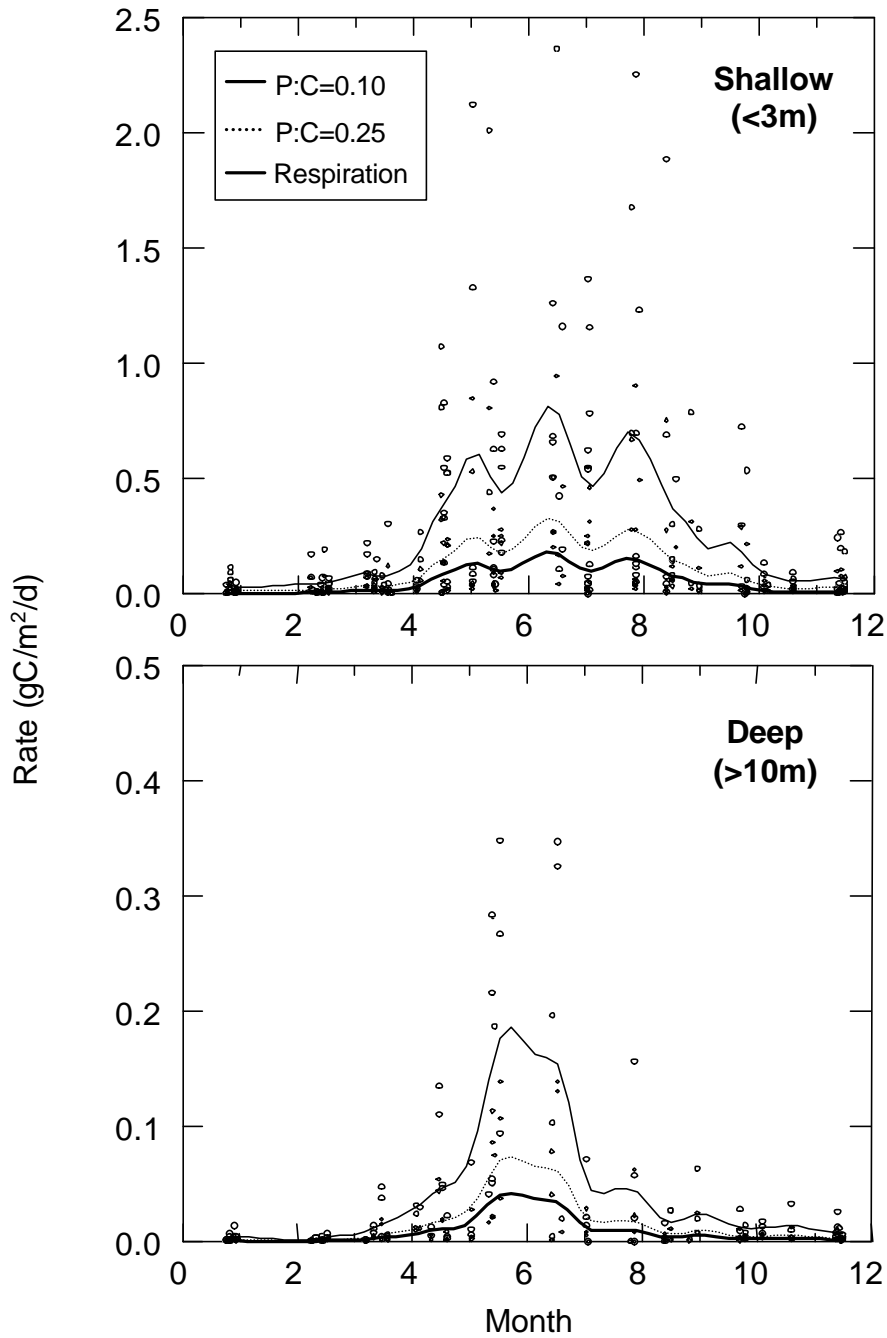


Fig I-6. Seasonal variation in C demand (ration) by macrobenthos in shallow and deep communities in mesohaline mainstem stations. High and low estimates of ration calculated as 10% and 25% production efficiency. Solid lines are distance weighted smoothed values from point estimates of ration at for each level of production efficiency.

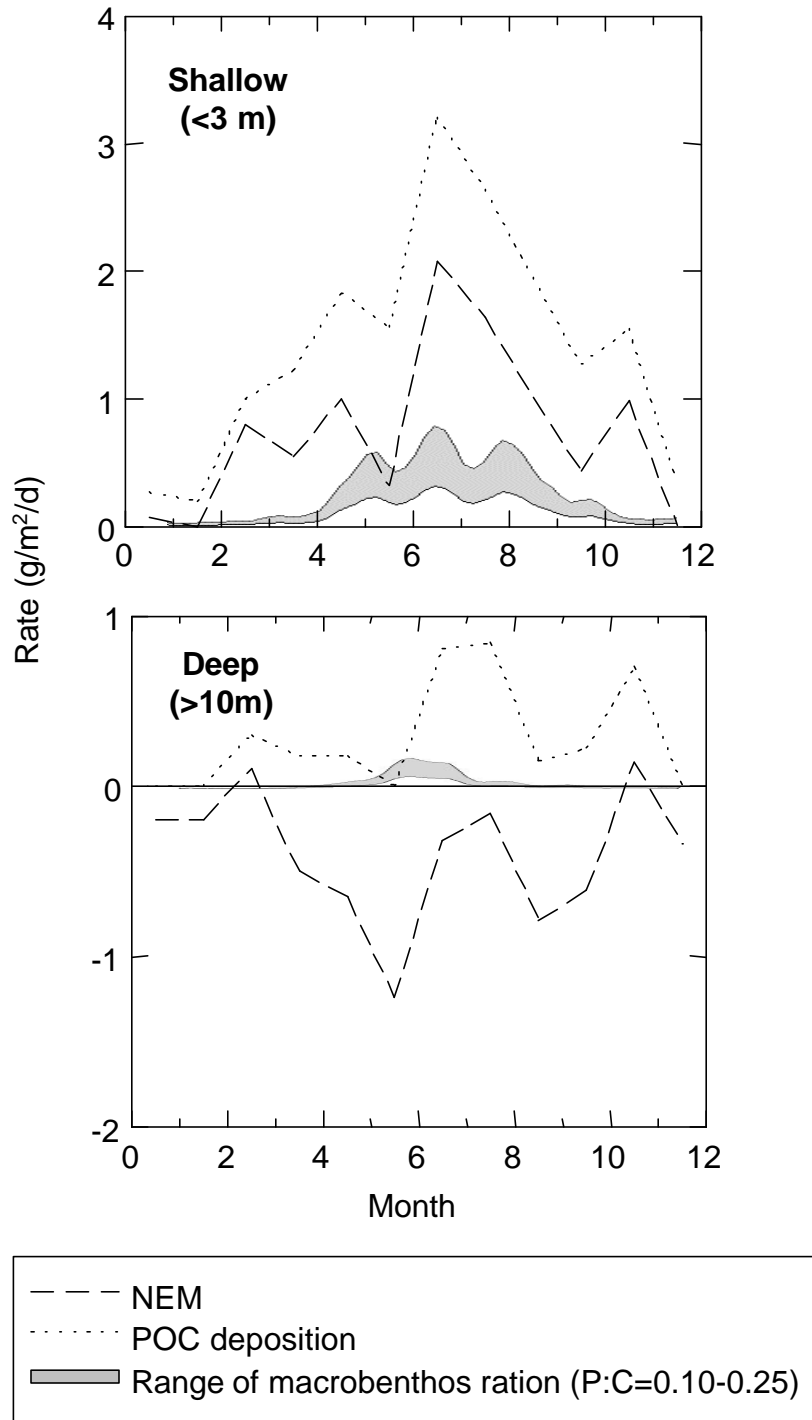


Fig. I-7. Composite data of NEM, POC deposition, and macrobenthic food ration for Chesapeake Bay mainstem.

Chapter II

Nutrient Enrichment, Habitat Variability and Trophic Transfer Efficiency in Food Webs of Estuarine Ecosystems

W. M. Kemp, M. T. Brooks and R. R. Hood

Abstract

We have developed a simple numerical model of estuarine ecosystem dynamics to explore how eutrophication and habitat variability might influence the efficiency by which primary production is transferred to growth of consumer organisms. This model is designed with a generic equation structure which is well documented by empirical studies and widely used in ecosystem and water quality modeling. Simulation experiments revealed that at low nutrient levels, trophic transfer efficiency (TTE) may be enhanced with increasing patchiness of resource availability, at both the individual and the ecosystem levels of conceptual organization. In contrast, resource variability has virtually no effect on TTE at higher nutrient levels. The model also suggested that, regardless of the variability of resource availability, there is an initial enhancement of transfer efficiency with increasing nutrient levels, followed by a drastic reduction in efficiency beginning at moderately eutrophic conditions. This catastrophic shift in trophic structure is attributable to a saturation of the ability of consumer organisms to utilize the increased primary production associated with nutrient enrichment. Under these conditions, an increasing fraction of the primary production is shunted to microbial food chains and associated respiratory losses and oxygen depletions. The steepness by which this reduction in efficiency (with nutrient enrichment) occurs is related to the strength of predation control at upper trophic levels, with more intense predation (e.g., associate with fisheries exploitation) resulting in sharper declines in efficiency. We argue that these results are robust and general, and that they may explain often observed reductions in relative fish production (per unit primary production) in response to eutrophication. Moreover, this pattern may be relevant to trends in Chesapeake Bay, and it may be broadly predictable using equation structures similar to those of the current Chesapeake Bay water quality model.

Introduction

A question of long-standing concern in ecology is the amount of fish production that can be derived from primary production in aquatic systems. To address this question it is essential to measure two key characteristics of the ecosystem's food web: 1) the efficiency of transfer between each trophic level; and 2) the average number of trophic transfers between primary producers and the fish of interest (e.g., Ryther 1969). The ratio of secondary to primary production, which is regulated by both of these mechanisms, can be referred to as the ecosystem's trophic transfer efficiency (TTE). These simple relationships have formed the basis for several estimates of potential regional and global fish production (e.g., Ryther 1969; Cushing 1990) and for resulting concerns about the

sustainability of current harvests (e.g., Pauly and Christensen 1995). These estimates, however, are critically dependent upon assumptions about trophic transfer efficiency between steps in the food chain and how this efficiency changes as a function of nutrient enrichment and primary productivity.

Recent analyses have suggested that TTE would tend to increase directly with primary production under nutrient-poor conditions, but would eventually saturate as nutrient levels continue to increase, such that TTE would remain unchanged with further increases in productivity (Iverson 1990). In contrast, comparative analyses of fish yield versus primary production among diverse aquatic ecosystems suggests that the ratio of fish yield to primary production actually increases with increasing primary production and associated nutrient enrichment (e.g., Nixon 1988). Recent discussions of global fisheries data, however, indicate a trend where increased fish yield in highly productive ecosystems may derive from harvesting organisms at lower trophic levels (Pauly et al. 1998). Indeed, there is growing evidence from lakes that the sustainable harvests of specific fish populations per unit primary production tend to decrease as aquatic ecosystems become highly eutrophic (e.g., Edmondson 1991). Although quantitative explanation for these changes in TTE with nutrient enrichment are generally lacking, it has been suggested that reduced TTE with eutrophication may result from changes in community structure and associated alteration of key trophic pathways (e.g., Landry 1977). These trophic change are often related to alterations in nutrient concentration ratios (e.g., Sanders et al. 1987; Turner and Rabblais 1994).

It remains an open question how and why the ratio of secondary-to-primary production might change with alterations in nutrient loading to aquatic ecosystems (Caddy 1993). This uncertainty is disturbing in light of two parallel worldwide trends of increases in both exploitation rates on fish populations (Pauly et al. 1998) and nutrient enrichment of aquatic systems (e.g., Nixon et al. 1986). Although it is anticipated that nutrient enrichment will lead to more total harvestable production, TTE may change dramatically with changes in nutrient loading. Conceivably, total fish production could even decline with nutrient enrichment if TTE were to decrease radically. Any expected relationship between nutrient enrichment and fish yield is likely complicated further by the fact that harvesting fish can significantly impact food-web structure through trophic cascade effects (e.g., Carpenter and Kitchell 1988). Thus, changes in top-down control imposed by human activities could potentially change TTE as well.

Over the last several decades, Chesapeake Bay has experienced a trend of increasing nutrient loading (Boynton et al. 1995), which has resulted in expanded conditions of seasonal hypoxia (e.g., Officer et al. 1984) and reductions in seagrass abundance and distribution (Orth and Moore 1983; Kemp et al. 1983). During the same period, harvest of carnivorous fish has been increasing (Houde and Rutherford 1993). Planned reductions in nutrient loading are expected to benefit fish habitats by improving conditions associated with seagrass and bottom water oxygen. Although fish production will also decline with nutrient reductions if TTE remains unchanged, other outcomes might be expected if TTE changes with nutrient loading. Thus, the relationship between

nutrient loading and TTE is a crucial element for conserving Bay resources in relation to nutrient waste management.

Large scale numerical simulation models are commonly used as tools to assist in establishing nutrient waste management strategies for estuaries such as Chesapeake Bay in relation to water quality and living resource conditions (Cercio and Cole 1993). If such models are to be of practical use, they must be structured in a way that will faithfully simulate, not only water quality variations, but also changes in TTE in response to nutrient loading. In addition to the general relationships between TTE and mean nutrient conditions, experimental studies suggest that trophic efficiencies for zooplankton are enhanced by the small-scale patchiness of phytoplankton distributions common in estuaries like Chesapeake Bay (e.g., Dagg 1977; Saiz et al. 1993). Such variations in zooplankton feeding efficiency might be substantially altered by small-scale pulses and patches of nutrients and algae. Current Chesapeake Bay management models (Cercio and Cole 1993) cannot simulate small scale variabilities, and it is thus unclear the degree to which these spatially aggregated computations will tend to underestimate TTE.

The purpose of this chapter is to conduct exploratory simulation modeling studies to investigate how trophic transfer efficiencies are altered with change in nutrient loading and resource variability (in time or space). We focus these studies on pelagic food webs because these are the primary conduits through which primary production is transferred to fish (Baird and Ulanowicz 1989). In this analysis, we use conventional model similar to those employed in the Chesapeake Bay water quality model, and we investigate the degree to which results depend on specific model structures.

Methods

The primary model developed in this study is structured around five state variables (Fig. 1d): dissolved inorganic nitrogen (N); herbivorous zooplankton (Z); large phytoplankton such as diatoms (P_L); small phytoplankton (P_S), and detritus (D). In addition, we have simplified and aggregated this five-compartment model (N- P_L - P_S -Z-D) into four (N-P-Z-D), three (N-P-Z) and two (P-Z) compartment models (Fig. 1 a-c). An alternative five-compartment model including fish (F) has also been developed, but will be discussed only briefly here. The terms describing interactions in all versions of this plankton model are identical, with only minor coefficient adjustments made to account for addition or deletion of pathways. Therefore, the description which follows relates specifically to this five-compartment version of the model (Fig. 1d).

The model, which is described by a series of five finite difference equations (Table 1), is calibrated in nitrogen units and uses conventional equation formulations which are described in detail elsewhere (Stickney et al. 1999). External forcing functions include insolation, water exchange rates and external concentrations of N. In the 3-5 compartment models external inputs of N are used to drive the model, while in the two-compartment version, there is no N state variable, and nutrients are taken up by P from an external variable. Nutrient uptake is described by standard Michaelis-Menten kinetics of the form, $\mu_m [N/(N + K_n)]$, where μ_m is maximum uptake (growth rate) for P and K_n is the

half-saturation coefficient. Photosynthesis versus light response functions use hyperbolic equations of the form $[1 - \exp(-I/I_k)]$, where I_k is the light saturation level.

To include the effects of varying food-chain length on trophic transfer efficiency the model was parameterized so that P_S dominates the phytoplankton biomass at low N concentrations and P_L dominates the phytoplankton biomass at high N concentrations. This is a realistic representation of the switch that commonly occurs from small to large phytoplankton dominance with increasing nutrient levels (e.g., Sanders et al. 1987). Both the large and small phytoplankton have a light- and concentration-dependent uptake rate of N, as well as a linear rate of senescence. The large phytoplankton exhibit a high sinking rate and a higher grazing preference by the zooplankton. Other differences between the phytoplankton compartments are evident in the senescence rate, uptake rate, and saturation coefficients (Table 2).

Zooplankton mortality is a key process which regulates the dynamics of the entire ecosystem (Steele and Henderson 1992). The base-run version of the model employs a quadratic mortality loss of the form, Z^b , where the version of this zooplankton closure term with $b = 2$ is thought to represent mortality inflicted by predators which are also dependent on Z, or inter-individual interactions which cause disease spread (Steele and Henderson 1992). Simulation experiments also utilize lower power functions ($b = 1.25, 1.5$), and a hyperbolic mortality which saturates at high values of Z. Zooplankton ingest large phytoplankton and detrital particles with equal preference, while their preference for the small phytoplankton is only 4% that for the larger particles. The sum of the preference values for zooplankton feeding equals one. At low N concentrations when P_S dominates the average food chain length is longer because more of the food supply for Z comes through a two step food chain (P_S to D to Z), whereas at high N concentrations most of the food supply for Z comes directly from P_L , a one step food chain.

Organic nitrogen losses associated with phytoplankton senescence and zooplankton egestion and mortality enter the detritus (D) compartment, which is meant to represent both dissolved and particulate non-living organic matter. The detritus in this model is considered to represent both detritus and bacteria and therefore constitutes a simplified microbial loop. The presence of bacteria is implied in the model through the respiratory losses from D which recycle nutrient back to N. Recycling of inorganic N also occurs via all respiratory pathways.

The model was built and run using Stella II computer software (High Performance Systems Inc., version 4.0). The model was run with a time-step of 0.1 day, and numerical integration were done using a fourth-order Runge-Kutta method. Model simulations were performed under a range of nutrient input conditions until steady-state levels were achieved, and values for state variables and flows were recorded. In some simulations, nutrient inputs were variable. The variability was introduced by using the Stella built-in function NORMAL, which produces a set of normally distributed random numbers with a given mean and standard deviation without variability to show the trophic transfer efficiency under steady-state conditions. Model performance was measured primarily in

terms of the trophic transfer efficiency (TTE), which was defined as the ratio of zooplankton growth to phytoplankton productivity for full model simulations.

Interacting effects of alterations in mean and variance of primary productivity levels were also examined at the level of the consumer population (Z). In this case, a proxy for TTE was defined as the ratio of zooplankton consumption and phytoplankton input. The zooplankton grazing function used in this analysis was a Holling Type III function, which is of the form, $G_m [P_2 / (P^2 + K_p^2)]$ (e.g., Scheffer 1991). This grazing equation was used here because it is thought to be most generally applicable (Holling 1959). This equation has the characteristic of changing from a second-order function at low food levels to a first-order function at middle food levels to a zero-order function at high food concentrations.

Results and Discussion

The five-compartment model (N- P_L - P_S -Z-D) was run for a 300 day simulation at low ($\approx 2 \mu\text{M}$), intermediate ($\approx 7 \mu\text{M}$) and high ($\approx 12 \mu\text{M}$) ambient N concentrations, which were regulated by adjusting concentrations of external N sources (Fig. 2). After initial transient behavior, biomass values achieved steady-state levels within 30 days at low and high nutrients; however, an oscillating pattern at intermediate concentrations continued past 100 days until it was internally damped. These cycling patterns suggests the possibility of an instability of the simulation at intermediate nutrient conditions. At low N concentrations, the total biomass is dominated by small phytoplankton; at intermediate nutrient levels all of the model compartments increase, but P_S still dominates the phytoplankton biomass. At high N concentrations large phytoplankton dominate, and there is a substantial increase in the amount of detritus in the system. The instability evident at the intermediate N concentrations occurs because the model is close to a transition from a low N, P_S dominated state to a high N state dominated by P_L and D. Note that the system is much better damped at both low and high N concentrations.

We explored this apparent shift in system state by running the model over a wide range of steady-state N concentrations from 1-12 μM . With the calibration parameter settings we observed a dramatic shift in biomass and production levels and partitioning at $N \approx 7 \mu\text{M}$. It is even clearer in this presentation (Fig. 3), that this catastrophic shift is characterized by a transition from P_S dominance at low N to P_L and D dominance at higher N. Although D biomass exceeds that of P_L at high nutrient levels, large algal production is substantially greater than the rate of D production from mortality and excretion. The relative significance of zooplankton also declines abruptly at the N transition, with the ratios $Z/(P_L + P_S)$ and Z/D both exhibiting dramatic declines at the transition, although the former also shows a slight increase with increasing N before the transition point (Fig. 4a). The ratio of phytoplankton to detritus [$(P_L + P_S)/D$] biomass declines relatively continuously over the entire N range, with only a small drop at the transition point (Fig. 4b). The ratio of phytoplankton to detritus production, however, declines up to the transition, at which point it jumps higher and continues to increase slightly with increasing N. Somewhat surprisingly, the relative importance of N recycling

(compared to exogenous input plus recycling) increases sharply with increasing N inputs from about 45% at low N to 60% at the state transition point; after this transition, the importance of recycling remains constant at about 70% of the total input to the N pool (Fig. 5).

The trophic transfer efficiency (TTE) of the model ecosystem responds strongly to changes in nutrient level, increasing from about 10% at low N to almost 30% at the transition point, at which TTE declines back to $\approx 10\%$ and remains relatively unchanged with increasing N (Fig. 6). Our initial interpretation was that the increasing TTE with N to the left of the transition point was attributable the increased consumption of P_L by Z, and the associated shortening of the average length of the food chain (e.g., Ryther, 1969; Landry 1977). However, as we shall demonstrate below, the actual explanation lies in the saturating nutrient uptake kinetics. The abrupt decline in TTE at the transition point and the subsequent gradual decline thereafter is related saturation of zooplankton grazing control over algal biomass. As the grazing saturates the model abruptly transitions to a new stable equilibrium state where zooplankton grazing no longer controls the amount of phytoplankton biomass in the system. This phenomenon of phase shift in phytoplankton-zooplankton interactions, which has been demonstrated previously using simple two-compartment (P-Z) models (e.g., Rosenzweig 1971; Scheffer 1991), has been interpreted as inherent chaotic behavior of these systems. Evidence from field experiments seems to support this general phase-shift pattern with nutrient enrichment (Scheffer 1991; Carpenter et al. 1995).

We investigated the generality of this relationship between TTE and nutrient enrichment through a series of numerical experiments and analyses. First we conducted the same simulation series recording variations in TTE with increases in N for four different versions of this plankton ecosystem model ranging from five to two compartments (Fig. 1a-d). Clearly, all four models exhibit similar patterns, with the transitions becoming more abrupt and the phase-shift point moving toward higher values of N with increased model complexity (Fig. 7). The relationships between TTE and N are scaled to maximum observed TTE to make results comparable in the face of necessary changes in model coefficients. We suspect that this pattern exists in more complex ecosystem simulation structures including those used in the Chesapeake Bay water quality model.

To test the mechanisms behind the observed phase shift, we conducted numerical experiments using the simplest two-compartment version of the model (Fig. 1a). Our first test involved changing the zooplankton feeding function from a saturating hyperbolic equation to a linear, first-order equation: the result was to retain the increases in TTE with N at low nutrients but to remove completely the phase shift (Fig. 8a). This confirms our interpretation that the phase shift is attributable to the saturation of zooplankton control on phytoplankton, but it leaves open the explanation for the initial increase in TTE with N. Before addressing that question, however, we also tested the response to variations in the structure of the closure or mortality term for zooplankton. Illustrated here are four different closure formulations. These include a power function of the form, $m_z Z^b$ where m_z is a mortality rate coefficient and b set equal to 1.5, and 2.0.

All of these power curve forms exert relatively strong top down control on the system because the predators never saturate and they respond instantly to increases in the Z population. With $b = 2.0$ this closure can be interpreted as cannibalism (Steele and Henderson 1992) or arising from some undefined predator population that varies in proportion to its prey. While the quadratic closure leads to abrupt catastrophic decline in TTE at a phase shift, the 1.5 power function exhibits a smooth (non-chaotic) transition from higher to lower values of TTE as N is increased beyond an “optimum N ” (Fig. 8b). Hence, it appears that, contrary to previous discussions (e.g., Scheffer 1991), this general pattern is not exclusive to equations with attractors and chaotic behaviors. The third and fourth mortality closure formulations are hyperbolic saturation functions of the forms, $Z(K_z + Z)^{-1}$ (Fasham et al. 1990), and $Z^2(Z^2 + K_z^2)^{-1}$ (Scheffer 1991), where K_z is a grazing half-saturation coefficient. The obvious interpretation of these equations is a hyperbolic rate for a satiable predator. With linear hyperbolic closure, the decline in TTE with N under high nutrient levels is no longer evident, while with the sigmoidal closure the shift is very dramatic (Fig. 8b).

It can be shown numerically and analytically that the initial increase in TTE at low N is the result of an increase in P growth rate relative to the advection/sinking loss rate, and that the N concentration where maximum TTE and subsequent decline occurs is inversely related to the P half-saturation constant for N uptake, K_p (Fig. 9). An analytical steady-state solution describing the initial increase and subsequent saturation of TTE with increasing N can be derived by assuming steady-state and setting the right-hand side of the differential equations for P and Z (Table 1) equal to zero. We assume that the quadratic loss term in the P equation is negligible at low N concentrations and that the grazing response in the Z equation is a linear function of P at low N concentrations. By rearranging these equations and combining, the resulting expression is $TTE_{init} = g_e \{1 - V_f / \mu_m [N/(N + K_p)]\}$. Thus, TTE depends on N at low nutrient concentrations according to an inverse hyperbolic function, which is also characterized by saturation with increasing N . As with the conventional rectangular hyperbolic formulation, this relationship shifts to the right with increasing values of K_p , (Fig. 9a). Change in the half-saturation coefficient for zooplankton grazing on phytoplankton also regulates the shape of this relationship, where increases in K_z shift the function to the left and reduce the abruptness of the decline at phase shift (Fig. 9b).

With the quadratic closure on P , the high N state is a P dominated, where losses due to flushing and density-dependent mortality are the primary means by which P is removed from the system. This condition is essentially similar to that which has developed in many lakes and estuaries subject to high anthropogenic nutrient loading and may also apply to some estuarine and coastal marine environments (e.g., Nixon et al. 1986). Eutrophication often leads to the development of blooms of “noxious” species, such as blue-green algae, which cannot be consumed and controlled by resident zooplankton species (Sanders et al. 1987; Turner and Rabalais 1995). Although the transition in the model is not associated with a change in species composition, the result is essentially similar. The high production is not controlled by grazing and is not transferred to higher trophic levels. In natural systems this often leads to accumulation of

organic detritus, funneling of the production to decomposers, and development of problems, such as anoxia.

We also considered the effect of introducing variability in resources availability in this aquatic ecosystem model. We examine this question at the level of the whole ecosystem and then take a closer look at the level of the grazer population. To simulate resource variability, we added a fluctuating component to the N supply in the model, while maintaining the same mean concentrations. The time-course model solutions do not change dramatically with variable (Fig. 10) versus constant N input (Fig. 2). At low N P_S dominates and the biomasses are generally low, while at high N concentrations the system transitions to a P_L and D dominance. At intermediate concentrations we once again see evidence of instability in the system. There are some interesting patterns in the time-course simulation (Fig. 10), where we see that the dominant periods of variation in the N pool appear to increase with mean N (Fig. 10, left hand panels). The variability in P_S , P_L , and Z all appear to be damped with increasing mean N level; however, D seems to retain its variance despite the nutrient conditions (Fig. 10, right panels). Although the introduction of variability does not fundamentally change the relationship between N concentration and TTE described above (Fig. 6), it tends to enhance TTE at very low and very high nutrient concentrations (Fig. 11). Variability in N also appears to move the transition point to the right and decrease TTE at intermediate concentrations (Fig. 11). The source of this increased trophic efficiency appears to be related to shifts in phytoplankton relative abundance and associated change in efficiency related to first-order part of the nutrient response kinetics.

We investigated changes in TTE with variability at the organism level by calculating zooplankton consumption and growth on variable food a specified feeding function. Although TTE is determined largely by the growth efficiency of the herbivore and the functional response of the herbivore to its prey, we focus here on how the amount and variability of phytoplankton biomass alters TTE as determined by the functional response curve of an herbivore to its prey. For generality, we use the sigmoidal Holling Type III feeding function, which encompasses the three basic types of feeding relations (second-, first- and zero-order functions) that are most often observed in nature. The sigmoidal function is analogous to a hyperbolic function a low-food threshold (i.e., an x-axis intercept) below which feeding ceases (Holling 1959). We generated a series of normal phytoplankton biomass distributions with different means and variances and then transformed them using the feeding function with K_p set at 1 and G_m at 3 day^{-1} . This procedure is analogous to non-linear, statistical transformations, such as the log transformation, which are commonly employed to change the shape of distribution to make it more normal. In this case we are applying the feeding function as a transformation to a series of normal phytoplankton distribution inputs. These inputs generate zooplankton growth rate distributions which tend to be non-normal because the transformation is non-linear. We ran 42 different combinations of mean and standard deviation of phytoplankton availability (7 means, each with 6 different SD values). The frequency distributions of zooplankton growth rates computed from these phytoplankton input series are shown (Fig. 12).

The ratio of the zooplankton growth to phytoplankton input is taken as a trophic efficiency, and results are summarized (Fig. 13). The pattern is clear in that transfer efficiency (TTE) increases with declining mean values of P down to $P = 0.5 K_p$, where variations are more complex. At higher values of P , increasing variance tends to cause a decrease in TTE; however, at low values of P (oligotrophic conditions), increased variance causes substantial increases in TTE until the standard deviation approaches 1.0 (Fig. 13). When we used a hyperbolic feeding function, the pattern was more consistent, where TTE declined with increasing variance regardless of the level of P . These model results suggest that in aquatic systems that are dominated by herbivores whose grazing is described by a sigmoidal feeding function, the effect of resource variability on TTE depends upon the trophic state of the system. Variability in food supplies associated with, for example, nutrient pulses or physical discontinuities, can substantially enhance trophic transfer efficiency (*i.e.*, by nearly a factor of two), but this will only occur when food supplies are limiting. As mean food concentrations increase the benefit imparted by variability rapidly diminishes and can actually reduce TTE as concentrations approach saturating levels.

Concluding Comments

According to our model analyses, increases in nutrient concentrations under oligotrophic conditions can result in significantly higher values of TTE due to enhancement of P growth rate when there are losses of P due to advection and/or sinking. Thus, in natural, nutrient-limited systems increased nutrient loading could result in disproportionately large increases in production at higher trophic levels due to increases in TTE. However, these results also suggest that there is a critical point above which increased nutrient loading can lead to substantially reduced TTE. There is anecdotal observations which suggest that such critical points exist in natural aquatic ecosystems, and this has obvious management implications. It implies that a relatively healthy system could undergo a sudden transition to an unhealthy state in response to a small increase in nutrient loading in the absence of abrupt changes in phytoplankton species composition. The fact that the strength of the decline in TTE at intermediate N concentrations is determined by the form of the mortality closure formulation has some important implications as well. It suggests that marine ecosystems with strong top-down control on the primary consumers will be more likely to experience abrupt declines in TTE with increasing eutrophication than those without strong top-down control. Since top-down control in aquatic systems can be modified by harvesting fish, it is possible that human activities could increase or decrease the probability of an abrupt decline in TTE with increased nutrient loading, depending upon the trophic level at which the harvesting occurs. Model analyses also suggest that spatial and temporal variability of resources contribute to changes in TTE; however, these effects appear to be relatively small except under oligotrophic conditions. The transition in TTE with increasing N (Fig. 6) occurs in our model ecosystem at N concentrations of about $7 \mu\text{M}$. It remains an open question as to where would such transition points occur on a nutrient-enrichment scale in natural ecosystems. Other important questions also need to be addressed. How do we recognize an approaching transition as systems undergo progressive eutrophication? What are the consequences of human exploitation of fish and other animals at higher trophic levels on

this TTE-nutrient relationship? Is Chesapeake Bay to the left or right of the point of maximum trophic efficiency on the TTE-nutrient gradient? Does the Chesapeake Bay water quality model produce these relationships? If so, where does it compute the Bay to be currently along this trend?

References

- Baird, D. and R. Ulanowicz. 1989. The seasonal dynamics of the Chesapeake Bay ecosystem. *Ecol. Monogr.* 59: 329-364.
- Boynton, W. R., J. H. Garber, R. Summers and W. M. Kemp. 1995. Inputs, transformations and transport of nitrogen and phosphorus in Chesapeake Bay and selected tributaries. *Estuaries* 18 (No. 1B): 285-314.
- Caddy, J. F. 1993. Towards a comparative evaluation of human impact on fishery ecosystems of enclosed and semi-enclosed seas. *Rev. Fish. Sci.* 1: 57-95.
- Carpenter, S. R., D. Christensen, J. Cole, K. Cottingham, X. He, J. Hodgson, J. Kitchell, S. Knight, M. Pace, D. Post, D. E. Schindler and N. Voichick. 1995. Biological control of eutrophication in lakes. *Environ. Sci. Technol.* 29: 784-786.
- Carpenter, S. R. and J. F. Kitchell. 1988. Consumer control of lake productivity. *BioScience* 38 (11): 764-769.
- Cerco, C. F., and T. Cole. 1993. Three-dimensional eutrophication model of Chesapeake Bay. *J. Environ. Engg.* 119: 1006-1025.
- Cushing, D. H. 1990. Plankton production and year-class strength in fish populations: an update of the match/mismatch hypothesis, *Adv. Mar. Biol.*, 26:
- Dagg, M. 1977. Some effects of patchy food environments on copepods. *Limnol. Oceanogr.* 22: 99-107.
- Edmunson, W. T. 1991. *The Uses of Ecology. Lake Washington and Beyond*, University of Washington Press, Seattle, WA.
- Fasham, M. J. R., et al. 1990. A nitrogen-based model of plankton dynamics in the oceanic mixed layer, *J. Mar. Res.*, 48, 591-639 (1990)
- Holling, C. S. 1959. Some characteristics of simple types of predation and parasitism. *Can. Ent.* 385-398.
- Houde, E. and E. Rutherford. 1993. Recent trends in estuarine fisheries: predictions of fish production and yield. *Estuaries* 16: 161-176.

- Iverson, R. L. 1990. Control of marine fish production. *Limnol. Oceanogr.*, 35:
- Kemp, W. M., Boynton, W. R., Twilley, R. R., Stevenson, J. C., Means, J. C. 1983. The decline of submerged vascular plants in upper Chesapeake Bay: Summary of results concerning possible causes. *Mar. Technol. Soc. J.* 17: 78-89.
- Landry, M. R. 1977. A review of important concepts in the trophic organization of pelagic ecosystems. *Helgolander wis. Meeresunters.* 30: 8-17.
- Nixon, S. W. 1988. Physical energy inputs and the comparative ecology of lake and marine ecosystems. *Limnol. Oceanogr.* 33: 1005-1025.
- Nixon, S. 1995. Coastal marine eutrophication: a definition, social causes, and future concerns. *Ophelia* 41: 199-219.
- Nixon, S.W., C.A. Oviatt, J. Frithsen and B. Sullivan. 1986. Nutrients and the productivity of estuarine and coastal marine systems. *J. Limnol. Soc. S. Africa* 12(1/2): 43-71.
- Officer, C.B., R.B. Biggs, J.L. Taft, L.E. Cronin, M.A. Tyler, and W.R. Boynton. 1984. Chesapeake Bay anoxia: origin, development and significance. *Science* 23: 22-27.
- Orth, R. J., and K. A. Moore. 1983a. Chesapeake Bay: An unprecedented decline in submerged aquatic vegetation. 222: 51-53.
- Pauly, D., and Christensen, V. 1995. Primary production required to sustain global fisheries, *Nature*, 374, 255-257.
- Pauly, D. et al. 1998. Fishing down the food chain, *Science*, 279, 860-863.
- Rosenzweig, M. L. 1971. Paradox of enrichment: Destabilization of exploitation ecosystems in ecological time. *Science* 171: 385-387.
- Ryther, J. H. 1969. Photosynthesis and fish production in the sea, *Science*, 166, 72-76.
- Scheffer, M. 1991. Fish and nutrients interplay determines algal biomass: a minimal model. *Oikos*. 62: 271-282.
- Saiz, E., P. Tiselius, P. Jonsson, P. Verity and G. Paffenhofer. 1993. Experimental records of the effects of food patchiness and predation on egg production of *Acartia tonsa*. *Limnol. Oceanogr.* 38: 280-289.
- Sanders, J. S. Cibik, C. D'Elia and W. Boynton. 1987. Nutrient enrichment studies in a coastal plain estuary: changes in phytoplankton species composition. *Can. J. Fish. Aquat. Sci.* 44: 83-90.

Steele, J. H., and E. W. Henderson. 1992. The role of predation in plankton models. *J. Plank. Res.*, 14, 157-172 (1992)

Stickney, H. L., D. Stoecker and R. Hood. 2000. The impact of mixotrophy on planktonic marine ecosystems. *Ecological Modeling*, in press.

Turner, R. E. and N. Rabalais. 1994. Coastal eutrophication near the Mississippi River delta. *Nature*. 368: 619-621.

Table II-1. Finite difference equations for five-compartment model of plankton trophic dynamics (N = dissolved inorganic nitrogen; D = detritus; P_L = large phytoplankton; P_S = small phytoplankton; Z = herbivorous zooplankton). Numerical calculations made at any time (t) starting with conditions at one time-step earlier (t - 1), where the time-step is dt.

Finite Difference Equations

$$\begin{aligned}
 N(t) &= N(t-dt) + (Re_z + Re_s + Re_l + Re_d + In_n - Up_l - Up_s - Ot_n) * dt \\
 D(t) &= D(t-dt) + (Mt_l + Mt_s + Mt_z + Df_z - Gz_d - Re_d - Ot_d - Sk_d) * dt \\
 P_L(t) &= P_L(t-dt) + (Up_l + In_l - Mt_l - Gz_l - Re_l - Ot_l - Sk_l) * dt \\
 P_S(t) &= P_S(t-dt) + (Up_s + In_s - Mt_s - Gz_s - Re_s - Ot_s - Sk_s) * dt \\
 Z(t) &= Z(t-dt) + (Gz_l + Gz_s + Gz_d - Mt_z - Re_z - Ot_z - Df_z) * dt
 \end{aligned}$$

Respiration and Excretion (Re) Rates

$$\begin{aligned}
 Re_z &= ((\xi_{al} - \xi_{gl}) * Gz_l) + ((\xi_{ad} - \xi_{gd}) * Gz_d) + ((\xi_{as} - \xi_{gs}) * Gz_s) \\
 Re_l &= (1-b) * (I_l * P_L^2) \\
 Re_s &= (1-b) * (I_s * P_S^2) \\
 Re_d &= r * D
 \end{aligned}$$

Mortality (Mt) and Defecation (Df) Rates

$$\begin{aligned}
 Mt_l &= b * I_l * (P_L)^2 \\
 Mt_s &= b * I_s * (P_S)^2 \\
 Mt_z &= p_z * (Z)^2 \\
 Df_z &= ((1 - \xi_{al}) * Gz_l) + ((1 - \xi_{as}) * Gz_s) + ((1 - \xi_{ad}) * Gz_d)
 \end{aligned}$$

Zooplankton Grazing (Gz) Rates

$$\begin{aligned}
 Gz_l &= (Gz_m * Z * \beta_l * (P_L - 0.01)) / ((\beta_l * P_L) + (\beta_s * P_S) + (\beta_d * D) + K_z) \\
 Gz_s &= (Gz_m * Z * \beta_s * P_S) / ((\beta_l * P_L) + (\beta_s * P_S) + (\beta_d * D) + K_z) \\
 Gz_d &= (Gz_m * Z * \beta_d * D) / ((\beta_l * P_L) + (\beta_s * P_S) + (\beta_d * D) + K_z)
 \end{aligned}$$

Phytoplankton Uptake (Up) Rates

$$\begin{aligned}
 Up_l &= \mu_{ml} * [1 - e^{(-I/Ik)}] * (N / (N + K_{nl})) * P_L \\
 Up_s &= \mu_{ms} * (1 - e^{(-I/Ik)}) * (N / (DIN + K_{ns})) * P_S
 \end{aligned}$$

Sinking (Sk) Rates

$$\begin{aligned}
 Sk_l &= c_l * P_L \\
 Sk_s &= c_s * P_S \\
 Sk_d &= c_d * D
 \end{aligned}$$

Table II-2: Definition of coefficients and values used in base run for five-compartment plankton model.

Parameter	Symbol	Value	Units
Assimilation efficiency for Z on D	ξ_{ad}	0.375	dimensionless
Assimilation efficiency for Z on P _L	ξ_{al}	0.75	dimensionless
Assimilation efficiency for Z on P _S	ξ_{as}	0.75	dimensionless
Zooplankton preference for D	β_d	0.49	dimensionless
Zooplankton preference for P _L	β_l	0.49	dimensionless
Zooplankton preference for P _S	β_s	0.02	dimensionless
Growth efficiency for Z on D	ξ_{gd}	0.15	dimensionless
Growth efficiency for Z on P _L	ξ_{gl}	0.30	dimensionless
Growth efficiency for Z on P _S	ξ_{gs}	0.30	dimensionless
Total irradiance	I	90.0	Watts/m ²
Light saturation parameter	I _k	75.0	Watts/m ²
Saturation constant for zoopl grazing	K _z	1.10	dimensionless
Saturation constant for N uptake by P _L	K _{nl}	1.00	day ⁻¹
Saturation constant for N uptake by P _L	K _{ns}	0.60	day ⁻¹
Predation on Zooplankton	p _z	0.12	day ⁻¹
Senescence rate for P _L	l _l	0.10	day ⁻¹
Senescence rate for P _S	l _s	0.12	day ⁻¹
Zooplankton maximum grazing rate	GZ _m	3.20	mmol/kg-sw
Maximum growth rate for LP	μ_{ml}	3.05	mmol/kg-sw
Maximum growth rate for SP	μ_{ms}	0.80	mmol/kg-sw
Detritus recycling rate	r	0.30	day ⁻¹
Partitioning of phytoplankton senescence	b	0.50	day ⁻¹
Sinking rate for P _L	c _l	0.18	day ⁻¹
Sinking rate for P _S	c _s	0.001	day ⁻¹
Sinking rate for D	c _d	0.01	day ⁻¹

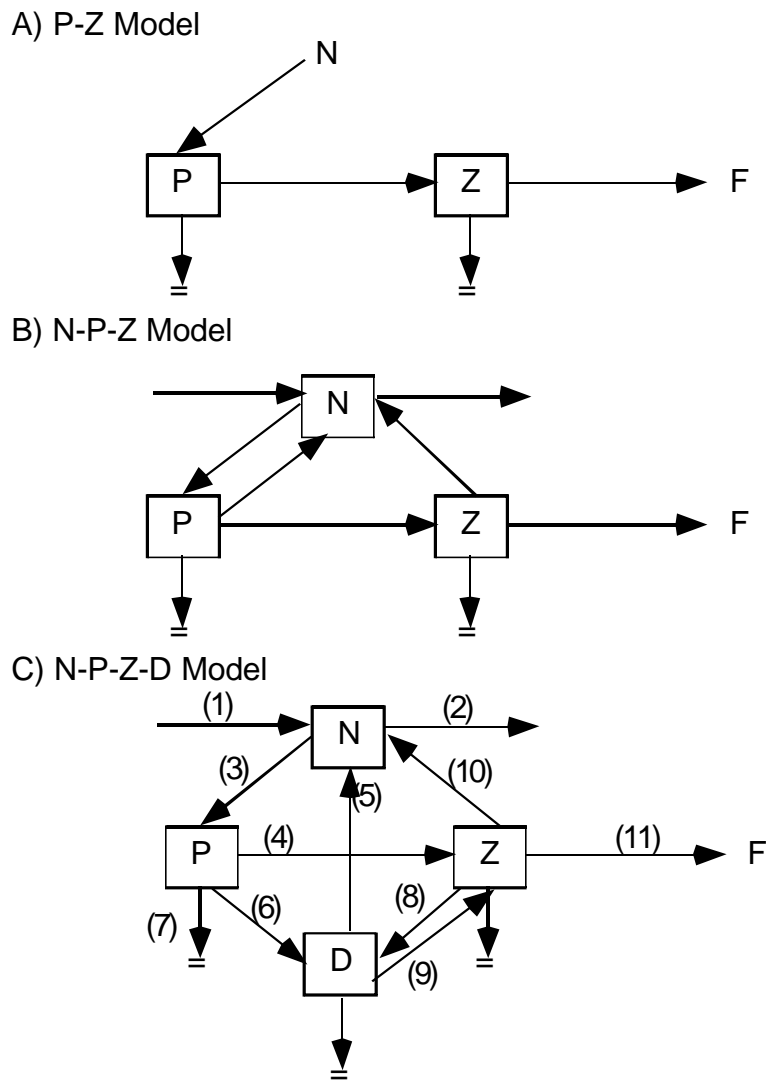
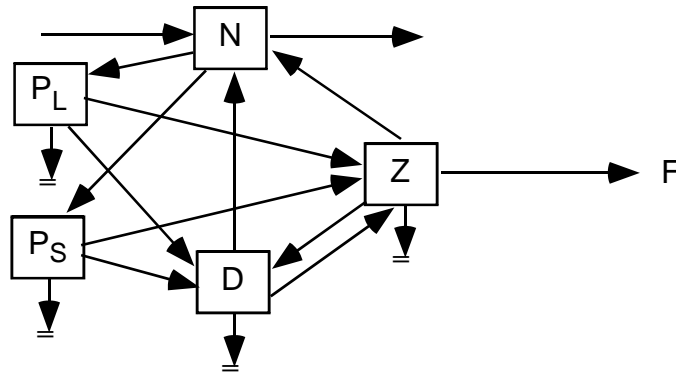


Fig. II-1A-C. Schematic sketches for three versions of the pelagic ecosystem model, with state variables indicated with boxes and trophic pathways and nutrient fluxes and indicated with arrows. State variables defined as: P = phytoplankton (L indicates large cells and S indicates small cells); Z = herbivorous zooplankton; N = dissolved inorganic nitrogen; D = detrital organic nitrogen (dissolved and particulate); F = zooplanktivorous fish. Arrows with double lines under them indicate respiration and imply N recycling.

D) N-P_L-P_S-Z-D Model



E) N-P-Z-D-F Model

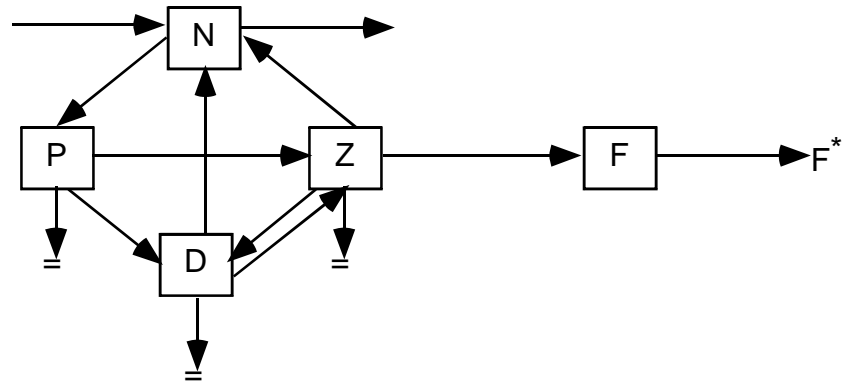


Fig. II-1D-E. Schematic sketches for two versions of the pelagic ecosystem model, with state variables indicated with boxes and trophic pathways and nutrient fluxes and indicated with arrows. State variables defined as: P = phytoplankton (L indicates large cells and S indicates small cells); Z = herbivorous zooplankton; N = dissolved inorganic nitrogen; D = detrital organic nitrogen (dissolved and particulate); F = zooplanktivorous fish. Arrows with double lines under them indicate respiration and imply N recycling.

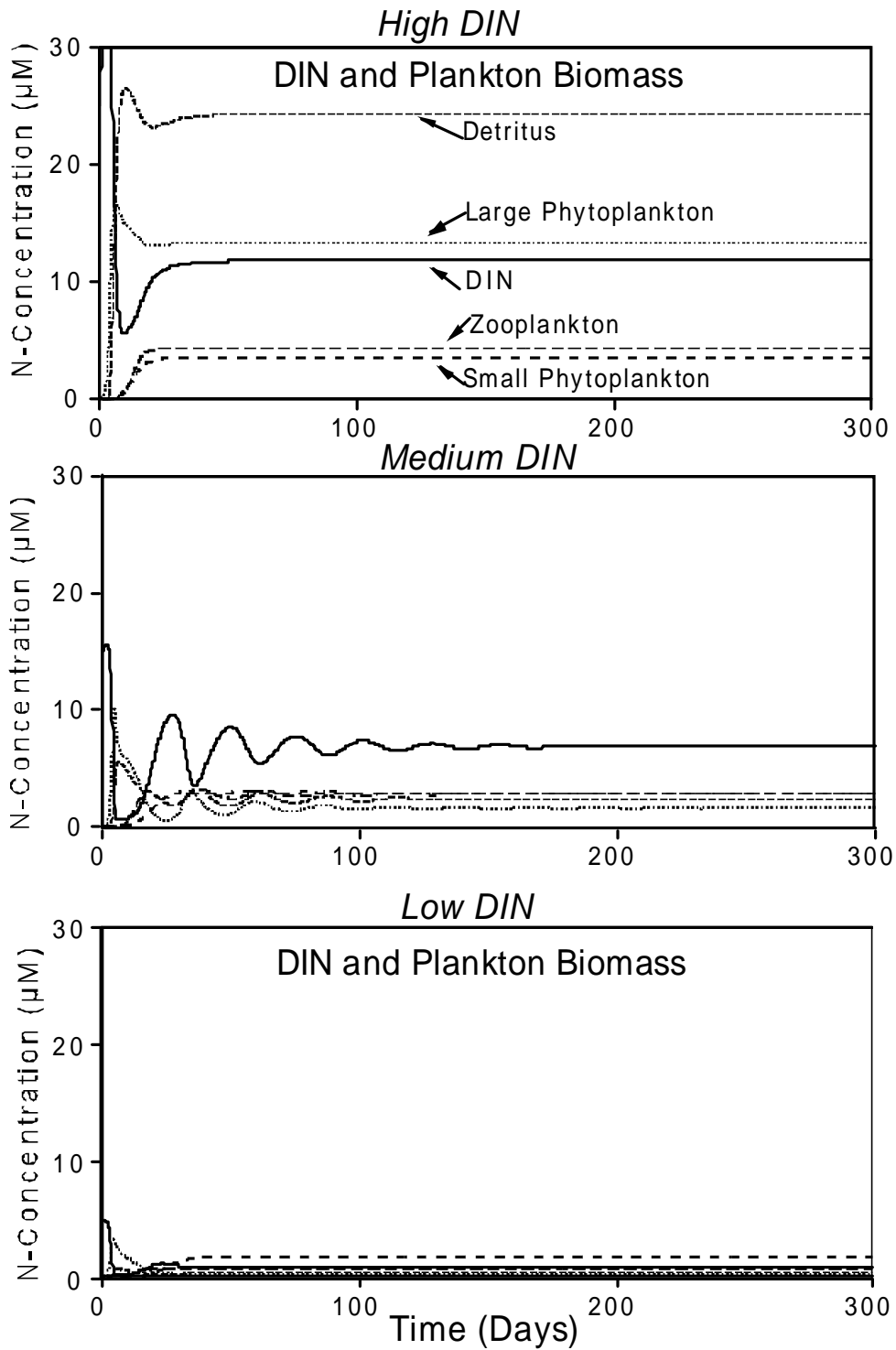


Fig. II-2. Time-course simulation of five-compartment pelagic ecosystem model (Fig. II-1d) under conditions of: a) high; b) intermediate; c) low nutrient inputs.

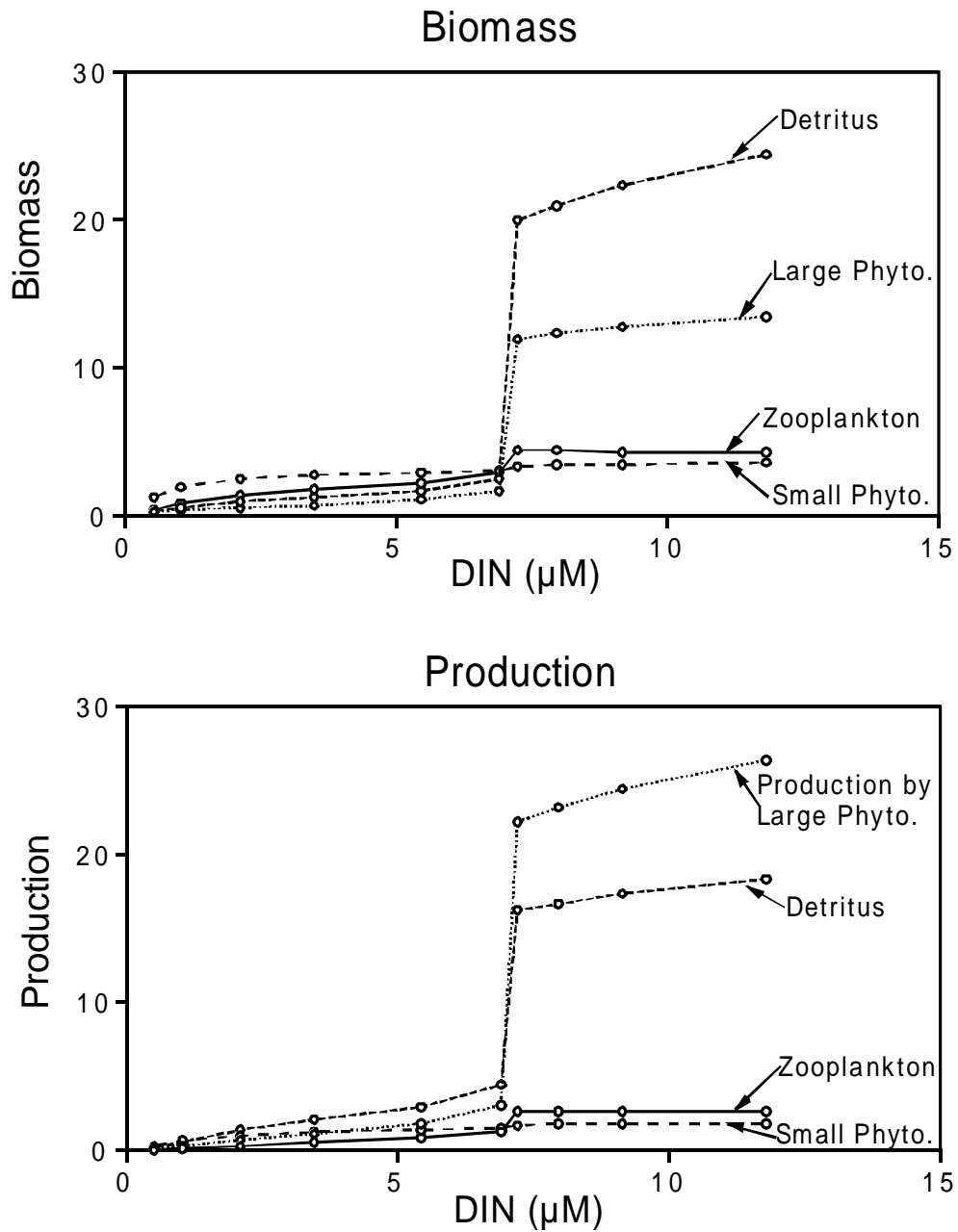
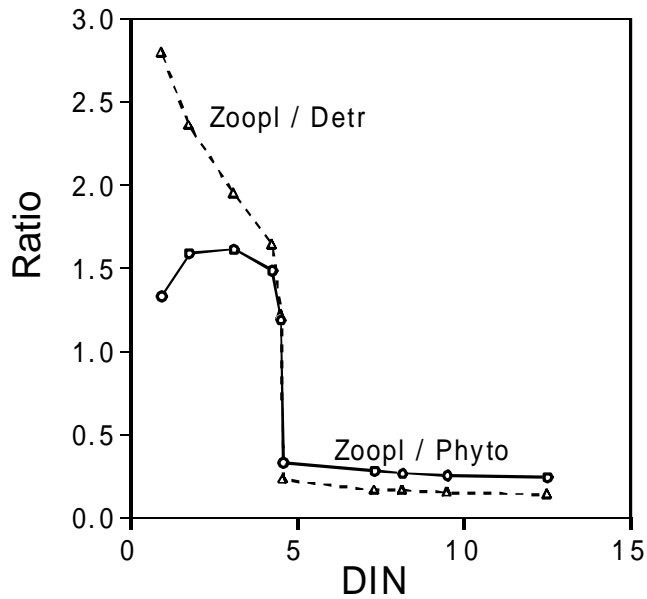


Fig. II-3. Variations in phytoplankton, zooplankton and detritus biomass (a) and production (b) with changes in nutrient loading to five-compartment pelagic ecosystem model (Fig. II-1d). Note the phase shift where DIN is approximately 7 μM .

A) Zooplankton Ratios



B) Phytoplankton / Detritus

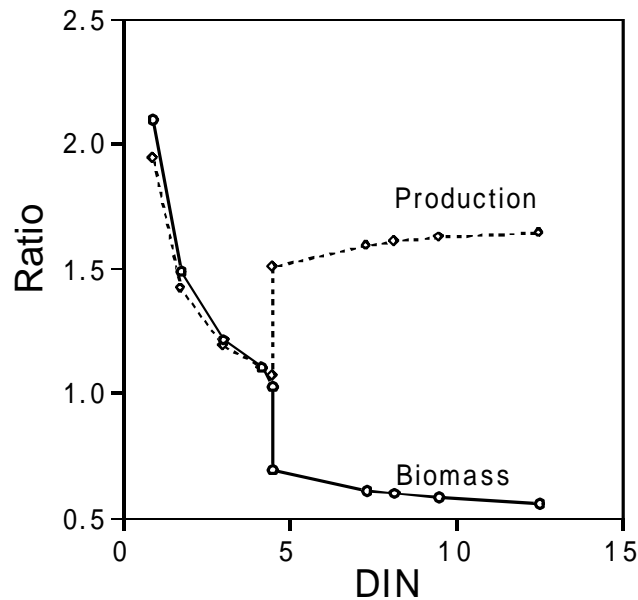


Fig. II-4. Variations in the biomass ratios of zooplankton/phytoplankton and zooplankton/detritus (a) and phytoplankton/detritus biomass and production (b) with changes in nutrient loading to five-compartment pelagic ecosystem model (Fig. II-1d). Note the phase shift at N approximately equal to 7 μ M.

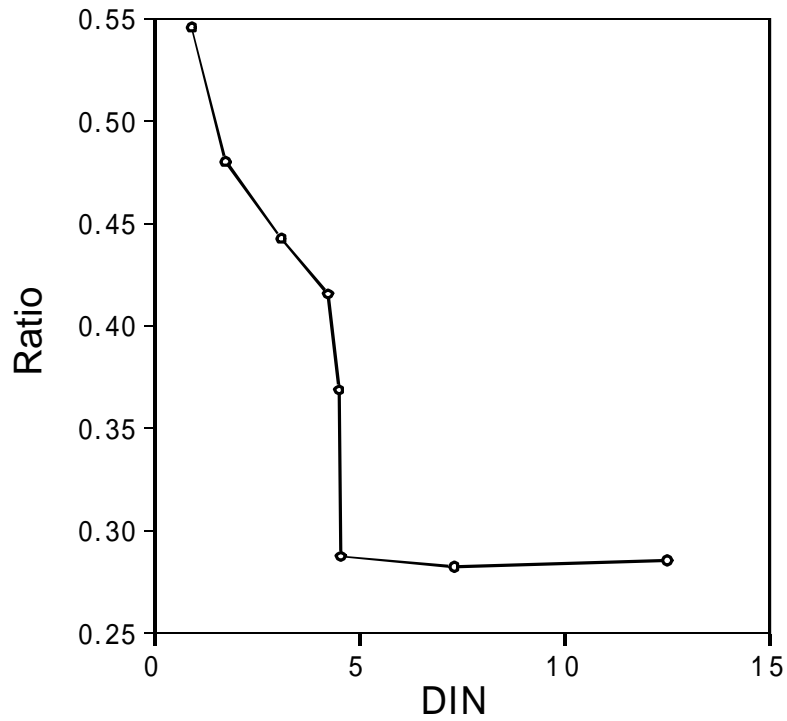


Fig. II-5. Variations in the ratio of external N-input to total flux of nitrogen input (external input + recycling) to N state variable with changes in nutrient loading from external sources to five-compartment pelagic ecosystem model (Fig. II-1d). Note the phase shift at N approximately equal to 7 μM .

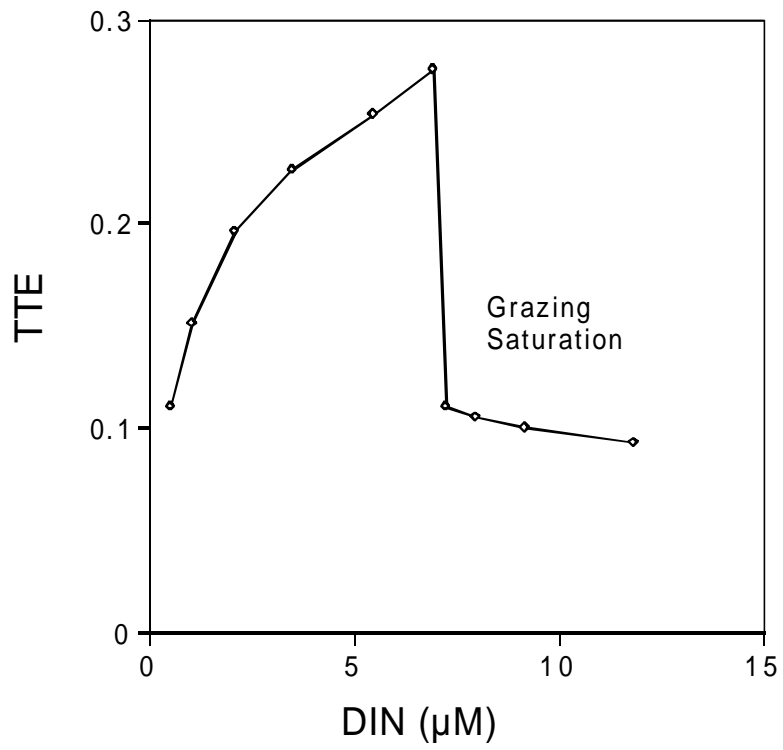


Fig. II-6. Variations in trophic transfer efficiency TTE with changes in nutrient loading to five-compartment pelagic ecosystem model (Fig. II-1d). Note the phase shift at N approximately equal to 7 μM .

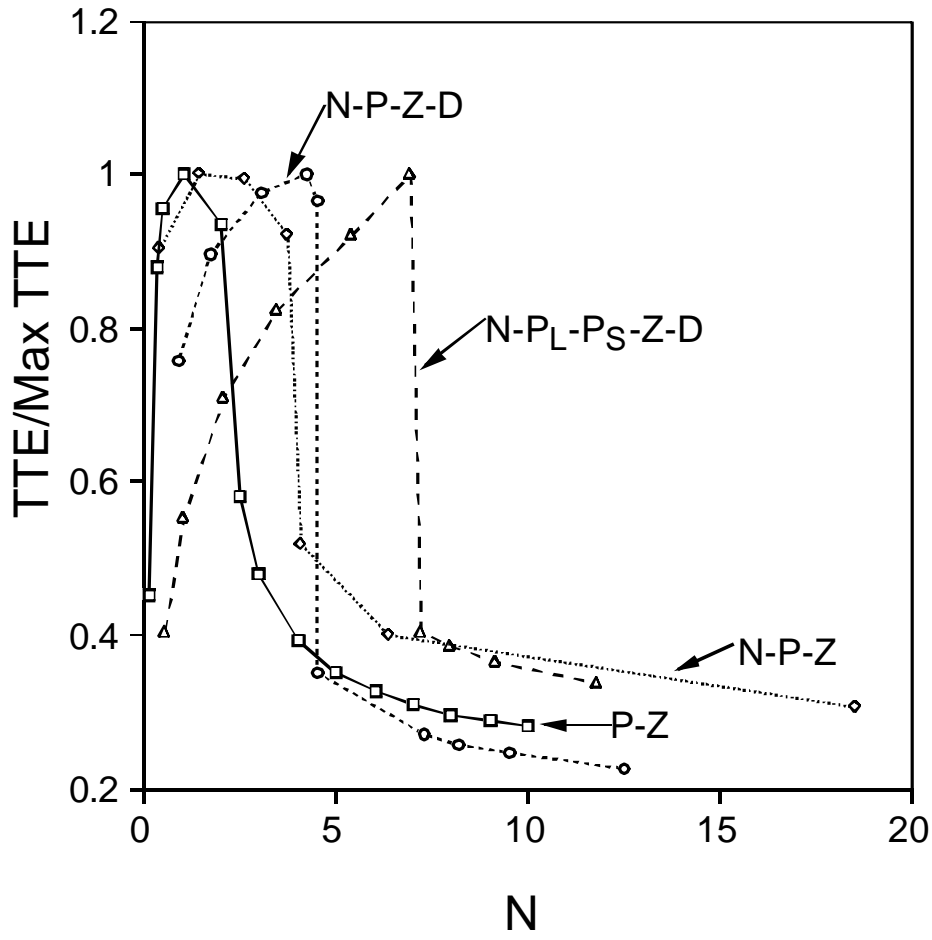


Fig. II-7. Effects of model complexity (Fig. II-1 a-d) on the relationship between trophic transfer efficiency (TTE) and nitrogen loading. Relationships are scaled to respective maximum TTE in each case for comparison; note that the phase shift point changes with model complexity.

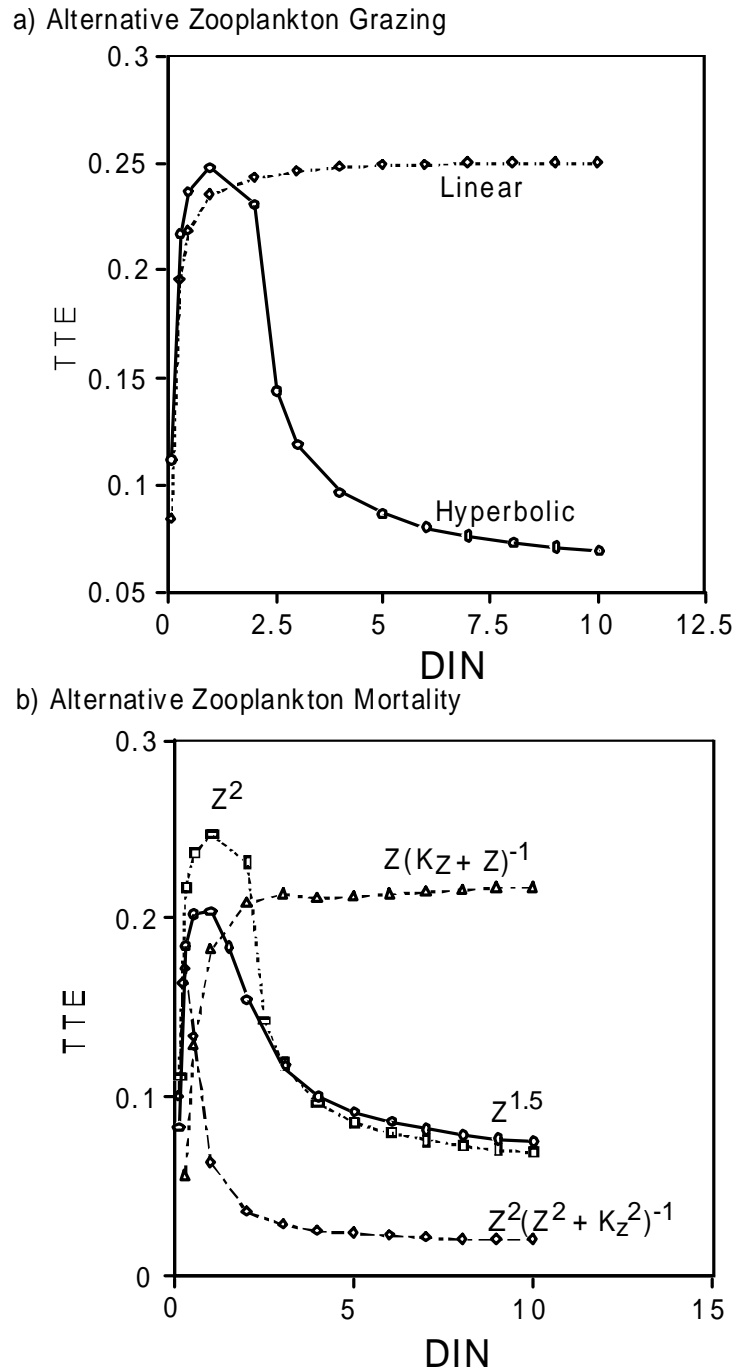
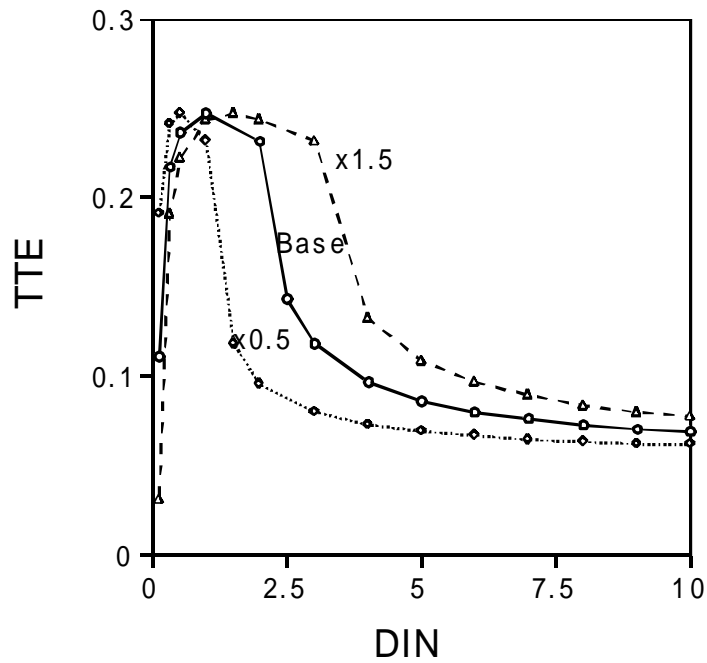


Fig. II-8. Effects of alternative zooplankton grazing equations (a) and alternative zooplankton mortality functions (b) on the relationship between trophic transfer efficiency (TTE) and nitrogen loading to two-compartment pelagic ecosystem model (Fig. II-1a). Note that the phase-shift disappears with linear grazing and hyperbolic mortality.

A) Half-Saturation of Phytoplankton on DIN



B) Half-Saturation of Zooplankton on Phytoplankton

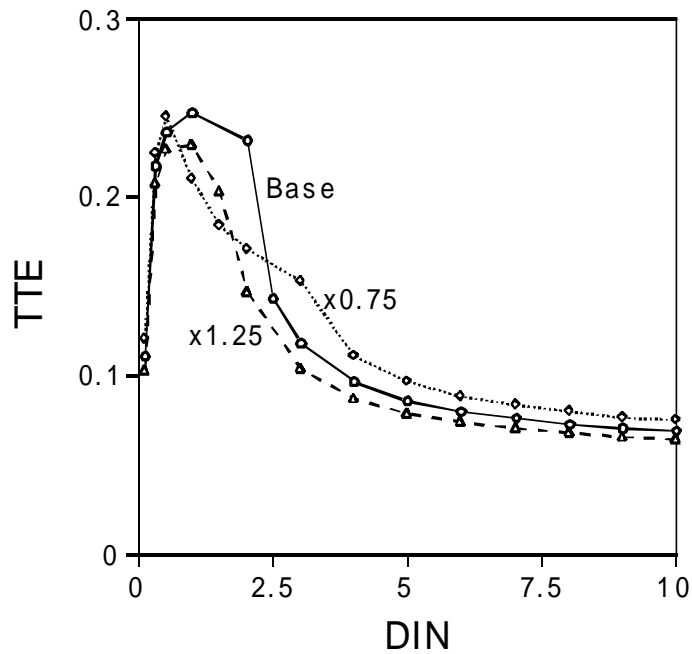


Fig. II-9. Effects of changing half-saturation coefficients for phytoplankton uptake of N (a) and zooplankton grazing on phytoplankton (b) for two-compartment pelagic ecosystem model (Fig. II-1a). Note that the phase-shift point changes with variations in half-saturation coefficients.

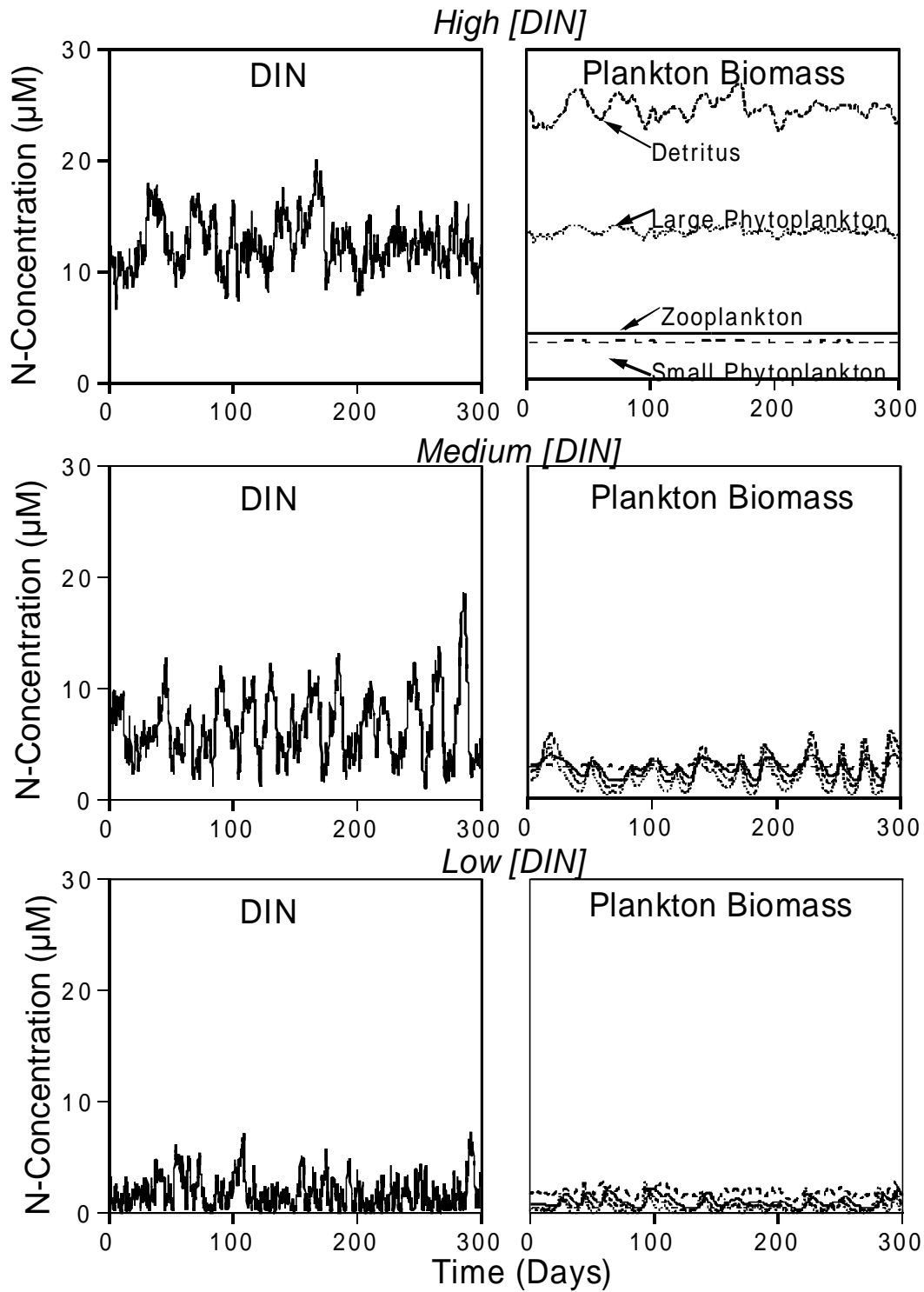


Fig. II-10. Time-course simulation of five-compartment pelagic ecosystem model (Fig. II-1d) under variable input conditions at: a) high; b) intermediate; c) low nutrient loading rates.

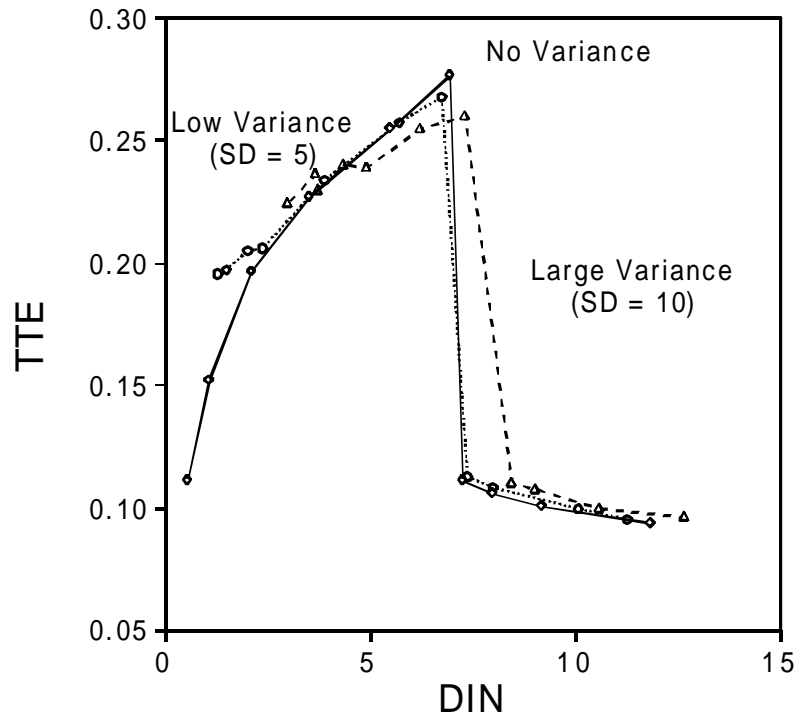


Fig. II-11. Variations in trophic transfer efficiency (TTE) with changes in nutrient loading to five-compartment pelagic ecosystem model (Fig. II-1-d) for conditions of no variance in N and low and high variance.

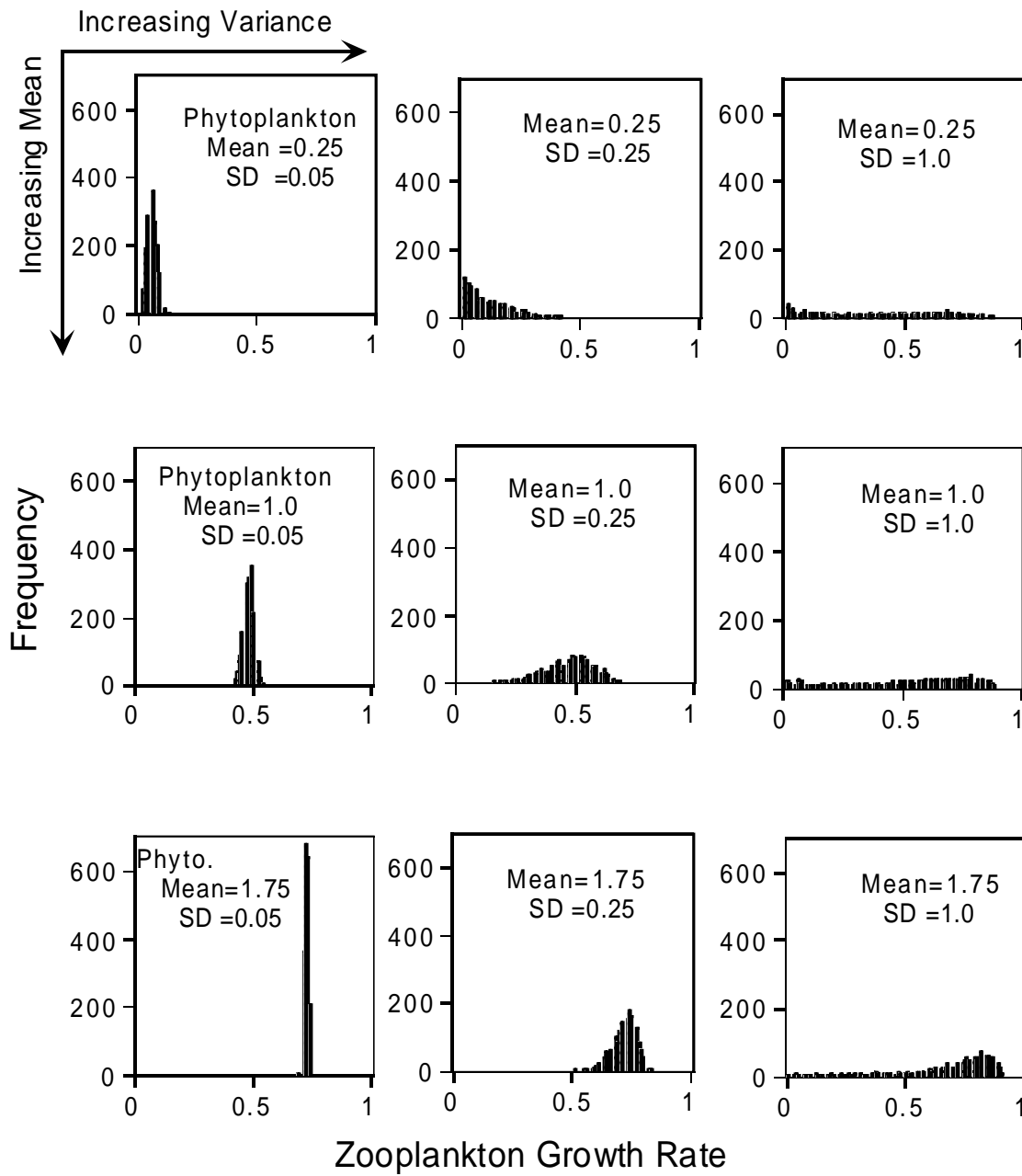


Fig II-12. Effects of changes in frequency distributions of phytoplankton (normal distributions with different mean and variances) on zooplankton growth using a Hollings Type III feeding function.

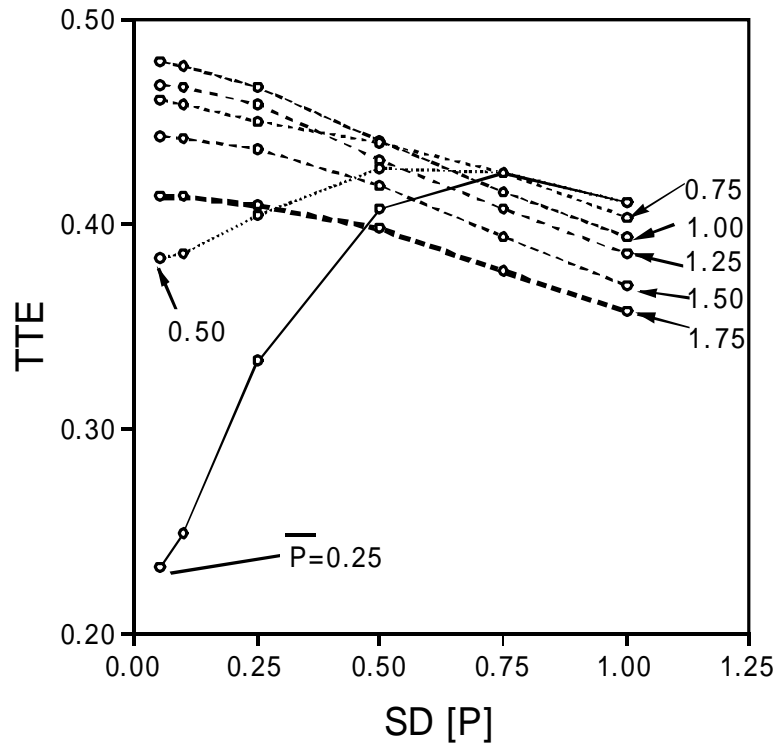


Fig. II-13. Summary of effects of variance in frequency distribution of phytoplankton food on trophic efficiency at which zooplankton grow on phytoplankton, considering interacting changes in mean and standard deviation of phytoplankton distributions.

Chapter III

Effects of Nutrients and Other Water Quality Variables on Submerged Aquatic Vegetation in Chesapeake Bay: Ecosystem Modeling Analyses

R.D. Bartleson, L. Murray, R.B. Sturgis and W.M. Kemp

Abstract

A numerical simulation model of an ecosystem associated with submerged aquatic vegetation (SAV) was formulated for several purposes: 1) to analyze and extrapolate mesocosm experimental results; 2) as a tool to conduct a dynamic assessment of habitat suitability for SAV growth at specific Chesapeake Bay sites using water quality monitoring data as inputs, and; 3) to investigate effects of water exchange rates and spatial distribution of SAV on plant-nutrient interactions. The model is used to examine, interpret, and extend mesocosm studies on nutrient effects at a range of nutrient supply rates and herbivorous grazer densities, as well as to examine the effect of initial concentrations and other variables. Simulation experiments revealed that the outcome of experimental nutrient additions could be largely controlled by the initial conditions, as well as biomass changes during the experiment. For example, high initial SAV biomass reduced light and nutrients available for algae, which prevented the overgrowth of algae at high nutrient addition rates. Model analysis showed that it is important to consider nutrient loading rate per unit plant biomass instead of concentration. Simulations of interactions between nutrient loading and trophic complexity showed little effect of grazers or fish at low nutrient addition and similar results with no grazers and with both grazers and fish. In the absence of grazers, SAV biomass responses to nutrient loading depended critically on water exchange rate. Grazers and fish could increase or decrease nitrogen cycling and retention depending on the nitrogen loading rate. A field calibrated version of the model was used to generate a tool for assessing SAV habitat suitability considering temporal variations in water quality conditions at specific Bay sites. The model successfully simulates inability of SAV to survive at a York River estuarine site with poor water quality conditions in spring but good conditions in summer. Dynamic simulations of SAV habitat suitability compare favorably with previously published static habitat criteria. Initial simulations of plant-nutrient interactions demonstrate the ability of plants to modify local nutrient conditions, and these mechanisms are placed in spatial calculations to demonstrate the importance of SAV bed patchiness and water residence time. Results demonstrate the diversity of uses for exploratory SAV ecosystem models in research and management applications.

Introduction

Many recent declines in abundance of seagrass and other submerged aquatic vegetation (SAV) populations world-wide have been attributed in part to nutrient enrichment (Orth and Moore 1983, Kemp et al. 1983, Lee and Olsen 1985, Twilley et al. 1985). Nutrients from agricultural runoff, sewage and other anthropogenic sources promote growth of epiphytic (Phillips et al. 1978, Harlin and Thorne-Miller 1981) and planktonic (Boynton et al. 1982) algae, which reduces light availability and consequently the growth rates of submerged plants (Short et al. 1995). In some environments, invertebrate grazing may effectively mitigate this effect of epiphyte overgrowth on SAV (Hootsmans and Vermaat 1985, Howard and Short 1986). However, the relative effectiveness of herbivorous grazing control on epiphytes tends to vary with season, region, and feeding mode of the grazer populations (Howard 1982; Brönmark 1985; Neckles et al. 1993). In addition, significant changes in the mortality of these grazers, which may result from predation or altered environmental conditions (e.g., Lubbers et al. 1990), can regulate the ability of grazers to control epiphyte growth. Ultimately, differences in trophic structure of the community associated with submersed plants can radically alter the plant responses to changes in nutrient levels.

Because of difficulties in determining the nutrient loading rate to a particular SAV bed in nature (e.g., Hemminga et al. 1991). Experimental ecosystems (mesocosms) have been widely used to study SAV ecosystem responses to nutrient loading and related environmental perturbations (e.g. Neckles et al. 1993, Twilley et al. 1985; Short et al. 1995; Sturgis and Murray 1997). Although most of these experiments demonstrate negative effects of nutrient enrichment on SAV, results have been variable (e.g., Burkholder et al. 1992; Taylor et al. 1995). These differences in experimental outcomes may be partially attributable to other factors such as: nutrient form and delivery mode, grazers abundance, seasonal timing, initial plant biomass, and water exchange rate.

Predicting effects of SAV on the ecosystem and of nutrients on SAV is difficult due to changing interactions of SAV with the water-column (hydrodynamics, and nutrients) across space. The magnitude of the interactions between SAV and the water column is related to the area of SAV coverage, and the volume exchanged, and most likely, the density and spatial pattern as well, since these may affect exchange and trapping. Submerged plant communities can reduce local nutrient concentrations when their biomass is high in relation to the volume of water that is exchanged with the adjacent system (e.g. McRoy and Barsdate 1970, Moore 1996). These local reductions in nutrients could result in reduced algal growth, and hence, improved conditions for SAV. Thus, it is imperative to consider the loading rate of nutrients per unit plant biomass when the impact of nutrients on SAV ecosystems is being investigated.

Extensive water quality monitoring programs in coastal ecosystems such as Chesapeake Bay provide a means by which the suitability of particular sites for SAV growth can be assessed (e.g., Batiuk et al. 1992; Dennison et al. 1992). In this case, statistical relationships between SAV presence and water quality conditions allow for water quality criteria to be generated to assess habitat suitability. Static calculations of habitat condition based on median values for these parameters are, however, limited in their ability to assess effects of short-term degradation of conditions in key seasons (e.g., Moore et al. 1996). What is needed is a numerical tool to make dynamic calculations of integrated SAV responses over the entire growing season for improved habitat assessment.

Numerical simulation models can be used to show the effects of nutrients on plant growth at a range of nutrient concentrations, supply rates and grazer densities. This can help elucidate the mechanisms involved in the nutrient/growth relationship, and produce better experimental designs and interpretations. Models can also be used to relate results from mesocosms experiments to field conditions. Several models of SAV production have examined responses to nutrient enrichment and grazing regulation of epiphyte growth (Wetzel and Neckles 1986; Kemp et al. 1995; Madden and Kemp 1996). These models have not simulated dynamics of the grazers themselves and feedback interactions among grazers, epiphytes and SAV. Spatially explicit SAV ecosystem models could also be used to examine effects of bed size, plant biomass and water exchange rates on plant-nutrient interactions. In principle, a numerical model could also be used to assess how variations in measured water quality conditions at a given site over a growing season affect the suitability of that site for SAV growth and survival.

Here we describe a revised numerical model of SAV ecosystems and demonstrate its use for three broad purposes: 1) to analyze and extrapolate mesocosm experimental results; 2) as a tool to conduct a dynamic assessment of habitat suitability for SAV growth at specific Chesapeake Bay sites using water quality monitoring data as inputs; 3) to investigate effects of water exchange rates and spatial distribution of SAV on plant-nutrient interactions.

Methods

Model Development

The model equations were developed from empirical relationships based on laboratory and field data from mesohaline Chesapeake Bay, other estuaries, and theoretical functions. The model structure is shown in Fig. III-1. The model was designed to track nitrogen (N), oxygen (O), and carbon (C) through the system's compartments. The model is structured around 19 state variables: SAV leaf C and N; SAV root C and N; SAV nonstructural C and N; epiphytic algae; benthic algae; phytoplankton; amphipods; fish; infauna; sediment labile organic

carbon; sediment refractory organic carbon; water column dissolved inorganic N; sediment porewater dissolved inorganic N; and dissolved oxygen. Data from mesocosm experiments (Sturgis and Murray 1997) were used to calibrate the model. The model used a time step of 15 minutes to capture diel effects of light on nutrients, production and respiration. Fourth order Runge-Kutta numerical integration was used.

The model simulations of mesocosm experiments were run at different inflow nutrient concentrations and exchange rates, with and without grazers, and maximum plant biomass was plotted. The model was also used to simulate plant-nutrient interactions in field conditions simulating mesohaline regions of Chesapeake Bay during the course of a growing season. Finally, the model was also configured to calculate SAV and epiphyte biomass and production using water quality data (nutrient concentrations, chlorophyll-*a*, total suspended solids, and light attenuation, K_d) as forcing functions to drive the model calculations.

Model Equations and Documentation

The structure of this model is similar to that described for previous simulation systems (Madden and Kemp 1996; Bartleson and Kemp 1991). A complete listing of the model equations and coefficients is provided in Appendix VI-A, and a brief description of the key model variables is provided below.

SAV Biomass; SL, SR and SC. SAV abundance was modeled as 3 compartments- Aboveground (*SL*), belowground (*SR*) and nonstructural carbohydrate (*SC*). Much of the model calibration is based on studies of the species, *Potamogeton perfoliatus*, in Chesapeake Bay. Carbon fixation by SAV was modeled as a function of light and nutrients. Maximum photosynthetic rate for SAV was 30 mg/g/h (Goldsborough and Kemp 1988). Limiting factors are modeled multiplicatively. The effect of light on maximum photosynthesis is calculated by using average I_k and K_m values (Harley and Findlay 1994, Goldsborough and Kemp 1988) of 350 and 150 $\mu\text{E m}^{-2} \text{d}^{-1}$. The effect of dissolved nitrogen on photosynthesis is modeled as a hyperbolic function of both sediment and water-column nitrogen with a K_s of 20 mg l^{-1} for sediment N and 14 mg l^{-1} for water-column N. Light available to the leaf is affected by water column attenuation, epiphyte coverage, macroalgae shading, and self-shading. Epiphyte shading is biomass specific (a coefficient of 0.11 /mgC/mg leaf C is used, which is from 0.15/ $\mu\text{g chl/cm}^{-2}$, 5 $\mu\text{g chl/mg ep C}$, and 3.7 $\text{cm}^2/\text{mg leaf C}$). Light attenuation due to epiphytic biomass is variable, so an ballpark value of 3/mg C/cm² (Staver, others) is used. This converts to 3.7/mgC/mg leaf C (@.75mg C/cm²). Since a portion of the photosynthetic area of the plants may not be covered, this number is reduced. Self-shading is estimated from the attenuation of leaves. Losses of leaf biomass include terms for plant respiration and senescence. The effect of temperature on respiration is assumed to be exponential with a Q_{10} of 2. The non-structural carbon pool is allocated to above or below-ground biomass depending on the existing biomass ratio. Root loss is due to

respiration and senescence. The effect of grazers is assumed to be negligible when grazers were excluded. If grazers were added, allometric relations were used to estimate grazing rates (Cattaneo and Mousseau 1995).

Phytoplankton, PO; Epiphytic Micro & Macroalgae, EP & MA. Algal carbon fixation was modeled as a function of temperature, light, and nutrients. The effect of temperature is assumed to be exponential with a Q_{10} of 2. This formulation (Kremer and Nixon 1978) is supported by several published values (Fasham et al. 1983, Bannister 1974). Maximum growth rates and temperature coefficients for algae were calibrated within the range of reported values (e.g., Talling 1957, Eppley 1972, Ojala 1993). The effect of light on maximum photosynthesis was calculated using the formulation of Talling (1957) modified for the effect of self-shading. Effects of dissolved inorganic nitrogen on photosynthesis was modeled as a hyperbolic function with a K_s of 10-30 mg m^{-3} (e.g., Goldman and Glibert 1983; Scavia 1980). Algal losses occur due to respiration, sinking, exudation, natural mortality, and export. Respiration is modeled as a function of temperature (Scavia et al. 1976), biomass and production. Reported specific respiration rates range from 0.02 to 1.2 d^{-1} (Geider 1992), or about 10% of P_{max} (Parsons et al. 1984).

Benthic Algae, AB. Benthic algal production is controlled by PAR, temperature, and N availability. Maximum growth rate is assumed to be 1/day (see phytoplankton). PAR is absorbed in the water column by phytoplankton and sediments and self-shading occurs at the sediment surface. The light half-saturation coefficient is assumed to be lower than for phytoplankton (Cahoon et al. 1993). Ammonium uptake is assumed to be from the sediments. Krom (1991) found that sediment uptake of ammonia-N was primarily from organic matter breakdown in the sediments. The nitrogen half-saturation coefficient is assumed to be the same as for phytoplankton. Outputs are to respiration and sediment organic carbon, where consumption by microorganisms, meiofauna and deposit-feeders occurs. Output to organic carbon is assumed to be an exponential function of biomass as well as a percentage of production.

Consumer Populations, AM & FI. Herbivorous and carnivorous animal variables were simulated using gammarid amphipods and killifish, respectively, as model organisms. Grazer concentrations used were in the mid-range (1.5 g C/tank) of those reported from shallow-water systems (e.g. Virnstein et al. 1983, Kemp et al. 1983). Individual amphipods in mesocosms were at least 7mm long at the beginning of the experiment. They were modeled in terms of their biomass for simplicity and to maintain bioenergetic consistency. Ingestion was modeled as a function of epiphyte and SAV biomass, and an allometric function of average amphipod size. Outflows are to respiration, excretion, and mortality. Respiration and excretion are linear functions of ingestion. Mortality was both natural and due to predation by fish if present. The killifish, *Fundulus heteroclitus*, was modeled based on animals of about 10g wet weight. In the mesocosm experiments, fish were allowed to feed in tanks for 4-8 hours/week in the fish treatments. Their

effect was, however, modeled as a bioenergetically equivalent continuous feeding by fewer fish (smaller biomass). Ingestion was a function of prey density. Outflows are to respiration and excretion. Respiration and excretion are linear functions of ingestion.

Dissolved nitrogen, NW. Dissolved inorganic nitrogen (DIN) in this model includes NH_4^+ , NO_3^- , and NO_2^- . Inflows to dissolved inorganic nitrogen are from the header tank and regeneration. Regeneration is a percentage of all except phytoplankton respiration terms and fish. NW was assumed to be regenerated at a ratio of 106C:16N. This ratio may be high; for example, the C:N ratio of copepods is higher than that of phytoplankton so they must be conserving N relative to C. The C:N ratio of organic state variables and flows except for phytoplankton respiration are assumed to be 6.625:1. Respiration of bacteria is coupled to N regeneration to keep a balance, although at high C:N ratios (>15:1), ammonium was not regenerated from natural assemblages of freshwater bacteria (Tezuka 1990). N excreted by predators (fish, ctenophores, crabs, etc.) is assumed to be 30% of ingestion (Purcell 1992). Mixing (described below) can result in a significant transfer of NW to the upper layer in the summer. Measured regeneration rates as high as $154 \text{ mg N m}^{-3} \text{ d}^{-1}$ (Bronk and Glibert 1993) are about twice as high as maximum values obtained in the model ($85 \text{ mg m}^{-3} \text{ d}^{-1}$). These rates are also measured in full light, representative of the surface layer, not the entire euphotic zone or a 24 hour average. The loss terms include outflow and uptake by autotrophs. Autotrophs take up NW in proportion to the amount of carbon fixed. Redfield's ratio (106C:16N) is used for the proportionality constant for algae and higher empirically measured ratios were used for SAV.

Dissolved oxygen, OW. Inflow to dissolved oxygen is from diffusion and phytoplankton production. Atmospheric diffusion is a function of the concentration difference, salinity and temperature (see Kemp and Boynton 1980). A photosynthetic quotient of 1.3 (Valiela 1984) is used as the ratio for oxygen produced per carbon fixed. Outflow is to water-column respiration, sediment oxygen demand, and diffusion. Flows are in stoichiometric relation to carbon flows (using an RQ of 0.9). The molar ratio for sediment carbon oxidation is 138:106 or 3.47 to 1 by mass (Valiela 1984). The oxidation of HS^- requires 2 moles of O_2 . Diffusion to the sediments is based on the difference between water column and sediment concentrations. A hyperbolically increasing proportion of sediment oxygen demand is derived directly from the water column as sediment oxygen concentration decreases. Oxygen units are mg l^{-1} .

Results and Discussion

Model Calibration and Validation

Simulation output from this model matched reasonably well the observed patterns for dissolved oxygen and dissolved inorganic nitrogen from mesocosm

experiments (Fig. VI-2). Simulated community production and respiration, as well as SAV growth rate and biomass, were comparable with mesocosm experimental data, but measured biomass of epiphytes and grazers diverged from model results. The model predicted that grazers would control epiphyte biomass in the high-grazer treatment and that epiphyte biomass would be higher in the low-grazer treatment. The measured epiphyte biomass was, however, not significantly different among treatments. Subsequent analyses suggest that discrepancy resulted from grazer-enhanced phosphorus recycling, which stimulated growth of inedible N-fixing epiphytic blue-green algae. Phosphorus was not explicitly included in this model. Other studies have reported blue-green algae dominating experimental epiphytic algal community in the presence of (Neckles et al. 1994). Including blue-green algae and phosphorus in future versions of the model would increase the model's ability to capture these processes.

Sensitivity Analysis and Initial Conditions

Responses of SAV leaf biomass to variations (by +50%) in selected parameter settings were examined for a medium-nutrient (with grazers) model (Fig. VI-3). There was a wide range of sensitivities of SAV biomass to coefficient variations from zero to 190% change. The lack of SAV response to increased DIN is attributable to the fact that SAV and epiphyte responses were already saturated at medium nutrient treatment (DIN = 17 μM) at the relatively high water exchange rates ($> 10 \text{ d}^{-1}$) used in this analysis (Fig. VI-4). This model simulation experiment led us to modify the water exchange rates used in subsequent mesocosm experiments. The SAV biomass was most sensitive to factors affecting growth rate, such as epiphyte growth or loss rates.

Model simulations also indicate that SAV response to nutrient additions is highly dependent on initial conditions prior to experimental treatment (Fig. VI-5). When initial epiphyte biomass was relatively large SAV biomass declined after 2 wk and did not start to recover until 8-10 wk into the experiment (Fig. VI-5, left panels). Epiphytic micro- and macro-algal growth reduced nutrients and shaded the SAV when no grazers were present. Amphipod grazers were able to keep the algae under control, however, if present in sufficient numbers. Under conditions of relatively high initial SAV temporal dynamics were different (Fig. VI-5, right panels). High SAV biomass reduced the available nutrients and light resulting in slower algal growth even when grazers were absent. These simulation experiments demonstrate the importance of using the model in the designing empirical mesocosm experiments. If the experiment was started with a high SAV biomass, nutrient input would have to be adjusted upwards to stimulate the epiphytes and have any grazing effect.

Effects of Grazing and Predation

Simulation studies indicated that grazers can significantly increase or decrease SAV response to nutrient enrichment and retention of nitrogen (Fig. VI-6 d, e, f) in an SAV ecosystem. These results are attributable to the stimulating effect of grazers on SAV primary production, through nutrient regeneration and removal of epiphytic algal biomass and associated light attenuation. When producer biomass is sufficiently high, much of the total nutrients in the system are tied up in plant tissues, and increased nutrient cycling and enhanced primary production tends to reduce the rate of nutrient outflow from the SAV bed. Adding fish, however, increased (Fig. VI-6 e, f) nitrogen cycling with moderate nutrient addition and decreased (Fig. VI-6 h and i) nitrogen cycling with high nutrient addition. Results were dependent on grazing rates and other factors. For example, when grazing rate was reduced under the moderate nutrient treatment with grazers (Fig. VI-6 e), epiphyte biomass remained high, such that responses of SAV and other components appear more like those predicted in the fish addition scenario (Fig. VI-6 f). In these mesocosm experiments, oxygen measurements allowed an estimate of community production and respiration, which were also computed by the model. Though the compartmentation can only be estimated, the total measured oxygen change correlated well with the modeled change.

Overall, the model was able to reproduce the experimental results on how trophic complexity (herbivorous grazing and predation on herbivores) altered SAV responses to nutrient addition. The modeled SAV growth rate compared reasonably well with data from the three treatments, control, grazer and grazers with fish (Fig. VI-7). The model simulation experiments do not support the hypothesis that fish predation will reduce grazers enough to increase the epiphyte load and decrease SAV production. Experimental results also failed to support this hypothesis, but they may have been complicated by experimental artifacts. Fish predation rates used in the model were based on limited data and may have been different in the mesocosms where the fish may behave differently. In the experiment, the fish were seen constantly preying on amphipods- and burrowing in the sediments.

SAV-Nutrient Interactions: Biomass, Exchange Rate, and Spatial Patterns

When SAV biomass is sufficiently high and water residence times sufficiently low, plant uptake of nutrient inputs can strongly reduce epiphyte growth. High plant biomass allows SAV to assimilate nutrient inputs and thereby maintain local concentrations low enough to preclude extensive epiphyte growth (Fig. VI-5, right panels). This drawdown of nutrients is a function of nutrient loading rate per unit plant biomass. At high biomass to loading ratios, significant reductions in nutrients can occur that can influence plant and algal growth. Since submersed plants can generally obtain much of their nutrients from the sediments,

they may out-compete epiphytic algae and phytoplankton, and experience enhanced light availability in the process. The ability of SAV to reduce local nutrient concentrations via uptake is also dependent on water exchange rates responsible for nutrient inputs and export. In the absence of grazers, SAV biomass actually increases with nutrient enrichment at relatively low ($< 2 \text{ d}^{-1}$) flushing rates (Fig. VI-4, lower panel). When water exchange rates are low enough, nutrients can be drawn down by SAV, especially when plant biomass is high.

The interior regions of SAV beds with relatively high plant biomass and low water exchange rates may experience drastically lower nutrients than in the external water entering the bed (e.g. Moore 1996). This interaction is illustrated in a simulation experiment (Fig. VI-8), where nitrogen concentrations are substantially reduced inside the bed over the course of the growing season (upper panel), and this effect is directly related to SAV biomass (lower panel). The difference between concentrations in day and night emphasizes the importance of photosynthetically driven nutrient assimilation as the mechanisms responsible for this effect. Hence, production of other autotrophs (epiphytic alga, phytoplankton) will be reduced if nutrients are decreased below saturating levels, and continued algal growth will become more dependent on nutrient recycling (e.g. Mullholland et al. 1992). Most SAV species obtain much of their nutrients from the sediments (e.g. Thursby and Harlin 1984), so dissolved nutrients in the overlying water are not as important for sustaining their growth. The theoretical basis of these dynamics are described in Appendix VI-B.

Spatial distributions of SAV beds will also alter these interactions between SAV and water column nutrients. This can be illustrated by placing a simple SAV-nutrient model into a spatial array, which allows for water and material exchange between adjacent cells through advective and diffusive processes, and for movement of organisms between cells. As an initial step toward developing a fully dynamic spatial SAV simulation system, we have set up a simple spatial array to compute nutrient concentrations in different hypothetical spatial arrangements. Example output from this computation is presented here (Fig. VI-9), contrasting spatial distributions of nutrient (DIN) concentration associated with one large SAV bed versus 15 small SAV patches, both occupying 60 of 120 cells in the spatial grid. This highly simplified calculation, with first-order nutrient uptake in SAV beds and constant 2-D turbulent diffusion, illustrates a 60% increase in mean DIN concentration over SAV cells for the patchy configuration compared to the homogeneous bed (Fig. VI-9). We anticipate that complex interactions among plants, epiphytes, phytoplankton, nutrient, light levels, and grazers, will produce highly non-linear dynamics in future versions of this spatial SAV model.

Dynamic Calculations of SAV Habitat Suitability

During the 1997-1998 project, we modified an existing SAV ecosystem dynamic simulation model for use in assessing habitat suitability. This model was

calibrated and verified with field and mesocosm data, and it was used to generate a closed-form relation between nutrient concentration (DIN, DIP) and biomass of epiphytic algae on SAV leaves. This output was combined with two empirical relations: 1) biomass-specific light attenuation vs. composition ratio of epiphytic material (chl_a/dry wt); 2) epiphyte composition ratio (chl_a/dry wt) vs. TSS in water column. A habitat-assessment model was developed as a spread-sheet computation based on these relations; this model is being used for assessing SAV habitat conditions (in terms of light available to support SAV growth) from data collected in the Bay monitoring program. This effort is described in our 1998 Final Report (Kemp et al. 1998). One problem with this model is that it is a static computation based on median values for monitoring data collected during the SAV growing season (Apr-Oct), and it does not consider dynamic interactions. It assumes that as long as average light conditions are above acceptable minimum values that the habitat is suitable for SAV growth. This approach assumes that the relations between light-photosynthesis and plant growth are all linear. There is growing evidence that these may be poor assumptions (e.g, Moore 1996).

We have, thus, incorporated existing empirical relations, which describe TSS effects on epiphyte mass and associated light attenuation, into the dynamic model computation. Model simulations are driven by water quality variables measured at fortnightly intervals in the monitoring program. We have used a field calibrated version of this model (e.g., Madden and Kemp 1996) to simulate seasonal variations in SAV and epiphyte biomass in relation to light, temperature and monitoring data on water quality conditions (DIN, DIP, TSS, Chl-*a*, K_d). This model also incorporates an empirical equation relating K_d to concentrations of TSS and Chl-*a* (Gallegos, 1999. SAV Technical Synthesis Report, EPA). To establish a baseline for comparison (TS2), the model was run with water quality variables set at constant values equal to the habitat criteria (Batiuk et al. 1992; Dennison et al. 1992). Sensitivity analyses (Fig. VI-10) revealed that the model is responsive to variations in DIN (or DIP) and particularly to total suspended solids (TSS) from the TS2 conditions. Although epiphyte biomass changed dramatically with variations in DIN, the corresponding changes in SAV biomass are muted. Responses of both SAV and epiphytes to TSS were strong, with a doubling of TSS (= 30 mg/l) above TS2 resulting in no survival of SAV or epiphytes. Although doubling of nutrients causes a tripling of epiphyte biomass, SAV biomass declined by only 10%. A 50% reduction in TSS resulted in increases in both SAV and epiphytes.

As a calibration exercise and demonstration of the model's potential utility, simulation experiments were conducted for two well-studied sites in the York River estuary (Moore 1996). Mean water quality conditions at the first of the York River sites, Clay Banks, are slightly poorer than mean conditions at the second site, Guinea Marsh. However, although SAV do not survive at Clay Banks, water quality conditions at both sites meet the SAV habitat criteria limitations (Moore 1996). At Clay Banks there is a characteristically strong pulse of turbid water in May-June, and it has been hypothesized that the inability of

SAV to grow at this site, despite reasonably good mean (and median) water quality conditions, may be because this spring turbidity pulse coincides with a critical period for SAV growth (Moore 1996). The simulation experiment revealed that, while modeled SAV growth at Guinea Marsh was robust, SAV could not survive at Clay Banks based on the water quality conditions monitored at these sites. Although light conditions at the plant leaf (PLL) ranged between 8 and 20 % of surface irradiance at Guinea Marsh, values declined to less than 5% for more than a month in late spring (Fig. VI-11, lower panel). These results are promising and may deserve further investigation as to the applicability of this approach for assessing SAV habitat suitability at diverse sites around the Bay.

This chapter illustrates a range of applications of exploratory SAV ecosystem modeling in addressing both research and management questions. Model experiments demonstrate the response of SAV to changes in nutrient inputs depends on plant biomass and bed spatial configuration, as well as on water exchange rates. Simulation studies also illustrate the importance of trophic interactions in modifying plant-nutrient interactions. Presumably, the mechanisms from which these results are derived also exist in the Chesapeake Bay water quality model (Cercio and Cole 1993), and it would be useful to investigate these dynamics in the larger computation platform. A field calibrated version resulted in a tool for assessing SAV habitat suitability considering temporal variations in water quality conditions at specific Bay sites. These results are encouraging and suggest that further exploratory modeling studies would continue to provide analyses that effectively will improve interpretation of monitoring data and large-scale modeling output.

Appendix VI-A. Documentation for SAV Model

Potamogeton perfoliatus; SL, SR and SC

SAV abundance was modeled as 3 compartments- Aboveground (SL), belowground (SR) and nonstructural carbohydrate (SC). Most of the model calibration is based on studies of *wasPotamogeton perfoliatus* in Chesapeake Bay. Carbon fixation by *P. perfoliatus* was modeled as a function of light and nutrients. Maximum photosynthetic rate for *P. perfoliatus* was 30 mg/g/h (Goldsborough and Kemp 1988). Limiting factors are modeled multiplicatively. The effect of light on maximum photosynthesis is calculated by using average I_k and K_m values (Harley and Findlay 1994, Goldsborough and Kemp 1988) of 350 and $150 \mu\text{E m}^{-2} \text{d}^{-1}$. The effect of dissolved nitrogen on photosynthesis is modeled as a hyperbolic function of both sediment and water-column nitrogen with a K_s of 20 mg l^{-1} for sediment N and 14 mg l^{-1} for water-column N. Light available to the leaf is affected by water column attenuation, epiphyte coverage, macroalgae shading, and self-shading. Epiphyte shading is biomass specific (a coefficient of $0.11 \text{ /mgC/mg leaf C}$ is used, which is from $0.15/\mu\text{g chl/cm}^{-2}$, $5 \mu\text{g chl/mg ep C}$, and $3.7 \text{ cm}^2/\text{mg leaf C}$). Light attenuation due to epiphytic biomass is variable, so an ballpark value of $3/\text{mg C/cm}^2$ (Staver, others) is used. This converts to $3.7/\text{mgC/mg leaf C}$ (@.75mg C/cm²). Since a portion of the photosynthetic area of the plants may not be covered, this number is reduced. Self-shading is estimated from the attenuation of leaves

Losses of leaf biomass include terms for plant respiration and senescence. The effect of temperature on respiration is assumed to be exponential with a Q_{10} of 2. The non-structural carbon pool is allocated to above or below-ground biomass depending on the existing biomass ratio. Root loss is due to respiration and senescence. The effect of grazers is assumed to be negligible when grazers were excluded. If grazers were added, allometric relations were used to estimate grazing rates (Cattaneo and Mousseau).

Algal Components - Phytoplankton; PO, Epiphytic Mass; EP, Macroalgae; MA

Algal carbon fixation is modeled as a function of temperature, light, and nutrients. The effect of temperature is assumed to be exponential with a Q_{10} 2. This formulation (Kremer and Nixon 1978) is supported by several published values (Fasham et al. 1983, Bannister 1974). Enzyme inhibition is known to occur at high temperatures among single species, but we assume that it does not occur among the whole assemblage of phytoplankton at the normal summer temperatures. Although the photosynthesis-temperature relationship is based on short term response, since phytoplankton size varies inversely with temperature (Malone et al.1991), there is an allometric basis for this formulation. The phytoplankton community could also adapt to the seasonal change in temperature and may be independent of temperature (Sheridan and Ulik 1976, Davison 1987). Maximum growth rates and temperature coefficients for PO are calibrated within the range of reported values (Talling 1957, Eppley 1972, Ojala 1993, etc.).

The effect of light on maximum photosynthesis is calculated by using the formulation of Talling (1957) modified for the effect of self-shading. The half saturation coefficients are averages of measured values in spring and summer. The Talling expression doesn't incorporate photo-inhibition and photo-inhibition is not a factor in the microcosms. An attenuation coefficient for self-shading of 0.002 per mg phytoplankton C is used (Steeman-Nielsen 1962). The effect of dissolved nitrogen on photosynthesis is modeled as a hyperbolic function with a K_s of 10 mg m⁻³ for PO (Goldman and Glibert 1983 obtained a K_s value of 0.5 μM or 7 μg l⁻¹) and 30 mg m⁻³ for PD (Scavia 1980). Diatom growth is additionally controlled by silica concentrations (forcing function) with a K_s of 0.2 μm (Conley and Malone 1992). Inputs of phytoplankton are determined by assuming a ratio of 70 mg C mg Chl⁻¹ (Malone 1982).

Phytoplankton losses occur due to respiration, sinking, exudation, natural mortality, and export. Respiration is modeled as a function of temperature (Scavia et al. 1976), biomass and production. Reported specific respiration rates range from 0.02 to 1.2 d⁻¹ (Geider 1992), or about 10% of P_{max} (Parsons et al. 1984). Respiration rates of flagellated species may be quite high relative to the diatoms due to their active nature (Geider and Osbourne 1989). Grazers of phytoplankton include copepods, protozoa, and menhaden. Copepods preferentially graze diatoms and while protozoans prefer other algal taxons (Burkhill et al. 1987) they still ingest significant amounts of diatoms. The model assumes that copepods prefer diatoms 5 to 1 over PO. Copepod grazing loss includes a percentage due to 'sloppy feeding'. Menhaden biomass is a forcing function peaking at 50 mg C m⁻³ in November (Brandt 1992) and consuming from 5 to 40% of their weight per day depending on temperature. Sinking is a percentage of biomass. Sinking rates of phytoplankton assemblages are determined by their composition (Pitcher et al. 1989), with diatoms sinking faster than dinoflagellates and microflagellates. Although sinking rates of individual diatoms are usually less than 1 m d⁻¹, gelatinous aggregations formed may sink 100 m d⁻¹ or more (Smetacek 1985). PD sinking rate of 0.3 d⁻¹ is assumed in the upper layer and 0.15 d⁻¹ in the lower water column to adjust for greater specific gravity. Silica limitation is assumed to increase sinking rates of diatoms. Culver and Smith (1989) found increased sinking rate with decreased nitrate concentrations. PO are assumed to sink more slowly than PD (0.2 in the upper layer, and 0.1 in the lower layer). Phytoplankton DOC release was significantly correlated (slope of 0.15) with production (Malone et al. 1991). Other measurements showed rates ranging from 0 to 15% of biomass (Eppley and Sloan 1965, Sellner 1976). Death, or density dependent mortality is an exponential function of biomass. Viral infection rates may increase with density (Sieburth et al. 1988).

Bacterioplankton; BP

Growth of bacterioplankton is a function of CD, NW, OW and temperature. Although assimilation rates of 1.2 g C g C⁻¹ h⁻¹ have been measured (Wetzel and Christian 1984), specific production in the bay ranges from 0.5 to 2

per day (Ducklow and Hill 1985). Production ranged from 52 to 680 mg C m⁻² d⁻¹ from September to November 1984. The Monod formulation is used and expresses growth as a function of dissolved and particulate organic matter. K_s values of eutrophic bacteria ranged from 112 mg C m⁻³ to over 100 g C m⁻³ for glucose (Semenov 1991 for review) which may be about the same as phytoplankton derived dissolved organic carbon (DOC). No good estimates are available for naturally occurring organic matter. V_{max} for glucose uptake ranged from 78 μ g to 50 g l⁻¹ (Semenov 1991). The effect of CD on growth depends on the percentage of CD that is derived from phytoplankton. The equation for uptake adjusts the rate depending on the percentage derived from phytoplankton exudation. Nitrogen does regulate DOM uptake however. The K_s for NW is assumed to be 2 mg m⁻³. Wheeler and Kirchman (1986) documented the uptake of dissolved nitrogen by bacterioplankton. The effect of temperature on uptake is exponential, with a Q_{10} of 2.7 (Shiah 1993). The percentage of bacterioplankton that are active is also affected by temperature (Mann and Hoppe 1978). The effect of NW and O₂ on growth are assumed to be hyperbolic. The K_s for O₂ is possibly below 0.2 (Shiah and Ducklow 1994) though 1 is used in the model.

Outflows include respiration, lysis and excretion, grazing and sedimentation of bacteria attached to detritus. Respiration is modeled as a linear function of uptake (Azam et al. 1983) and to a lesser degree a function of biomass and temperature. Respiration is not modeled solely as a function of biomass due to the ability of some species to survive long periods of starvation (Novitsky and Morita 1978). The affect of temperature on respiration may vary significantly and depend on substrate concentration (Pomeroy et al. 1991). We chose to use a small value that allowed biomass to increase with temperature, and to ensure an adequate food supply for protozoans. Lysis is modeled as an exponential function of biomass to account for density dependent mortality. Proctor and Fuhrman (1990) reported that 60% of the mortality of bacterioplankton in coastal and open ocean environments may be due to viruses. Phages lysed 2 to 24% of the bacterial population per hour in waters off Denmark (Heldal and Bratbak 1991). Excretion rates are negligible (Azam et al. 1983) so a small percentage (0.05 d⁻¹) of biomass is assumed to be lost. Sedimentation is a linear function of biomass and CP.

Amphipods AM

Grazer concentrations used were in the mid-range (1.5 g C/ tank) of those reported from shallow-water systems (e.g. Virnstein et al. 1983, Kemp et al. 1983). Gammarid amphipods were used as the model grazer. Individuals were at least 7mm long at the beginning of the experiment. They were modeled as biomass for simplicity. Ingestion was modeled as a function of epiphyte and SAV biomass, and an allometric function of average amphipod size. Outflows are to respiration, excretion, and mortality. Respiration and excretion are linear functions of ingestion. Mortality was both natural and due to predation by fish if present.

Fish FI

Fundulus heteroclitus of about 10g wet weight were used for 4-8 hours/week in the fish treatments. Their effect was modeled as a continuous function of a smaller biomass. Ingestion was a function of prey density. Outflows are to respiration and excretion. Respiration and excretion are linear functions of ingestion.

Dissolved nitrogen; NW

Dissolved nitrogen includes NH_4^+ , NO_3^- , and NO_2^- . Inflows to dissolved nitrogen are from the header tank and regeneration. Regeneration is a percentage of all except phytoplankton respiration terms and fish. NW is assumed to be regenerated at a ratio of 106C:16N. This ratio may be high; for example, the C:N ratio of copepods is higher than that of phytoplankton so they must be conserving N relative to C. The C:N ratio of organic state variables and flows except for phytoplankton respiration are assumed to be 6.625:1. Respiration of bacteria is coupled to N regeneration to keep a balance, although at high C:N ratios (>15:1), ammonium was not regenerated from natural assemblages of freshwater bacteria (Tezuka 1990). N excreted by predators (fish, ctenophores, crabs, etc.) is assumed to be 30% of ingestion (Purcell 1992). Mixing (described below) can result in a significant transfer of NW to the upper layer in the summer. Measured regeneration rates as high as $154 \text{ mg N m}^{-3} \text{ d}^{-1}$ (Bronk and Glibert 1993) are about twice as high as maximum values obtained in the model ($85 \text{ mg m}^{-3} \text{ d}^{-1}$). These rates are also measured in full light, representative of the surface layer, not the entire euphotic zone or a 24 hour average.

The loss terms include outflow loss and uptake by autotrophs and bacterioplankton. Phytoplankton take up NW in proportion to the amount of carbon fixed. Redfield's ratio (106C:16N) is used for the proportionality constant. To maintain Redfield's ratio, the uptake ratio N:C is adjusted to the ratio of respiration and exudation to gross production. Bacterioplankton take up DN in proportion to the percentage of phytoplankton exudation in the CD pool. Since phytoplankton include some partially heterotrophic forms, DOC exudation is assumed to have some amino-acids as well as nitrogen free molecules such as glycolic acid. Dinoflagellates possibly migrate vertically to obtain N and or avoid predation (Valiela 1984). This may increase the upward flux of nutrients through the pycnocline. Luxury uptake of phytoplankton mixed into the lower layer may also increase upward flux. To model this, if DN UP is less than 20 mg m^{-3} , 10% of the demand is supplied by the lower layer. A randomized (pulsing) mixing term is used to increase nitrogen flux to the upper layer. Though denitrification is thought to occur at the pycnocline during anoxic periods (e.g. Brettar and Rheinheimer 1991) it isn't modeled.

Dissolved organic matter; CD

The major constituents of dissolved organic carbon (DOC) in estuaries are humic acids of terrestrial origin which are relatively refractory to microbial decomposition (Mantoura 1981). A smaller proportion of total DOC is from direct release from phytoplankton and indirect release from grazing and excretion of zooplankton (Lancelot 1979, Roman et al. 1988). Only the labile fraction is modeled here. Surface water values of labile DOC averaged 270 mg C m^{-3} in spring and 420 mg C m^{-3} in summer (Jonas and Tuttle 1990), although total DOC ranges from 1.5 to 6.5 mg l^{-1} . Inflow to the CD compartment includes phytoplankton exudation and SAV excretion, and a percentage of lysed phytoplankton and bacteria. DOC exudation from phytoplankton is assumed to be 100% dissolved, while dead phytoplankton is assumed to be 25% dissolved. DOC production rates in 1988 averaged 72 and $120 \text{ mg m}^{-3} \text{ d}^{-1}$ in spring and summer respectively (Malone et al. 1990). Loss is bacterial uptake (described above).

Dissolved oxygen; OW

Inflow to dissolved oxygen is from diffusion and phytoplankton production. Atmospheric diffusion is a function of the concentration difference, salinity and temperature (see Kemp and Boynton 1980). A photosynthetic quotient of 1.3 (Valiela 1984) is used as the ratio for oxygen produced per carbon fixed. Outflow is to water-column respiration, sediment oxygen demand, and diffusion. Flows are in stoichiometric relation to carbon flows (using an RQ of 0.9). The molar ratio for sediment carbon oxidation is 138:106 or 3.47 to 1 by mass (Valiela 1984). The oxidation of HS^- requires 2 moles of O_2 . Diffusion to the sediments is based on the difference between water column and sediment concentrations. A hyperbolically increasing proportion of sediment oxygen demand is derived directly from the water column as sediment oxygen concentration decreases. Oxygen units are mg l^{-1} .

Benthic Algae, AB

Benthic algal production is controlled by PAR, temperature, and N availability. Maximum growth rate is assumed to be 1/day (see phytoplankton). PAR is absorbed in the water column by phytoplankton and sediments and self-shading occurs at the sediment surface. The light half-saturation coefficient is assumed to be lower than for phytoplankton (Cahoon et al. 1993). Ammonium uptake is assumed to be from the sediments. Krom (1991) found that sediment uptake of ammonia-N was primarily from organic matter breakdown in the sediments. The nitrogen half-saturation coefficient is assumed to be the same as for phytoplankton. Outputs are to respiration and sediment organic carbon, where consumption by microorganisms, meiofauna and deposit-feeders

occurs. Output to organic carbon is assumed to be an exponential function of biomass as well as a percentage of production.

Infaunal deposit feeders, BD

Major taxa include the polychaetes *Heteromastus filiformis*, *Scolecopides viridis* and *Nereis succinea* (Kemp and Boynton 1981). Ingestion is an exponential function of temperature, and a hyperbolic function of dissolved oxygen and sediment POC concentration. Maximum ingestion rates of labile and refractory carbon are 4 and 2% day⁻¹ respectively before the temperature correction. Temperature controls survival and growth in the polychaetes *Polydora ligni* (Rice and Simon 1980), *Capitella capitata* and *Neanthes arenaceodentata* (Oshida and Reish 1974). The temperature coefficient for ingestion gives a Q_{10} of 2. The half-saturation coefficient for oxygen is assumed to be 2 mg l⁻¹. Food supply influenced brood size of *S. benedicti* (Levin and Creed 1986), fecundity and size of *Polydora ligni* (Zajac 1985) and population growth in *Capitella* sp. (Tenore and Chesney 1985). The half-saturation coefficients for refractory and labile carbon are calibrated. Outflows are to respiration, defecation, and mortality. Respiration and excretion are linear functions of ingestion. *Abarenicola pacifica* respiration was about 2% d⁻¹ and was not related to feeding (Taghon 1988). The model assumes that 5% of ingested C is excreted (Grémare et al. 1989), and 10% is respired (Taghon 1988). Resting respiration is assumed to be 0.2 % d⁻¹ (Taghon 1988).

Sediment organic carbon, CL, CR

Sediment organic carbon is separated into labile (CL) and refractory (CR) fractions based on the ability of the organic matter to be decomposed (Billen et al. 1989). A third, more recalcitrant form is not modeled. For calibration, pool sizes were estimated from measurements of chlorophyll in the surface sediments, and measurements of decomposition rates (Burdige 1991, Sampou et. al. 1989) using the "G model" approach (Bernier 1972). Inputs include sedimentation and infauna excretion. Carbon is deposited to the sediments from phytoplankton, amphipod excretion and algal and plant senescence and is divided 50:20 into the two sub-compartments, the remainder being considered recalcitrant. All deposited material is assumed to have the same ratio of labile, refractory and recalcitrant carbon.

Outputs include consumption and respiration. Sediment POM is consumed by meiofauna, both aerobic and anaerobic bacteria, and by deposit-feeding infauna. Aerobic respiration (of meiofauna and bacteria) is simulated as an exponential function of temperature ($Q_{10} = 2$), a linear function of OS and a hyperbolic function of carbon. The hyperbolic function is used because something besides oxygen (e.g. pH) may limit aerobic respiration at high carbon concentrations. The rate coefficients

for biological utilization of labile and refractory fractions are based on geochemical experiments (e.g. Westrich and Berner 1984) which found decomposition rates ranging from 0.01-0.05 day⁻¹ for CL and from 0.0002-0.001 day⁻¹ for CR. Aerobic respiration consumes up to six mmoles C m⁻² d⁻¹ during periods when the bottom water is oxygenated (72 mg m⁻² d⁻¹). Metabolizable POC pools at sampling stations R64 and DB were 24.84 and 36.84 g C m⁻² respectively (Roden 1990). Seasonal sediment organic carbon concentrations in the top one cm of sediments in 8-11 m of water range from 2.5 to 3.5% dry weight (Boynton et al. 1988). Chlorophyll content in the top cm ranged from near 0 to 0.025 % dry weight (0 to 1.25%). This translates to 12.5 g metabolizable carbon m⁻². Denitrification consumes labile carbon (at a ratio of 0.96 C:N) and is equal to nitrification. The equation for nitrification is described below. Anaerobic decomposition is a function of temperature, and carbon, and a negative power function of oxygen, while aerobic respiration is an exponential function of temperature, a hyperbolic function of carbon and is positively correlated with oxygen. Sulfate reduction is dependent on particulate carbon, temperature and inversely affected by sediment oxygen (see HS and NS for further description). The ratio of carbon consumed to sulfate reduced is 0.75 mg /mg. Sulfate reduction accounts for greater than 75% of the carbon mineralization (Roden 1990) in mid bay sediments. Consumption by deposit feeders is described below.

Sediment dissolved inorganic nitrogen, NS

Inflow to NS is ammonification of organic nitrogen; including aerobic and anaerobic decomposition, and deposit feeder excretion. A C:N ratio of 6.6:1 is assumed for all organic matter. A percentage of the nitrogen from buried material is assumed to enter the NW pool. Outputs of the sediment NS pool are nitrification-denitrification and diffusion. Nitrification is modeled as a hyperbolic function of NS and sediment oxygen concentration, and an exponential function of temperature. The reported K_s values range from 0.1 to 700 μM NH₄⁺ (to 500 mg m⁻²) and <1 to 16 μM O₂ (Henriksen and Kemp 1988). The effect of temperature on nitrification fits the Arrhenius equation with a Q₁₀ between 2 and 3.3 (see Henriksen and Kemp 1988 for review). Nitrification rates in various estuaries, including Chesapeake Bay range to greater than 30 mg m⁻² d⁻¹ (Henriksen and Kemp 1988). Denitrification is coupled with nitrification. Diffusion is a percentage of ammonium concentration and thus, is highest in the summer.

Appendix VI-B. Theoretical Basis for SAV Nutrient Interactions in Space.

Although the question of how water exchange rate and SAV biomass and spatial distribution affect plant-nutrient interactions can be generally grasped at an intuitive level, it can also be explained in more theoretical terms. We do this using a simple diffusion-reaction model to describe how changes in nutrient concentration within the seagrass bed depend on the balance between plant uptake (reaction) and physical replenishment (diffusion). Although many other processes are also involved, the simplest model is

$$dC/dt = D [d^2C/dx^2] - uptake \quad (1)$$

where the d's are differential operators, D is the diffusion coefficient (which is proportional to mixing energy in the system), x is a measure of horizontal distance across the bed, and C is the nutrient concentration. By integrating this equation (1) with respect to x (Fick's First Law), we can compute flux of nutrients (F) from outside into the seagrass bed

$$F = D [dC/dx] - k C_i \quad (2)$$

where C_i is the nutrient concentration in the bed, and k is the nutrient uptake rate coefficient, assuming first-order kinetics. Under steady state conditions, F equals zero, and Eq. 2 simplifies to

$$D [dC/dx] = k C_i . \quad (3)$$

The differential $[dC/dx]$, which defines the nutrient concentration gradient from outside to inside the seagrass bed, can be approximated by $[C_o - C_i]/r$. Here, C_o is the nutrient concentration outside the bed (assumed to be constant for this calculation), and r is the mean distance from outside to the bed's center, assuming a semi-infinite plane bed. With this approximation, Eq. 3 simplifies to

$$(D/r) (C_o - C_i) = k (C_i). \quad (4)$$

Solving Eq. 4 for C_i results in the expression

$$C_i = C_o (D/r) [(D/r) + k]^{-1} \quad (5)$$

which simplifies to the following

$$C_i = C_o (D) [(D) + r(k)]^{-1}. \quad (6)$$

This equation (6) describes the dependence of local nutrient concentrations (in the middle of a seagrass bed) on four variables: 1) turbulent diffusion (D); 2) external

nutrient concentration (C_o); 3) uptake rate coefficient (k , which would be dependent on plant biomass); and 4) mean width (r) of the bed.

The relative dependence of C_i on these variables changes with the balance between diffusion (D) and uptake r (k). From Eq. 6 it is clear that when rates of physical replenishment greatly exceed uptake rates ($D \gg r$ (k)), C_i approaches C_o , and seagrass beds have little effect on local nutrient concentrations. Conversely, when the uptake rate greatly exceeds the physical exchange rate ($D \ll r$ (k)), Eq. 6 can be approximated and rearranged to examine the concentration ratio in relation to the flux ratio

$$C_i / C_o = D [r (k)]^{-1}. \quad (7)$$

In this case, the ratio of internal to external nutrient concentrations is directly proportional to the mixing energy (D) and inversely related to uptake rate (k) and mean bed width (r). This is the case that we intuitively hypothesized earlier in this proposal (p. 2). Thus, the relative reduction in nutrient concentration within the seagrass bed is large when physical exchange rates are low, uptake rates are high and mean bed size is large. It is interesting to note that when D is approximately equal to r , the relative reduction in concentration is independent of both D and r , as indicated by the simplified version of Eq. 7, $C_i / C_o = (1 + r)^{-1}$. Under these conditions bed size is the dominant controlling factor, a point of relevance to this proposal.

While this analysis may be interesting and perhaps intuitively appealing, it represents a highly simplified situation. It does not take into account several complicating, but potentially important, factors, including higher-order uptake kinetics, dependence of D on biomass and/or r , and dependence of C_o on k . It remains to be seen how these relationships might change under actual estuarine conditions, and to what degree the conclusions reached in this analysis depend on its simplifying assumptions. Hence, we are proposing here a research project to investigate relationships among nutrients, mixing, SAV biomass and bed dimensions with field experiments, numerical simulations and statistical analyses of SAV spatial distributions.

References

- Azam, F., T. Fenchel, J. G. Field, J. S. Gray, L. A. Meyer-Reil and F. Thingstad. 1983. The ecological role of water-column microbes in the sea. *Mar. Ecol. Prog. Ser.* 10:257-263.
- Azam, F., T. Fenchel, J. G. Field, J. S. Gray, L. A. Meyer-Reil and F. Thingstad. 1983. The ecological role of water-column microbes in the sea. *Mar. Ecol. Prog. Ser.* 10:257-263.
- Bannister, T. T. 1974a. Production equations in terms of chlorophyll concentration, quantum yield, and upper limit to production. *Limnol. Oceanogr.* 19:1-12.
- Bartleson, R. D. and W. M. Kemp. 1991. Preliminary ecosystem simulations of estuarine planktonic-benthic interactions: The planktonic submodel. Chesapeake Research Consortium Publication, 4-6 December, Baltimore Maryland
- Batiuk, R., R. Orth, K. Moore, J. C. Stevenson, W. Dennison, L. Staver, V. Carter, N. Rybicki, R. Hickman, S. Kollar and S. Bieber. 1992. Submerged aquatic vegetation habitat requirements and restoration targets: a technical synthesis. USEPA Chesapeake Bay Program, Annapolis Maryland.
- Batiuk, R. A., P. Bergstrom, W. M. Kemp, E. Kock, L. Murray, J. C. Stevenson, R. Bartleson, V. Carter, N. B. Rybicki, J. M. Landwehr, C. Gallegos, L. Karrh, M. Naylor, D. Wilcox, K. Moore, and S. Ailstock. 2000. Chesapeake Bay submerged aquatic vegetation water quality and habitat-based requirements and restoration targets: A second technical synthesis. US EPA Chesapeake Bay Program, Annapolis, MD.
- Berner, R. A. 1972. Sulfate reduction, pyrite formation, and the oceanic sulfur budget, p. 347-361. *In* D. Dryssen and K. Jagner (eds.) *The changing chemistry of the oceans.* Almqvist and Wiksell, Stockholm.
- Billen, G., S. Dessery, C. Lancelot and M. Maybeck. 1989. Seasonal and interannual variations of nitrogen diagenesis in the sediments of a recently impounded basin. *Biogeochem.* 8:73-100.
- Boynton, W. R. 1982. Ecological role and value of submerged macrophyte communities: A scientific summary., p. 428-502. *In* E. G. Macalaster (eds.) *Chesapeake Bay Program Technical Studies: A Synthesis.* U. S. Environmental Protection Agency, NTIS, Springfield, VA.
- Boynton, W. R., J. Garber, J. Barnes and W. M. Kemp. 1988. Ecosystem processes component. Level 1 report to state of Maryland Department of the Environment.

- Univ. Maryland Center for Environmental and Estuarine Studies. Solomons MD. NTIS, Ref. No. (UMCES) CBL 88-2.
- Brandt, S. B., D. M. Mason and E. V. Patrick. 1992. Spatially-explicit models of fish growth rate. *Fisheries* 17:23-35.
- Brettar, I. and G. Rheinheimer. 1991. Denitrification in the Central Baltic: evidence for H₂S-oxidation as motor of denitrification at the oxic-anoxic interface. *Mar. Ecol. Prog. Ser.* 77:157-169.
- Bronk, D. A. and P. M. Glibert. 1993. Application of a ¹⁵N tracer method to the study of dissolved organic nitrogen uptake during spring and summer in Chesapeake Bay. *Mar. Biol.* 115:501-508.
- Brönmark, C. 1985. Interactions between macrophytes, epiphytes and herbivores: an experimental approach. *Oikos* 45:26-30.
- Burdige, D. J. 1991. The kinetics of organic matter mineralization in anoxic marine sediments. *J. Mar. Res.* 49:727-761.
- Burkholder, J. M., K. M. Mason and H. B. Glasgow, Jr. 1992. Water-column nitrate enrichment promotes decline of eelgrass *Zostera marina* : Evidence from seasonal mesocosm experiments. *Mar. Ecol. Prog. Ser.* 81:163-178.
- Burkill, P. H., R. F. Mantoura, C. Llewellyn and C. A. Owens. 1987. Microzooplankton grazing and selectivity of phytoplankton in coastal waters. *Mar. Biol.* 93:581-590.
- Cahoon, L. B., G. R. J. Beretich, C. J. Thomas and A. M. McDonald. 1993. Benthic microalgal production at Stellwagen Bank, Massachusetts Bay, USA. *Mar. Ecol. Prog. Ser.* 102:179-185.
- Cattaneo, A. and B. Mousseau. 1995. Empirical analysis of the removal rate of periphyton by grazers. *Oecologia* 103:249-254.
- Cerco, C. F. and T. Cole. 1993. Three-dimensional eutrophication model of Chesapeake Bay. *Journal of Environmental Engineering* 119:1006-1025.
- Conley, D. J. and T. C. Malone. 1992. Annual cycle of dissolved silicate in Chesapeake Bay: implications for the production and fate of phytoplankton biomass. *Mar. Ecol. Prog. Ser.* 81:121-128.
- Culver, M. E. and W. O. S. Jr. 1989. Effects of environmental variation on sinking rates of marine phytoplankton. *J. Phycol.* 25:262-270.
- Davison, I. R. 1987. Adaptation of photosynthesis in *Laminaria saccharina* (Phaeophyta) to changes in growth temperature. *J. Phycol.* 23:273-283.

- Dennison, W. C., R. J. Orth, K. A. Moore, J. C. Stevenson, V. Carter, S. Kollar, P. W. Bergstrom and R. A. Batiuk. 1993. Assessing water quality with submersed aquatic vegetation. Habitat requirements as barometers of Chesapeake Bay health. *Bioscience*. 43:86-94.
- Ducklow, H. W. and S. M. Hill. 1985. The growth of heterotrophic bacteria in the surface waters of warm core rings. *Limnol. Oceanogr.* 30:239-259.
- Eppley, R. W. and P. R. Sloan. 1965. Carbon balance experiments with marine phytoplankton. *J. Fish Res. Bd. Canada* 22:1083-1097.
- Eppley, R. W. 1972. Temperature and phytoplankton growth in the sea. *Fishery Bull.* 1063-1085.
- Fasham, M. J. R., P. M. Holligan and P. R. Pugh. 1983. The spatial and temporal development of the spring phytoplankton bloom in the Celtic Sea, April 1979. *Prog. Oceanogr.* 12:87-145.
- Geider, R. J. and B. A. Osborne. 1989. Respiration and microalgal growth: A review of the quantitative relationship between dark respiration and growth. *New Phytol.* 112:327-340.
- Geider, R. J. 1992. Respiration: Taxation without representation, p. 333-360. In P. G. Falkowski and A. D. Woodhead (eds.) Primary productivity and biogeochemical cycles in the sea. Plenum Press, New York.
- Goldman, J. C. and P. M. Glibert. 1983. Kinetics of inorganic uptake by phytoplankton, p. E. J. Carpenter and D. G. Capone (eds.) Nitrogen in the marine environment. Academic Press, New York.
- Goldsborough, W. J. and W. M. Kemp. 1988. Light responses of a submersed macrophyte: implications for survival in turbid tidal waters. 69:1775-1786.
- Gremare, A., J. M. Amouroux and J. Amouroux. 1989. Modeling of consumption and assimilation in the deposit-feeding polychaete *Eupolymnia nebulosa*. *Mar. Ecol. Prog. Ser.* 54:239-248.
- Harley, M. T. and S. Findlay. 1994. Photosynthesis-irradiance relationships for three species of submersed macrophytes in the tidal freshwater Hudson River. *Estuaries* 17:200-205.
- Harlin, M. M. and B. Thorne-Miller. 1981. Nutrient Enrichment of Seagrass Beds in a Rhode Island Coastal Lagoon. *Mar. Biol.* 65:221-229.

- Heldal, M. and G. Bratbak. 1991. Production and decay of viruses in aquatic environments. *Mar. Ecol. Prog. Ser.* 72:205-212.
- Hemminga, M. A., P. G. Harrison and F. van Lent. 1991. The balance of nutrient losses and gains in seagrass meadows. *Mar. Ecol. (Prog. Ser.)*. 71:85-96.
- Henriksen, K. and W. M. Kemp. 1988. Nitrification in estuarine and coastal marine sediments: Methods, patterns and regulating factors., p. 207-249. *In* T. H. Blackburn and J. Sørensen (eds.) Nitrogen cycling in coastal marine environments. John Wiley publ., New York.
- Hootsmans, M. J. M. and J. E. Vermaat. 1985. The effect of periphyton-grazing by three epifaunal species on the growth of *Zostera marina* L. under experimental conditions. *Aquatic Botany* 22:83-88.
- Howard, R. K. 1982. Impact of feeding activities of epibenthic amphipods on surface-fouling of eelgrass leaves. *Aquat. Bot.* 14:91-97.
- Howard, R. K. and F. T. Short. 1986. Seagrass growth and survivorship under the influence of epiphyte grazers. 24:287-302.
- Jonas, R. B. and J. H. Tuttle. 1990. Improving Chesapeake Bay water quality: Influence of rafted oyster aquaculture on microbial processes and organic carbon. Chesapeake Research Consortium Publication, 4-6 December Baltimore Maryland.
- Kemp, W. M. and W. R. Boynton. 1980. Influence of biological and physical factors on dissolved oxygen dynamics in an estuarine system: implications for measurement of community metabolism. *Estuar. Coast. Mar. Sci.* 11:407-431.
- Kemp, W. M., Boynton, W. R., Twilley, R. R., Stevenson, J. C., Means, J. C. 1983. The decline of submerged vascular plants in upper Chesapeake Bay: Summary of results concerning possible causes. *Mar. Technol. Soc. J.* 17:78-89.
- Kemp, W. M., W. R. Boynton and A. J. Hermann. 1995. Simulation models of an estuarine macrophyte ecosystem, p. 262-278. *In* B. P. a. S. E. Jørgensen (eds.) Complex ecology. Prentice Hall, Englewood Cliffs, NJ.
- Kremer, J. N. and S. W. Nixon. 1978. A coastal marine ecosystem simulation and analysis. 1 ed. Ecological Studies. Springer-Verlag, New York
- Krom, M. D. 1991. Importance of benthic productivity in controlling the flux of dissolved inorganic nitrogen through the sediment-water interface in a hypertrophic marine ecosystem. *Mar. Ecol. Prog. Ser.* 78:163-172.

- Lancelot, C. 1979. Gross excretion rates of natural marine phytoplankton and heterotrophic uptake of excreted products in the Southern North Sea, as determined by short-term kinetics. *Mar. Ecol. Prog. Ser.* 1:179-186.
- Lee, V. and S. Olsen. 1985. Eutrophication and management initiatives for the control of nutrient inputs to Rhode Island coastal lagoons. *Estuaries* 8:191-202.
- Levin, L. A. 1986. Effects of enrichment on reproduction in the opportunistic polychaete *Treblospio benedicti* (Webster): A mesocosm study. *Biol. Bull.* 171:143-160.
- Lubbers, L., W. R. Boynton and W. M. Kemp. 1990. Variations in structure of estuarine fish communities in relation to abundance of submersed vascular plants. *Mar. Ecol. Prog. Ser.* 65:1-14.
- Madden, C. J. and W. M. Kemp. 1996. Ecosystem model of an estuarine submersed plant community: Calibration and simulation of eutrophication responses. *Estuaries* 19 (2B):457-474.
- Malone, T. C. 1982. Phytoplankton photosynthesis and carbon-specific growth: light-saturated rates in a nutrient-rich environment. *Limnol. Oceanogr.* 27:226-235.
- Malone, T. C. and H. W. Ducklow. 1990. Microbial biomass in the coastal plume of Chesapeake Bay: Phytoplankton-bacterioplankton relationships. *Limnol. Oceanogr.* 35:296-312.
- Malone, T. C., H. W. Ducklow, E. R. Peele and S. E. Pike. 1991. Picoplankton carbon flux in Chesapeake Bay. *Mar. Ecol. Prog. Ser.* 78:11-22.
- Mantoura, R. F. C. 1981. Dissolved organic constituents in estuaries. United Nations Environmental Programme, New York, 259-265
- McRoy, C. P. and R. J. Barsdate. 1970. Phosphate absorption in eelgrass. *Limnol. Oceanogr.* 15:6-13.
- Moore, K. A., H. A. Neckles and R. J. Orth. 1996. *Zostera marina* (eelgrass) growth and survival along a gradient of nutrients and turbidity in the lower Chesapeake Bay. *Mar. Ecol. Prog. Ser.* 142:247-259.
- Moore, K. A. (1996). Relationships between seagrass growth and survival and environmental conditions in a lower Chesapeake Bay Tributary. Ph.D. Thesis, University of Maryland at College Park
- Mulholland, P. J. and A. D. Rosemond. 1992. Periphyton response to longitudinal nutrient depletion in a woodland stream: Evidence of upstream-downstream linkage. *J. N. Am. Benthol. Soc.* 11:405-419.

- Neckles, H. A., R. L. Wetzel and R. J. Orth. 1993. Relative effects of nutrient enrichment and grazing epiphyte-macrophyte (*Zostera marina* L.) dynamics. *Oecologia* 93:285-295.
- Neckles, H. A., E. T. Koepfler, L. W. Haas, R. L. Wetzel and R. J. Orth. 1994. Dynamics of epiphytic photoautotrophs and heterotrophs in *Zostera marina* (Eelgrass) microcosms: responses to nutrient enrichment and grazing. *Estuaries* 17:597-605.
- Novitsky, J. A. and R. Y. Morita. 1978. Possible strategy for the survival of marine bacteria under starvation conditions. *Mar. Biol.* 48:289-295.
- Ojala, A. 1993. Effects of temperature and irradiance on the growth of two freshwater photosynthetic cryptophytes. *J. Phycol.* 29:278-284.
- Orth, R. J. and K. A. Moore. 1983. Chesapeake Bay: An unprecedented decline in submerged aquatic vegetation. 222:51-53.
- Oshida, P. and D. J. Reish. 1974. The effects of various water temperatures on the survival and reproduction in polychaetous annelids, p. 63-77. *In* (eds.) Preliminary Report, marine studies of San Pedro Bay, California, Part III.
- Parsons, T. R., M. Takahashi and B. Hargrave. 1984. Biological Oceanographic Processes. Third Edition ed. Pergamon Press, New York
- Phillips, G. L., D. Eminson and B. Moss. 1978. A mechanism to account for macrophyte decline in progressively eutrophicated freshwaters. *Aquat. Bot.* 4:103-126.
- Pitcher, G. C., D. R. Walker and B. A. Mitchell-Innes. 1989. Phytoplankton sinking rate dynamics in the southern Benguela upwelling system. *Mar. Ecol. Prog. Ser.* 55:261-269.
- Pomeroy, L. R., W. J. Wiebe, D. Deibel, R. J. Thompson, G. T. Rowe and J. D. Pakulski. 1991. Bacterial responses to temperature and substrate concentration during the Newfoundland spring bloom. *Mar. Ecol. Prog. Ser.* 75:143-159.
- Proctor, L. M. and J. A. Fuhrman. 1990. Viral mortality of marine bacteria and cyanobacteria. *Nature* 343:60-62.
- Purcell, J. E. and D. A. Nemazie. 1992. Quantitative feeding ecology of the hydromedusan *Nemopsis bachei* in Chesapeake Bay. *Mar. Biol.* 113:305-311.
- Rice, S. A. and J. L. Simon. 1980. Intraspecific variation in the pollution indicator polychaete *Polydora ligni* (Spionidae). *Ophelia* 19:79-115.

- Roden, E. E. 1990. Sediment sulfur cycling and its relationship to carbon cycling and oxygen balance in the Chesapeake Bay. Ph.D. Dissertation, University of Maryland, College Park
- Roman, M. R., H. Ducklow, J. Fuhrman, C. Garside, P. Glibert, T. Malone and G. B. McManus. 1988. Production, consumption, and nutrient cycling in a laboratory mesocosm. *Mar. Ecol. Prog. Ser.* 42:39-52.
- Sampou, P. 1989. Effects of eutrophication on the biogeochemical cycling of carbon, oxygen, sulfur and energy in coastal marine ecosystems. Ph.D. Dissertation, University of Rhode Island, Kingston.
- Scavia, D., B. J. Eadie and A. Robertson. 1976. An ecological model for the Great Lakes, p. 629-633. *In* W. R. Ott (eds.) Environmental modeling and simulation. EPA 600/9-76-016 (U. S. Environmental Protection Agency), Washington, DC.
- Scavia, D. 1980. An ecological model of lake Ontario. *Ecol. Modelling* 8:49-78.
- Sellner, K. G. and M. E. Kachur. 1987. Chapter 1. Phytoplankton: Relationships between phytoplankton, nutrients, oxygen flux and secondary producers, p. 287. *In* K. L. Heck (eds.) Ecological Studies in the Middle Reach of the Chesapeake Bay Calvert Cliffs. Springer Verlag, New York.
- Semenov, A. M. 1991. Physiological Bases of Oligotrophy of Microorganisms and the Concept of Microbial Community. *Microb. Ecol.* 22:239-247.
- Sheridan, R. P. and T. Ulik. 1976. Adaptive photosynthesis responses to temperature extremes by the thermophilic cyanophyte *Synechococcus lividus*. *J. Phycol.* 12:255-261.
- Shiah, F. K. (1993). Multi-scale variability of bacterioplankton abundance, production and growth rate in temperate estuarine ecosystems. Doctoral Dissertation, University of Maryland, College Park.
- Shiah, F. and H. W. Ducklow. 1994. Temperature and substrate regulation of bacterial abundance, production and specific growth rate in Chesapeake Bay, USA. *Mar. Ecol. Prog. Ser.* 103:297-308.
- Short, F. T., D. M. Burdick and J. E. K. III. 1995. Mesocosm experiments quantify the effects of eutrophication on eelgrass, *Zostera marina*. *Limnol. Oceanogr.* 40:740-749.
- Sieburth, J. M., P. W. Johnson and P. E. Hargraves. 1988. Ultrastructure and ecology of *Aureococcus anophagefferens* gen. et sp. nov. (Chrysophyceae): The dominant picoplankton during a bloom in Narragansett Bay, Rhode Island, Summer 1985. *J. Phycol.* 24:416.

- Smetacek, V. S. 1985. Role of sinking in diatom life history cycles: ecological, evolutionary, and geological significance. *Mar. Biol.* 84:239-251.
- Staver, K. (1984). Responses of epiphytic algae to nitrogen and phosphorus enrichment and effects on productivity of the host plant, *Potamogeton perfoliatus* L., in estuarine waters. M.S., Univ of Md
- Stemann-Nielsen, E. 1962. On the maximum quantity of plankton chlorophyll per surface unit of a lake or the sea. *Int. Rev. ges. Hydrobiol.* 47:333-338.
- Sturgis, R., and L. Murray. 1997. Scaling of nutrient inputs to submersed plant communities: temporal and spatial variations. *Mar Ecol Prog Ser* 152:89-102.
- Taghon, G. L. 1988. The benefits and costs of deposit feeding in the polychaete *Abarenicola pacifica*. *Limnol. Oceanogr.* 33:1166-1175.
- Talling, J. F. 1957b. The phytoplankton population as a compound photosynthetic system. *New Phytol.* 56:133-149.
- Taylor, D. I., S.W. Nixon, S.L. Granger, B.A. Buckley, J.P. McMahon, H.-J. Lin. 1995. Responses of coastal lagoon plant communities to different forms of nutrient enrichment- a mesocosm experiment. *Aquat. Bot.* 52:19-34.
- Tenore, K. R. and E. J. Chesney, Jr. 1985. The effects of interaction on rate of food supply and population density on the bioenergetics of the opportunistic polychaete, *Capitella capitata* (type 1). *Limnol. Oceanogr.* 30:1188-1195.
- Tezuka, Y. 1990. Bacterial Regeneration of Ammonium and Phosphate as Affected by the Carbon:Nitrogen:Phosphorus Ratio of Organic Substrates. *Micro. Ecol.* 19:227-238.
- Thursby, G. B. 1984. Root-exuded oxygen in the aquatic angiosperm *Ruppia maritima*. *Mar. Ecol. Prog. Ser.* 16:303-305.
- Twilley, R. R., W. M. Kemp, K. W. Staver, J. C. Stevenson and W. R. Boynton. 1985. Nutrient enrichment of estuarine submersed vascular plant communities. 1. Algal growth and effects on production of plants and associated communities. *Mar. Ecol. Prog. Ser.* 23:179-191.
- Valiela, I. 1984. Marine ecological processes. Springer Verlag, New York
- Virnstein, R. W., P. S. Mikkelsen, K. D. Cairns, M. A. Capone, W. K. Taylor and H. O. Whittier. 1983. Seagrass beds versus sand bottoms: The trophic importance of their associated benthic invertebrates. *Fla. Sci.* 46:363-381.

- Westrich, J. T. and R. A. Berner. 1984. The role of sedimentary organic matter in bacterial sulfate reduction: The *G* model tested. *Limnol. Oceanogr.* 29:236-249.
- Wetzel, R. L. and R. R. Christian. 1984. Model studies on the interactions among carbon substrates, bacteria and consumers in a salt marsh estuary. *Bull. Mar. Sci.* 601-614.
- Wetzel, R. L. and H. A. Neckles. 1986. A model of *Zostera marina* L. photosynthesis and growth: simulated effects of selected physical-chemical variables and biological interactions. *Aquat. Bot.* 26:307-323.
- Wheeler, P. A. and D. L. Kirchman. 1986. Utilization of inorganic and organic nitrogen by bacteria in marine systems. *Limnol. Oceanogr.* 31:998-1009.
- Zajac, R. N. 1985. The effects of sublethal predation on reproduction in the spionid polychaete *Polydora ligni* Webster. *J. Exp. Mar. Biol. Ecol.* 88:1-19.

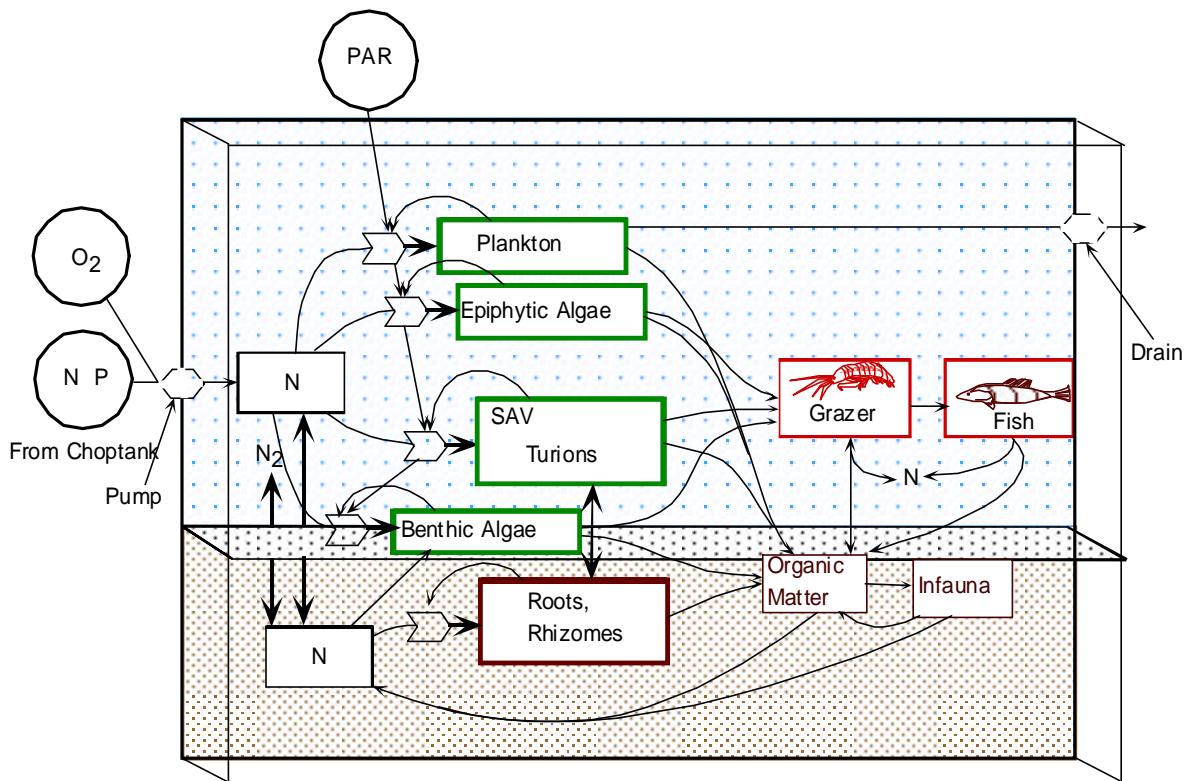


Fig. III-1 General structure of SAV model is shown. Some material flows are left out for simplicity. N is modeled in stoichiometry with C except in SAV where structural and nonstructural N and C are modeled separately.

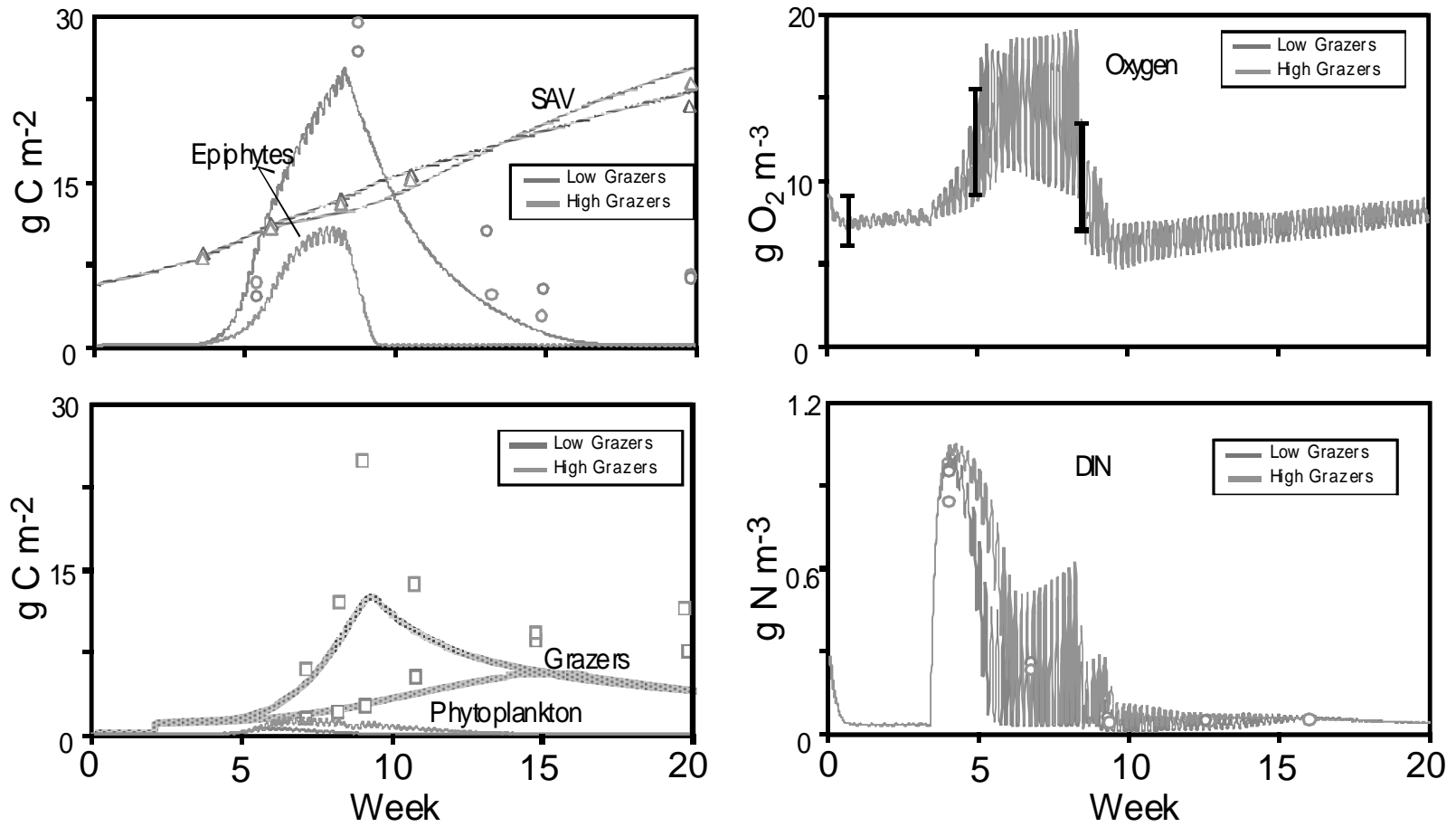


Fig. III-2. Model results are shown with data from the 1995 mesocosm experiment. The system behavior is in the right range, but the biomasses aren't exactly what the model predicts.

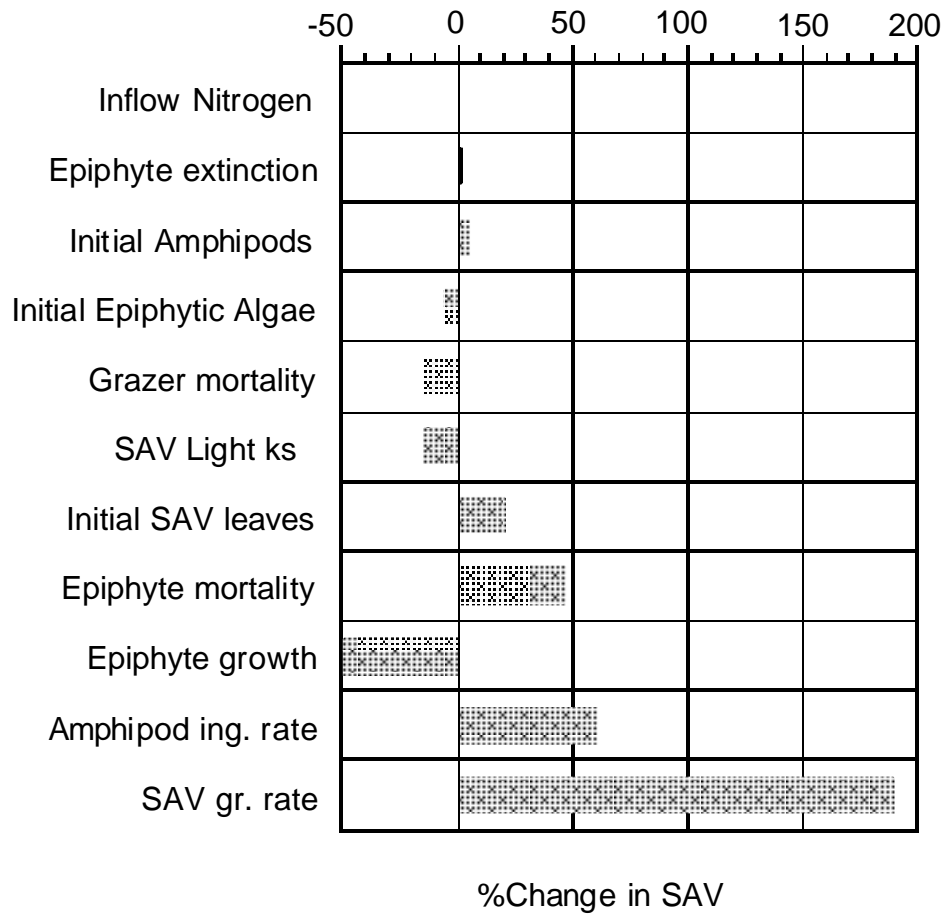


Fig. III-3 Sensitivity analysis showing percent change in SAV leaf biomass after 23 weeks for a 50% increase in the variable

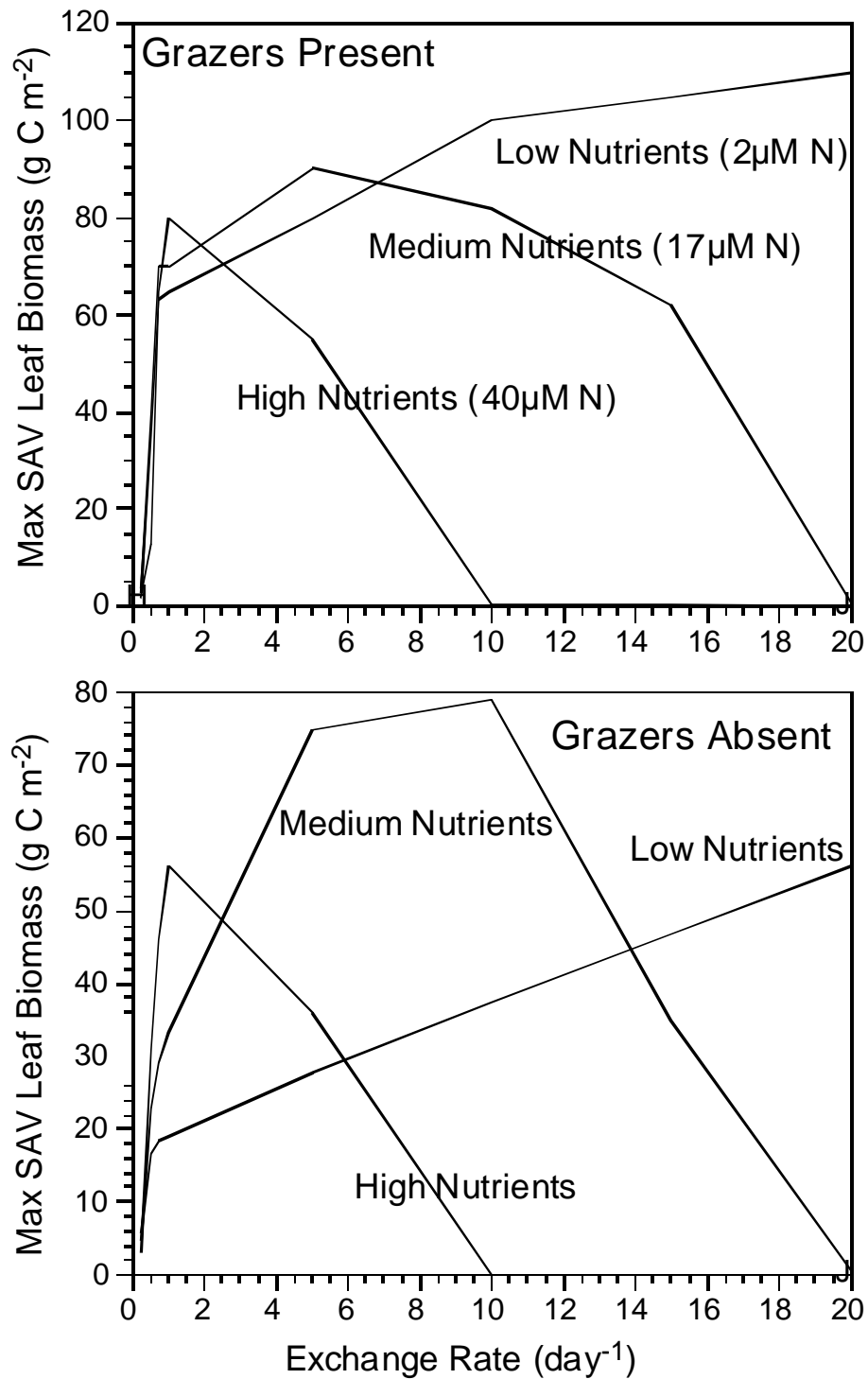


Fig. III-4 Effect of interaction of exchange rate, nutrients and grazers on SAV biomass.

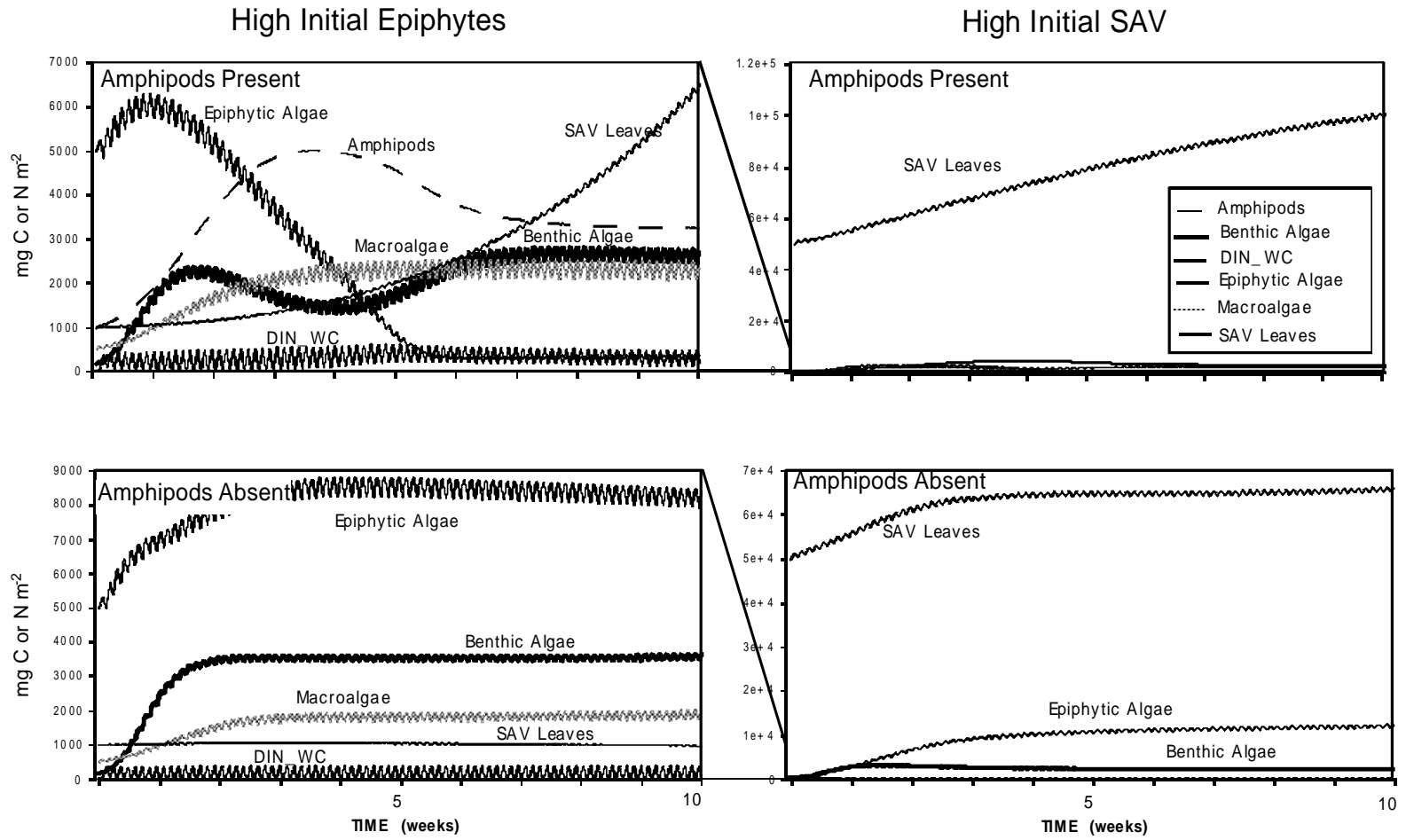


Fig. III-5. Effects of initial conditions on model state variables over the course of an experiment.

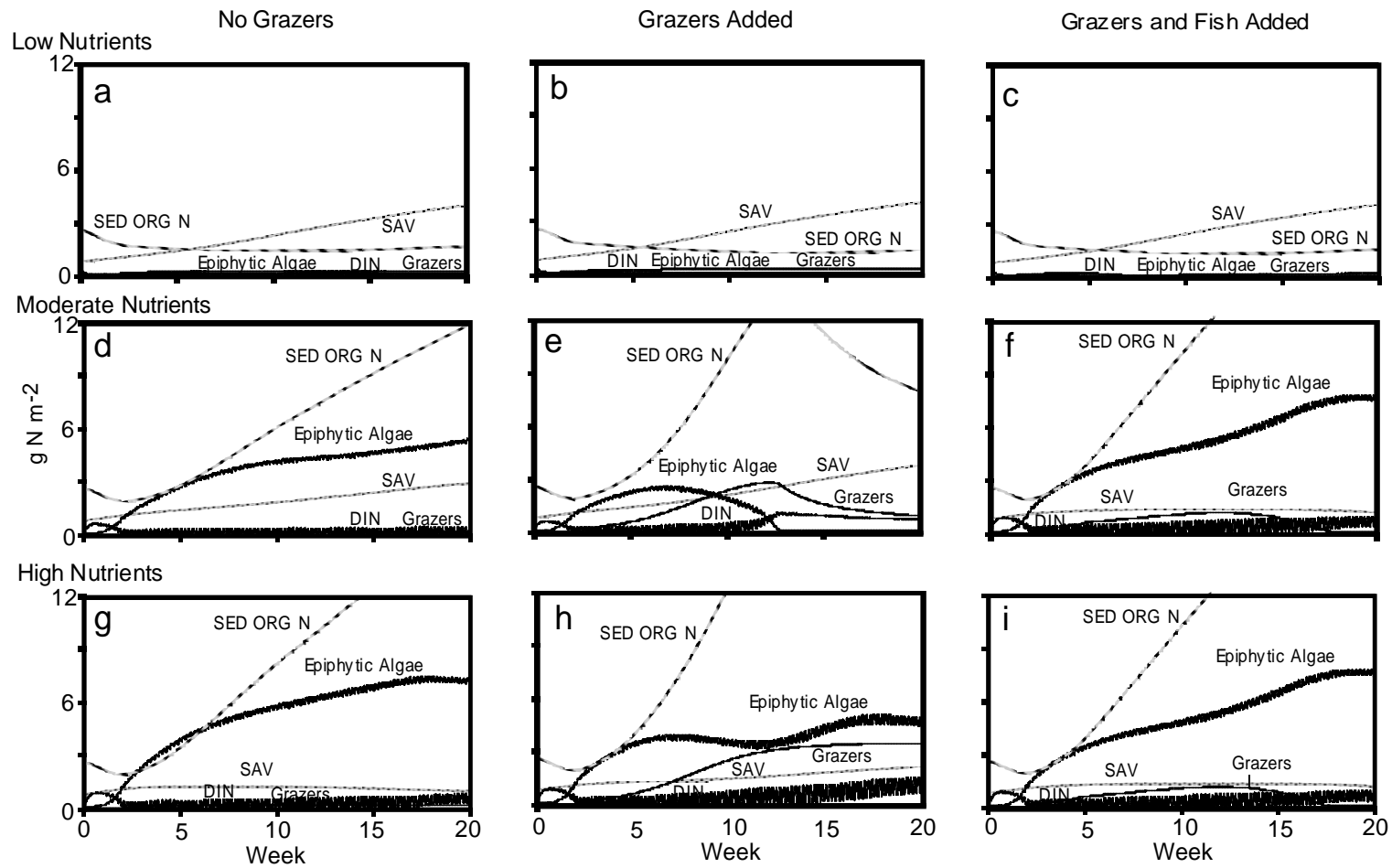


Fig. III-6. Model runs showing the results of mesocosm nutrient addition to SAV mesocosms containing no grazers (first column), grazers (second column), and grazers with fish (third column).

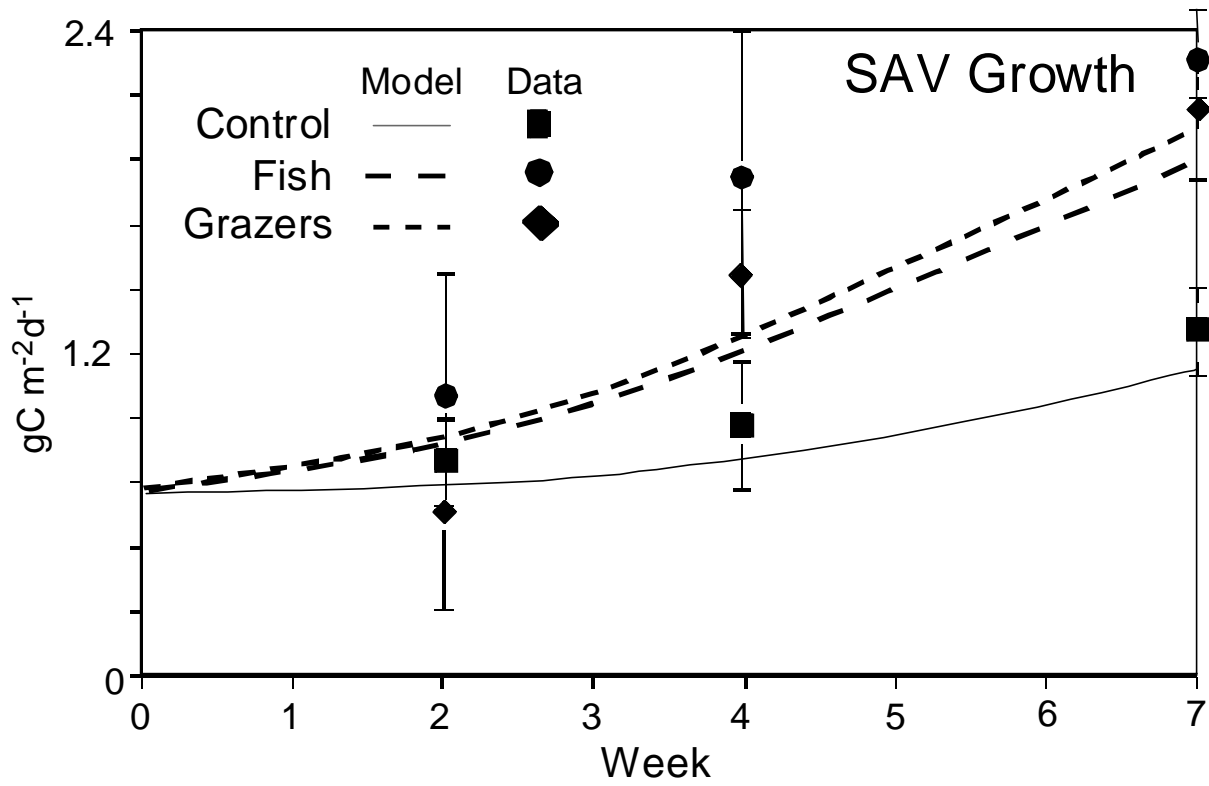


Fig. III-7. Effect of treatment on SAV growth in mesocosm experiments and in simulations.

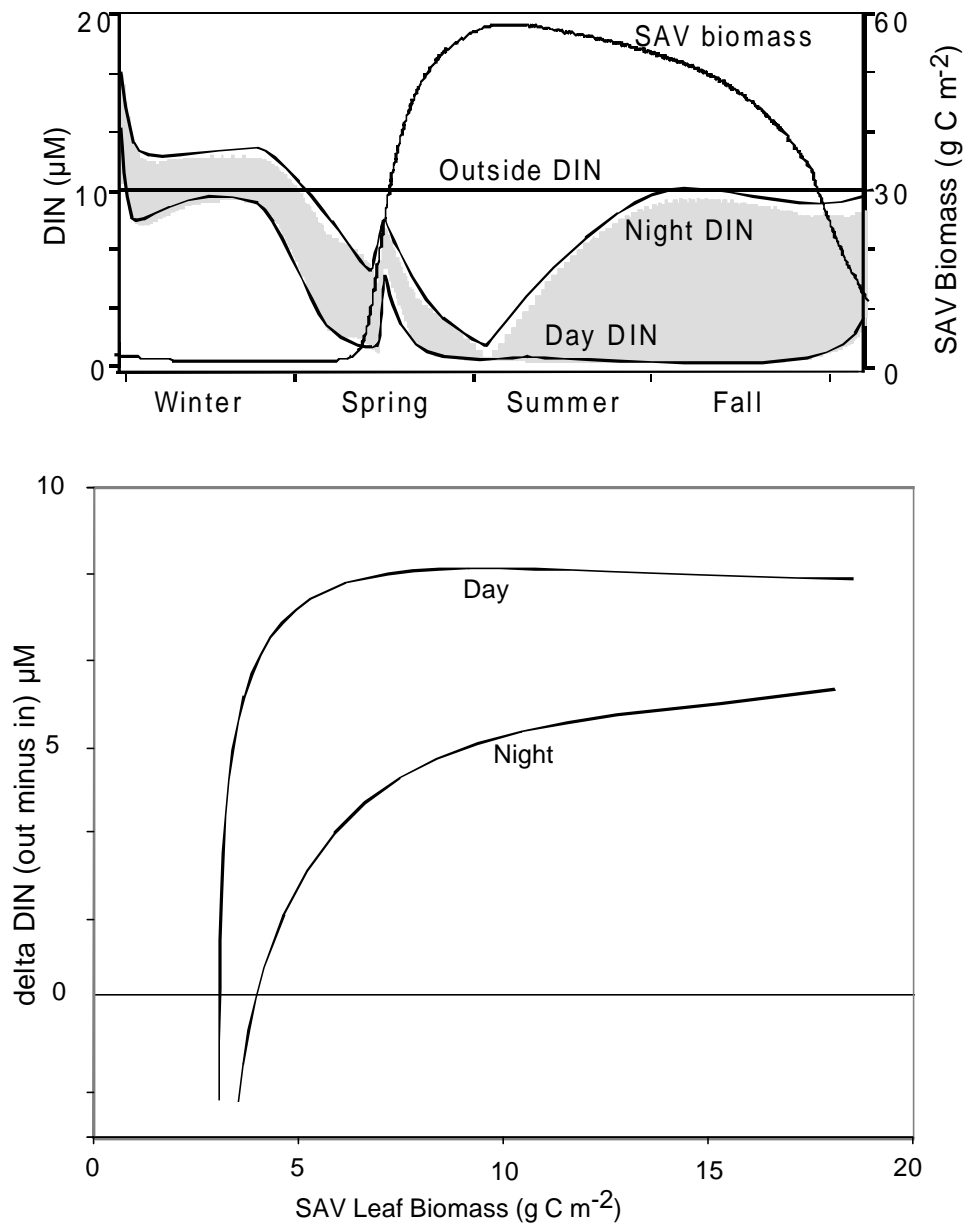
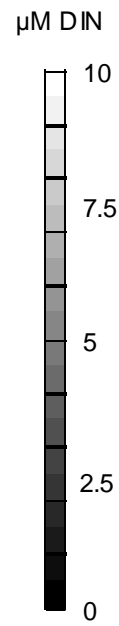
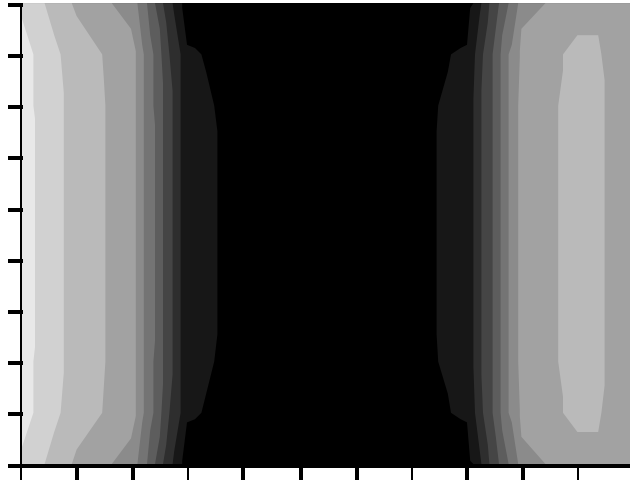


Fig. III-8. Upper Panel--Simulated seasonal cycle of mean SAV biomass and nutrient (dissolved inorganic nitrogen, DIN) concentrations outside and within (mid-day and late-night) the plant bed. External concentration is held constant for this simulation. Notice how maximum difference in nutrient concentration occurs in early summer, and how diel variation in difference increases during the summer-fall period. Lower Panel--Relationship between difference in DIN inside to outside SAV bed (delta DIN) in daytime and night time versus plant leaf biomass in a model of a mesocosm. Notice how SAV effect on delta DIN saturates at lower biomass levels for daytime concentrations.

Large contiguous SAV bed occupying one 60-cell patch (6 x 10)



Patchy SAV bed occupying 60 cells distributed in 15 equal-size, evenly-spaced patches (each 2 x 2 cells)

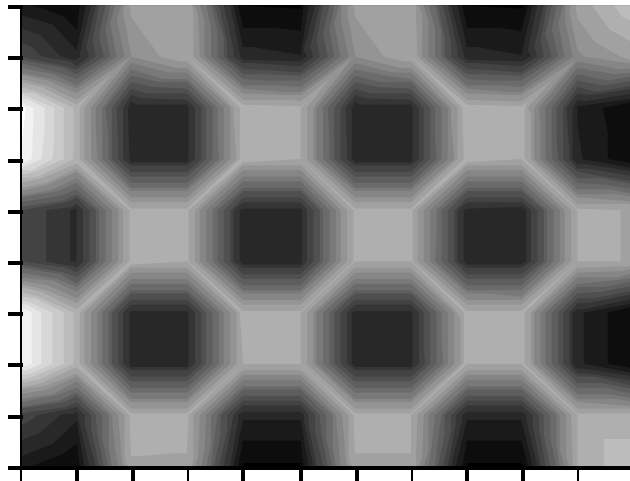


Fig. III-9. Results of spreadsheet calculation showing nutrient concentrations over space as a result of uptake in patchy and continuous SAV.

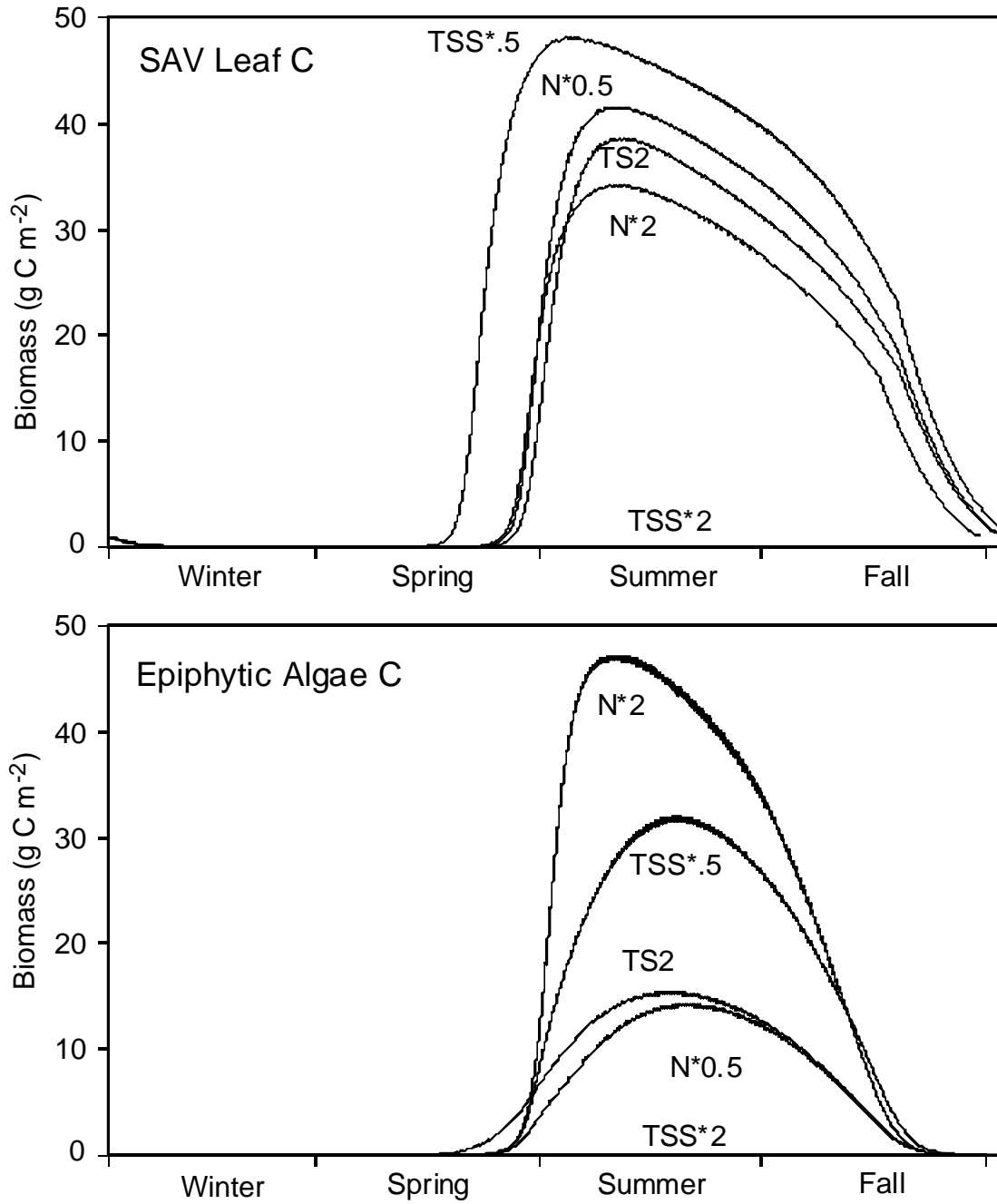


Fig. III-10. Effect of TSS and DIN on SAV and epiphyte biomass over the course of a season in a simulation model run.

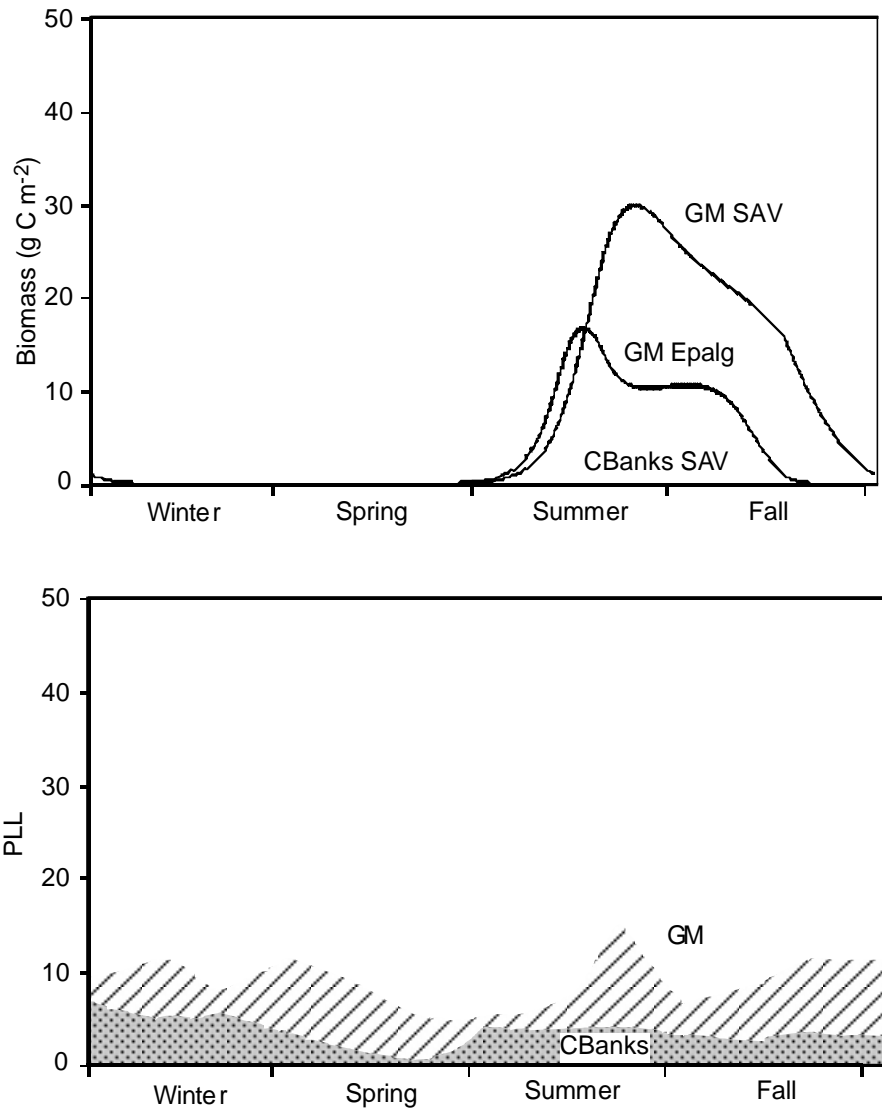


Fig. III-11. Seasonal run showing modeled SAV biomass using data from two York River sites: Guinea Marsh (GM) and Clay Banks (CBanks).

Chapter IV

Tree-Structured Models of Water Quality and Submersed Aquatic Vegetation in Chesapeake Bay

J. D. Hagy

Abstract

Restoration of nearshore, submerged aquatic vegetation (SAV) is a major environmental management objective, which it is generally agreed will require improvement of water quality, specifically those components of water quality that contribute to light attenuation and the potential for biofouling of SAV leaves. One challenge to relating water quality to the survival of submersed aquatic vegetation is that the available data for SAV do not characterize the physiological state of the SAV, but merely its abundance. This leads to the likelihood of discontinuous response functions, such as thresholds. In addition, the relevant water quality variables interact, so their effects are not additive. A tree-structured non-parametric data analysis technique called CART is introduced as an effective tool for quantifying context-sensitive responses and interactions, discontinuous responses, and for analyzing data with challenging statistical distributions. Tree-structured models were developed for all of Chesapeake Bay and tributaries, and for individual salinity zones. Model performance was superior to previously described discriminant models. Salinity zone-specific models were most successful, identifying total suspended solids (TSS) as the most important variable in low salinity areas, TSS and chlorophyll-a as most important in mesohaline areas, and dissolved inorganic nitrogen as most important in higher salinity areas. Dissolved inorganic phosphorus was a more important variable than expected.

Introduction

Hagy and Boynton (1997; 1998) investigated the relationship between water quality at the main channel water quality stations and the presence of submersed aquatic vegetation (SAV) in the most adjacent shallow water areas. There were two objectives of their analysis. The first was to develop a model to predict SAV survival in littoral zones from main channel water quality information, which constitutes the vast majority of past and planned water quality monitoring in Chesapeake Bay. The second objective was to evaluate whether (and how), the empirically-established SAV habitat criteria could be applied to main channel water quality data to ascertain expected increases in SAV coverage in Chesapeake Bay as water quality improvements are observed at the mid-Channel stations. This would aid in specifying water quality restoration goals for river and Bay channels that are relevant in a known way to SAV restoration, an objective with well-established ecological value. One issue is whether there are equivalent trade-offs among the 5 variables for which criteria have been established (dissolved inorganic nitrogen (DIN), dissolved inorganic phosphorus (DIP), total suspended solids (TSS), chlorophyll-a, and secchi depth). Since TSS and Chlorophyll-a contribute to light

attenuation and secchi depth is a direct measure of light attenuation, trade-offs among TSS and chlorophyll-a might be expected.

Hagy and Boynton (1997) used a parametric discriminant analysis, a classification technique, to classify USGS 7.5-minute quadrangles among one of three groups: "UN" sites had a median SAV coverage of zero; the "SN" group sometimes had no SAV, or had a minimum SAV coverage of zero, but a median SAV coverage greater than zero. The "AS" group had minimum SAV coverage greater than zero. Quantification via a continuous variable was avoided because a target coverage (e.g. area less than 1m deep or TIER II restoration goals) by which SAV coverage could be scaled (e.g. to express as "percent of restoration goal") was not available. The explanatory variables included in the model include salinity zone, chlorophyll-a concentration (Chl-a), total suspended solids concentration (TSS), dissolved inorganic nitrogen concentration (DIN), dissolved inorganic phosphorus concentration (DIP), and secchi depth. These are the variables required to establish compliance with the SAV habitat criteria. Growing season medians were calculated for each year (varying growing season by salinity zone; Batiuk et al. 1992), then long term medians were taken for each site.

Application of multivariate analysis of variance (MANOVA) showed that water quality varied among these groups of sites (Hagy and Boynton 1997). Discriminant analysis was able to predict with some success which sites were AS, SN or UN sites on the basis of water quality at adjacent mid-channel water quality stations, but the parametric model exhibited spurious interactions among water quality variables that resulted from violations of model assumptions. Hagy and Boynton (1998) improved significantly upon this analysis using a non-parametric approach. This approach was able to classify 78% of AS or SN sites correctly and 76% of UN sites on the basis of the water quality variables that constitute the SAV habitat criteria. However, as noted by Hagy and Boynton (1998) the utility of this model for management purposes is reduced because it cannot be visualized graphically or summarized in a concise mathematical statement. Model performance could only be evaluated on the basis of performance. Like some kinds of simulation models, the explanatory power of the model is not great and it can only be used by those with access to the appropriate computer software (SAS in this case) and the knowledge to use it.

Methods

As in Hagy and Boynton (1997) and Hagy and Boynton (1998), SAV coverage data, tabled by USGS 7.5-minute quadrangle were used for this study. These data provide the best match of spatial resolution between water quality monitoring data and SAV coverage data. These data were obtained via the SAV Internet site at the Virginia Institute of Marine Science. Because the USGS 7.5-minute quadrangles vary enormously in the amount of potential SAV habitat within each one, it was not possible to analyze coverage data directly, for the same reasons noted by Hagy and Boynton (1997) and Hagy and Boynton (1998). A classification-based measurement of SAV abundance was used to avoid this problem. This approach applies a binary recoding to the SAV coverage

for any year and in any quad. Specifically, "0" indicates no SAV and "1" indicates SAV is present. Three categories of coverage describe the long-term status of SAV at any locations. "AS" indicates that in no year was SAV ever completely absent. "SN" indicates that in some years SAV was absent, but that it was present in more than 50% of the years. "UN" indicates that SAV was absent in more than 50% of the years. In addition to this coding system, frequencies of SAV presence were analyzed directly using CART regression models. This permits, for example, distinguishing a site that had SAV in all but 1 year (an "SN" site) from a site that had SAV in only 6 of 10 years (also an "SN" site), thereby retaining more information. Finally, the binary codes were analyzed directly using CART to determine if interannual changes in status could be related to water quality changes. In fact, sites changed status only a relatively small number of times, and such models did not yield useful results.

Water quality inputs to the models were generated in the same manner as reported by Hagy and Boynton (1997) and Hagy and Boynton (1998). Specifically, all water quality variables represent growing season medians of surface water quality, calculated as suggested for the SAV habitat criteria by Batiuk et al. (1992). Long-term water quality characterizations are medians of annual growing season medians.

Results and Discussion

Classification and Regression Tree Models for SAV

A series of analyses were conducted using CART classification models to see if greater predictive ability could be achieved than with discriminant analysis. Many different models could be constructed using CART, each with different variables, but similar predictive success. One such model assigned 82% of the AS sites and 75% of the UN sites correctly in a separate (resubstitution) test sample (Fig IV-1). Higher accuracy (>90%) was achieved for classifying the learning sample. This model divides all quads into 4 groups or "terminal nodes." When $DIP \leq 0.006 \text{ mg l}^{-1}$, 43 of 64 observations were AS sites and 80% of sites were either AS or UN. These sites had salinity from 0-22 ppt, but had a low average TSS, chlorophyll-a, and DIN and a high average secchi depth (Table IV-1). Among sites with $DIP > 0.006 \text{ mg l}^{-1}$, only 22 of 90 were AS sites. All of these had $TSS \leq 18.525 \text{ mg l}^{-1}$ and most were in lower salinity areas (Fig. IV-1). Thus, terminal node #2 sites (Fig. IV-1) consisted of higher-nutrient low salinity sites that tended to support SAV. Node #3 sites, which had salinity $> 7.958 \text{ ppt}$ had lower DIN and DIP concentrations, lower TSS, slightly higher chlorophyll-a and higher secchi depth than node #2 sites (Table 1), but 29 of 40 quads were UN sites. This reveals strong differences in water quality tolerances across salinity zones, to be discussed later. All but one of the 28 sites with $DIP > 0.006 \text{ mg l}^{-1}$ and $TSS > 18.525 \text{ mg l}^{-1}$ were UN sites. These sites all had salinity $< 12 \text{ ppt}$, and had lower DIN and DIP than node #2 sites. The accuracy of this model is comparable or superior to the non-parametric discriminant analysis, and was achieved with a simpler and easily visualized model. Three main conclusions can be reached from this model: (1) water quality criteria are different for

low salinity areas; (2) SAV does not survive, even in low salinity areas when $TSS > 18.5 \text{ mg l}^{-1}$, and (3) SAV presence is very likely when DIP is very low.

More focused models were developed by dividing the observations into salinity zones. In addition to removing the correlation among salinity and water quality, this approach recognizes the importance of different SAV species and growth-form differences associated with salinity zones. In particular, some low salinity species form a leaf canopy on the water surface, allowing them to receive more light than would be predicted by the depth of the water and water clarity (Batiuk et al. 1992). As an initial point of departure, the salinity zones associated with the SAV habitat criteria were used (<0.5 , $0.5-5$, $5-18$, >18 ppt). Subsequently, these were collapsed into three zones by combining the tidal fresh and oligohaline zones. Finally, initial data analysis for observations with salinity >5 indicated that major changes occurred not at 18 ppt, but perhaps at 12 ppt. This may reflect the near absence of SAV from the 5-12 ppt region. Including the 5-12 ppt observations with higher salinity sites re-introduces the problem of salinity-water quality-SAV correlations. Thus, CART models are presented below for three salinity zones - oligohaline (<5 ppt), mesohaline (5-12 ppt) and polyhaline (>12 ppt).

Tidal Fresh and Oligohaline SAV

Tidal fresh and oligohaline areas of Chesapeake Bay have been recognized as distinct habitats with regard to SAV by the establishment of different SAV habitat criteria for these areas (Batiuk et al. 1992). We examined the SAV habitat requirements in these areas using CART. There were 44 quads in which the average salinity was less than 5 ppt. Of these sites, 21 were UN sites, 4 were SN sites, and 19 were AS sites, as defined above (Figure IV-2, upper panel). While all the SAV habitat criteria were included as candidate variables, the final CART model included only two variables, TSS and DIP and two splitting rules (Figure IV-2, upper panel). The model correctly classified all the AS sites and 86% of the UN sites. TSS was the most important variable, although chlorophyll-a was also lower when TSS was lower and secchi depth was higher (Table IV-2). Among the 20 sites for which $TSS \leq 19.25 \text{ mg l}^{-1}$, 80% (16) were AS sites, and 15% (3) were SN sites. Among the 24 sites for which TSS was greater than 19.25 mg l^{-1} , 83% (20) were UN sites, 13% (4) were AS sites, and 1 site was an SN site. Among the higher TSS sites, all 3 AS sites were areas in which DIP was very low, less than 0.008 mg l^{-1} . These SAV beds, located in the Elk and Sassafras Rivers, and in creeks adjacent to the Gunpowder Rivers contained a variety of SAV species, but always included *Myriophyllum spicatum*, a canopy forming exotic species. This analysis shows that (1) TSS is an important variable for predicting SAV survival in oligohaline and freshwater habitats, (2) as measured in channel stations, slightly higher TSS than the SAV habitat criteria can be tolerated and (3) low DIP may be able to compensate for otherwise excessively high turbidity.

An equivalent regression tree analysis (Figure IV-2, lower panel) arrived at a similar conclusion. As with the classification tree, $TSS \leq 19.25 \text{ mg l}^{-1}$ was the primary splitting rule and $DIP \leq 0.008 \text{ mg l}^{-1}$ was a secondary splitting rule. Most sites with

TSS \leq 19.25 mg l⁻¹ had SAV in all years. Among those with higher TSS, those with DIP \leq 0.008 mg l⁻¹ usually had SAV, while those with higher DIP did not. Ironically, the lower DIP concentrations were also associated with very high chlorophyll-a (>40 μ g l⁻¹), suggesting that perhaps mid-channel phytoplankton facilitated SAV survival by outcompeting epiphytes for DIP while not adversely affecting the ability of the canopy forming SAV plants to obtain light.

Logistic regression was used as an alternative parametric technique for evaluating the same problem (Figure IV-3). In this analysis, a non-linear transformation (the LOGIT transformation) was used to relate the frequencies of binary events (SAV present or not) to continuous variables, in this case TSS. The model has a very satisfactory functional form and fit for this prediction problem. However, it appears that the discrete function suggested by CART may better fit the threshold type response evident in the data (Fig. IV-3). Moreover, the CART model effectively deals with the context-sensitive effect of DIP in this case.

Since all the water quality variables varied among terminal nodes, average values within each terminal node for each water quality variable are summarized in Table IV-2. Sites in terminal #1 typically had some SAV and on average experienced median water quality in compliance with the SAV habitat criteria. Note, however, that the primary splitting rule in the CART model, TSS \leq 19.25 mg l⁻¹ is the observed criteria for SAV presence, not the average value in node #1. Terminal #2 includes sites where summer phytoplankton biomass was very high, as was TSS. These sites had low secchi depth and therefore K_d far in excess of the habitat criteria. However, DIP concentrations were very low, and SAV persisted, probably in either very shallow waters or by forming a leaf canopy on the water surface. Sites in Terminal #3 rarely had any SAV and had excessively high TSS and chlorophyll-a. DIN and DIP concentrations were also higher. The SAV habitat criteria (Batiuk et al. 1992) for tidal fresh and oligohaline areas would partition into node #1, and therefore appear to ensure SAV survival. The requirement for TSS $<$ 15 mg l⁻¹ is prudent since this analysis does not distinguish between canopy-forming SAV and other species, nor does it indicate the requirements for SAV survival beyond the shallowest water to the 1 m depth contour.

Mesohaline and Polyhaline SAV

Unlike the low salinity areas in which about half of the sites were UN sites and half were AS sites, the mesohaline and polyhaline areas each had much greater concentration of one category. The mesohaline region had relatively few vegetated sites while the polyhaline region a greater number of vegetated sites. Because of the disparity in fraction of vegetated sites, empirical analyses that include both mesohaline and polyhaline sites tended to relate SAV presence to correlates of salinity, in the same manner as if tidal fresh sites were included, except in the opposite sense. Thus, mesohaline sites and polyhaline sites were considered separately. While Batiuk et al. (1992) defined mesohaline as 5 ppt - 18 ppt and polyhaline as > 18 ppt, initial analyses using CART suggest that factors explaining SAV presence changed when salinity was

greater than 12 ppt. Thus, the 110 quads in which salinity was > 5 ppt were divided into two groups, those with 5-12 ppt salinity (mesohaline) and those with salinity > 12 ppt (polyhaline).

Among the quads with salinity 5-12 ppt (mesohaline), 70% were UN sites. There were only 7 AS sites and 6 SN sites. This reduced the effectiveness of empirical approaches for identifying satisfactory water quality conditions for this salinity range compared to other salinity ranges. Like the low salinity regions, the primary splitting rule was based on TSS. In fact, if TSS was excluded from the model, no other variable or combination of variables could predict SAV coverage classes nearly as well. When $TSS > 15.75 \text{ mg l}^{-1}$, 93% of sites were UN sites, one was an SN site, and there were no AS sites (Figure IV-4). These sites also had, on average, chlorophyll-a, DIN and DIP in excess of the SAV habitat criteria (Table IV-4). Among sites with $TSS \leq 15.75 \text{ mg l}^{-1}$, most (57%) were still UN sites. However, the subset of these sites with chlorophyll-a less than 9.7 mg l^{-1} included more AS sites than UN sites. The AS sites in Terminal #1 include portions of Tilghman and Kent Islands bordering Eastern Bay, portions of Tilghman Island adjacent to Choptank River, several areas in the lower Potomac River, and a creek off the upper eastern shore of Chesapeake Bay. The AS sites in Terminal #2 include areas of the lower Chester River, lower Choptank River, and Eastern Bay. Overall, this analysis confirms the TSS habitat requirement of 15 mg l^{-1} for TSS in mesohaline areas, a more stringent requirement than for lower salinity areas. The other habitat requirements, particularly DIN and DIP, were not predictive when applied to these main channel water quality data. However, it is possible that if TSS and chlorophyll-a were reduced, that DIN and DIP would have to be reduced further to prevent epiphyte fouling.

Among quads with salinity greater than 12 ppt, 58% were AS sites, 30% were UN sites and 10% were SN sites. The CART classification model (Figure IV-5) classified 80% of UN sites and 95% of AS sites correctly, while erroneously classifying the 8 SN sites as either UN or AS sites. Unlike either of the lower salinity cases, the most primary splitting variable when salinity > 12 ppt was DIN. When $DIN > 0.11 \text{ mg l}^{-1}$, 12 of 15 sites were UN sites. The one AS site with $DIN > 0.11$ included creeks adjacent to the Deal Island State Wildlife Management Area on the Manokin River, perhaps indicating that more favorable water quality prevailed along this very natural shoreline. Of potential importance is the fact that $DIP \leq 0.01$ emerged as a nearly equivalent and successful splitting rule. For these data satisfying $DIP \leq 0.01$ implies $DIN < 0.11$, with the exception of very few observations. The primary importance of nutrients rather than TSS in the model suggests that in these higher salinity areas, epiphyte fouling may be a more important light attenuation mechanism than water column light attenuation. While TSS does appear as a splitting rule for the model (Figure IV-5), all sites with $TSS > 8.98 \text{ mg l}^{-1}$ had $DIP \leq 0.006 \text{ mg l}^{-1}$, and most had $DIP \leq 0.003 \text{ mg l}^{-1}$. The critical DIN nutrient concentration is slightly lower than the habitat criterion for DIN.

An analogous regression tree analysis, examining the percent of years with SAV vs. water quality suggests a slightly higher DIN criterion, $DIN \leq 0.119 \text{ mg l}^{-1}$ (Figure IV-6). Quads with DIN between the two criteria had intermittent SAV coverage, whereas

those with $\text{DIN} > 0.119 \text{ mg l}^{-1}$ were usually unvegetated in all years. A case by case examination of quads with $\text{DIN} \leq 0.110 \text{ mg l}^{-1}$, but with intermittent SAV coverage or no SAV coverage provides alternative explanations or hypotheses for the apparently nonsensical splitting rules on chlorophyll-a and TSS in Figure IV-6 (Table IV-4).

Integrated Model Performance

While the CART models were developed separately for each salinity region, their combined performance can be evaluated by forming a composite classification tree in which the first two splitting rules divide the observations into the appropriate salinity regions. Table IV-5 shows the predictive performance of the combined models, as well as the success of the CART model for each salinity region. When SAV was always present, the criteria established by the model were met 92% of the time. When SAV was not present, the criteria were not met 86% of the time. Thus, this model was highly successful for both predicting the present and absence of SAV on the basis of water quality variable.

Relationship Between This Study and Established Water Quality Criteria and Management Models

The SAV habitat criteria, as reported by Batiuk et al. (1992) are a good point of departure for the process of identifying water quality requirements for SAV and monitoring progress toward meeting those goals. Based on the present analysis, if water quality persisted at the limits of the habitat criteria for each variable in each salinity zone, SAV would be present where salinity < 5 ppt and where salinity > 12 ppt, but not in the mesohaline Bay. In the mesohaline reaches of the Bay, chlorophyll-a would have to be less than $10 \mu\text{g l}^{-1}$, a more stringent requirement.

This study and our earlier reports (Hagy and Boynton 1997, Hagy and Boynton 1998) have shown that the water quality variables that have been identified as SAV habitat criteria are intercorrelated. For example, in a principle components analysis, most of the variability is explained by two quantities, one of which is an index of nutrient concentrations (DIN, DIP), while the other is an index of water clarity indicators (chlorophyll-a, TSS, secchi depth). As a consequence, one can conclude that separate consideration of 5 habitat criteria can be confusing and even misleading, since the variables do not vary independently in the ecosystem. The joint importance of these factors has been expressed in recent research via the concept of "percent light at leaf." (Batiuk et al. 2000) This concept integrates the factors known to be the most important eutrophication impacts on SAV (but does exclude sediment oxygen stress, for example). Our results do not directly refute or support these results and associated models. Instead, we identify empirically the simplest water quality criteria that effectively predict long-term presence (i.e. survival) of SAV in different regions of Chesapeake Bay. Three significant strengths of such a simple model are (1) low data requirements, (2) easy of application, and (3) good communicability. Like any model, these models do not address all possible factors. Instead, they focus on ambient (mid-channel) water quality factors and neglect other factors that may affect SAV survival such as exposure and possible

feedback effects of SAV beds on nearshore water quality. The greatest management value of these models lies in their good combination of effectiveness and simplicity. For example, one need only know the growing season median TSS concentration to predict SAV presence in areas where salinity < 12 (Fig IV-2, Fig. IV-4), even though some information about other factors might improve the prediction somewhat. Similarly, for salinity > 12, one need only know the DIN concentration to predict SAV presence for the majority of locations (Fig IV-5). Again, more information will provide greater certainty. The strength of these models is that a great deal of information has been distilled to generate a simple pictorial representation that illustrates, from an SAV perspective, minimum water quality restoration goals for TSS and DIN in two major salinity zones (Table IV-6). More mechanistic approaches remain extremely valuable from both a scientific and management perspective, but these models show that sophisticated methods are not needed illustrate the strong relationships between SAV and water quality that are present in Chesapeake Bay.

Appendix IV-A: Introduction to Tree Structured Data Analysis

Tree-structured data analysis is a very promising alternative to traditional statistical analysis. Its advantages are particularly significant where larger databases are becoming more common and computer technology is bringing more computational capabilities to bear on data analysis. Tree-structured data analysis lends itself particularly well to "data mining" problems where many potential explanatory variables are being considered and one cannot be certain *a priori* which variables will be most important, how they may interact, and what the functional form of the relationships will be. Common applications include decision-making in the medical professions, credit-risk analysis, marketing, and investments. The science of ecology is a potential beneficiary of data analysis techniques and associated software driven by these profitable areas of the economy.

Since we have not evaluated tree-structured methodologies in general, we will focus the discussion at this point on the particular algorithm and associated computer software that we used. The CART, which stands for "Classification and Regression Trees," was developed and described at length by Breiman et al. (1984). As the name implies, the algorithm can address both classification problems with discrete variables and regression problems with continuous variables. Salford Systems, Inc. offers a commercially available implementation of CART in cooperation with the statistical researchers that developed the algorithm. This implementation provides a user-friendly graphical interface, simplifies the application of this powerful data analysis approach, and provides useful graphical and diagnostic output that aids in model building and evaluation. While referring the mathematically-inclined to Breiman et al. (1984), we undertake a more conceptual discussion of CART, drawing substantially on Steinburg and Colla (1995), the technical documentation provided with Salford Systems' CART implementation. Undoubtedly, some of the features of CART are also characteristic of other tree-structured approaches; however, we will describe them as features of CART and will hereafter refer to tree-structured data analysis as "CART."

Technically, the algorithm underlying CART can be called "binary recursive partitioning." Unlike some technical terms, this designation is particularly descriptive. CART begins with all of the data (observations) in a single group, or node. The observations are then divided into exactly two groups, hence "binary partitioning." These two groups are known as "child nodes." Allocation of observations to child nodes is determined by the answer to a "yes" or "no" question that pertains to one of the explanatory variables (or, optionally, a linear combination of several explanatory variables). This question is determined such that the distributions of observations on the target variable in the child nodes is as disparate as possible. In the case of a classification problem, the child nodes will differ in the frequency of the classes. In a regression context, the child nodes will have different mean or median values for the target variable. The term "recursive" applies because once observations have been allocated from the parent node to one of the two child nodes, the algorithm operates on the observations in the child nodes in the same manner. Each child node is considered a parent node, and then the observations are partitioned to one of two child nodes.

One of the more remarkable features of the CART algorithm is the manner in which the questions, or "splitting rules" are determined. Suppose that the data contain 1,000 observations on 5 explanatory variables. Then, there is a maximum of 5,000 possible splitting rules. To determine which rule partitions the observations optimally, CART simply tries all 5,000 candidate rules. If there are categorical variables among the explanatory variables, there will be less candidate rules, but the algorithm is identical. While this approach ensures that the algorithm finds the optimum splitting rule for the parent node, the algorithm cannot "look ahead" to determine which splitting rule which make the best model in the end. In particular, the algorithm cannot identify the most useful model. Thus, despite the power of the analytical algorithm there remains an essential role for use of scientific insight by the analyst. Ultimately teasing a useful model from CART requires careful work despite the apparently automatic nature of the algorithm.

CART continues the recursive binary partitioning, or "tree growing" process until nodes contain fewer than 10 observations or cannot be split further (e.g. all observations have the same value for the target variable.). In this manner the so-called "maximum tree" is produced. While more complex models always explain more variability among the observations, whether in CART or multiple regression, performance for new observations may not be as good as expected due to "overfitting." For this reason, algorithms to penalize overfitting of models (e.g. adjusted r^2 in multiple regression) have been developed. In CART, complex trees can simply be "pruned," eliminating first the least explanatory splitting rules. The basis for such pruning can be a user-specified trade-off between model complexity and amount of variability explained, or by comparing the performance of the model against a test dataset that is excluded from the analysis completely. This may be accomplished via cross-validation, often the more appropriate technique for smaller data sets. In CART, cross-validation sets aside a fraction of the observations (the default option is 10%), then generates a tree, calculating the error rates

on the test data. Subsequently, each of the other 9 groups containing 10% of the observations is utilized. Once the most complex tree has been developed, the optimal complexity is determined either by choosing the tree that makes the best predictions for the test data. The investigator may choose an even simpler tree, electing to sacrifice a small amount of explanatory power for a more easily interpreted model.

To avoid the appearance of over-enthusiasm, it is important to note some of the weaknesses of tree-structured data analysis relative to other techniques for data analysis. The most obvious weakness of tree-structured models is that their performance is poor when only a small number of observations are available. CART models may not work at all with insufficient data. While a parametric regression model with 10 or fewer observations may give precise predictions, success with CART is unlikely with so few observations. Generally, more than 100 observations are needed (Steinburg and Colla 1995). Moreover, if the data do satisfy the assumptions of parametric statistical models, or if prior mechanistic knowledge allows one to specify functional forms *a priori*, parametric modeling approaches may be more powerful. This leads to the possibility that CART can be used as a hypothesis generating tool, whereas more focused studies using traditional statistical approaches may be used to refine predictions and test hypotheses.

References

- Batiuk, R., R. Orth, K. Moore, W. Dennison, J. Stevenson, L. Staver, V. Carter, N. Rybicki, R. Hickman, S. Kollar, S. Bieber, and P. Heasley. 1992. Chesapeake Bay Submerged Aquatic Vegetation Habitat Requirements and Restoration Targets: A Technical Synthesis. US EPA Chesapeake Bay Program, Annapolis, MD.
- Batiuk, R. A., P. Bergstrom, W. M. Kemp, E. Kock, L. Murray, J. C. Stevenson, R. Bartleson, V. Carter, N. B. Rybicki, J. M. Landwehr, C. Gallegos, L. Karrh, M. Naylor, D. Wilcox, K. Moore, and S. Ailstock. 2000. Chesapeake Bay submerged aquatic vegetation water quality and habitat-based requirements and restoration targets: A second technical synthesis. US EPA Chesapeake Bay Program, Annapolis, MD.
- Breiman, L., J. Friedman, R. Olshen, and C. Stone. 1984. Classification and Regression Trees. Pacific Grove: Wadsworth.
- Hagy, J. D. and W. R. Boynton. 1997. Analysis of the relationship of submerged aquatic vegetation distribution to water quality distribution in Chesapeake Bay and tributaries. **In:** W. M. Kemp et al. Ecosystem Model of the Chesapeake Bay Relating Nutrient Loadings, Environmental Conditions, and Living Resources. US EPA Chesapeake Bay Program, Annapolis, MD.
- Hagy, J. D. and W. R. Boynton. 1998. Analysis of the relationship of submerged aquatic vegetation distribution to water quality distribution in Chesapeake Bay and tributaries. Chapter 3. **In:** W. M. Kemp et al. Ecosystem Model of the Chesapeake Bay Relating Nutrient Loadings, Environmental Conditions, and Living Resources. US EPA Chesapeake Bay Program, Annapolis, MD.
- Kemp, W. M., R. Bartleson, S. Blumenshine, W. R. Boynton and J. D. Hagy. 1998. Ecosystem models of the Chesapeake Bay relating nutrient loadings, environmental conditions, and living resources. US EPA Chesapeake Bay Program, Annapolis, MD,
- Steinburg, D. and P. Colla. 1995. CART: Tree-Structured Non-Parametric Data Analysis. San Diego, CA. Salford Systems.

Table IV-1. Averages of growing season median water quality in each of the terminal nodes established in the CART model in Figure IV-1.

Variable	Terminal #1	Terminal #2	Terminal #3	Terminal #4
Number of Quads	64	22	40	29
% AS Sites	67%	73%	15%	0%
Salinity Range (ppt)	0-3,11-22*	0-7.92	7.99-27	0-12.57
Chlorophyll-a ($\mu\text{g l}^{-1}$)	12.02	6.86	10.77	17.96
Total Suspended Solids (mg l^{-1})	11.56	14.93	11.21	28.04
Dissolved Inorganic N (mg l^{-1})	0.120	0.914	0.144	0.355
Dissolved Inorganic P (mg l^{-1})	0.004	0.030	0.012	0.020
Secchi Depth (m)	1.32	0.689	1.16	0.475

* Salinity distribution is bi-modal, with no sites where salinity is 3-10 ppt.

Table IV-2. Averages of growing season median water quality in each of the terminal nodes established in the CART models in Figure IV-2.

Variable	Terminal #1	Terminal #2	Terminal #2
Number of Quads	20	6	18
% Years Vegetated	Med = 100	Med = 90	Med = 0
Chlorophyll-a ($\mu\text{g l}^{-1}$)	8.0	38.4	20.89
Total Suspended Solids (mg l^{-1})	14.2	25.67	28.64
Dissolved Inorganic N (mg l^{-1})	1.02	0.125	0.48
Dissolved Inorganic P (mg l^{-1})	0.023	0.004	0.020
Secchi Depth (m)	0.69	0.35	0.46

Table IV-3. Averages of growing season median water quality in each of the terminal nodes established in the CART classification model for the mesohaline (salinity 5-12 ppt) region. Median percentages of vegetated years are shown for a nearly equivalent CART regression model; however, in the regression model the secondary splitting rule is $\text{chl-a} \leq 7.053 \mu\text{g l}^{-1}$.

Variable	Terminal #1	Terminal #2	Terminal #3
Number of Quads	9	19	15
% AS Sites	44%	16%	0%
% Years Vegetated	Med = 100%	Med = 20%	Med = 0%
Chlorophyll-a ($\mu\text{g l}^{-1}$)	7.14	15.56	16.42
Total Suspended Solids (mg l^{-1})	11.53	10.45	22.25
Dissolved Inorganic N (mg l^{-1})	0.373	0.135	0.191
Dissolved Inorganic P (mg l^{-1})	0.028	0.007	0.018
Secchi Depth (m)	0.98	1.12	0.63

Table IV-4. Locations of quads with $DIN \leq 0.11 \text{ mg l}^{-1}$ but with no SAV in some or all years and hypotheses suggesting an alternative explanation or hypothesis to a water quality based classification. Two exceptions are three sites in Patuxent River where exceptionally high chlorophyll-a concentrations, a water quality based explanation may have caused the lack of SAV.

Quad	Location	DIN	% Yrs. w/SAV	Alt. Hypothesis/Explanation
143, 186	Cape Charles, Fisherman's Is.	0.017	50	High energy environment
90	Cape Lookout	0.040	10	High energy, low habitat availability
81	Pt. No Point	0.050	0	High energy, low habitat availability
82	Richland Pt. (nr Honga R.)	0.050	80	Small persistent beds, disappeared 94-96
98	Smith Point	0.051	0	High energy environment
177	New Point Comfort, VA	0.051	80	Small potential habitat
60	Patuxent River	0.056	20	High chlorophyll-a
61	Patuxent River / Calv. Cliff	0.055	30	High chlorophyll-a (Pax), exposure (Calv. Cliffs)
151	Little Creek	0.064	20	Exposure, Development in Creek?
102	Beasley Bay nr. Pocomoke R.	0.068	70	High TSS
70	Patuxent River	0.084	20	High Chlorophyll-a
72	Barren Island, MD	0.086	70	Disappeared 94-96
178	Bethel Beach, VA	0.103	50	High Energy Environment

Table IV-5. CART model performance data (confusion matrices) for the composite model (top group) and for each of the salinity-zone specific models.

Actual Class	Predicted Class			% Correct
	All Salinity Regions			
	UN	SN	AS	
UN	60	0	11	85
SN	6	0	12	0
AS	4	0	60	94
Tidal Fresh/Oligohaline (≤ 5 ppt)				
UN	18	0	3	86
SN	0	0	4	0
AS	0	0	19	100
Mesohaline (5-12 ppt)				
UN	27	0	3	90
SN	4	0	2	0
AS	3	0	4	57
Polyhaline (>12 ppt)				
UN	15	0	5	75
SN	2	0	6	0
AS	1	0	38	97

Table IV-6. CART model-based habitat criteria for three salinity zones of Chesapeake Bay and tributaries describing necessary, but not necessarily sufficient mid-channel water quality conditions likely to lead to SAV growth and survival in adjacent littoral zones.

	TSS	Chl-a	DIN	DIP
Tidal Fresh/Oligohaline	$\leq 19 \text{ mg l}^{-1}$	-	-	≤ 0.008 if TSS $> 19 \text{ mg l}^{-1}$
Mesohaline	$\leq 15 \text{ mg l}^{-1}$	$\leq 9 \text{ } \mu\text{g}^{-1}$	-	-
Polyhaline	-	-	$\leq 0.1 \text{ mg l}^{-1}$	$\leq 0.006 \text{ mg l}^{-1}$

Classification Tree

Target Variable: SAV Coverage Class

Explanatory Variables: TSS, Chlorophyll-a, DIP, Secchi Depth

Restrictions: None

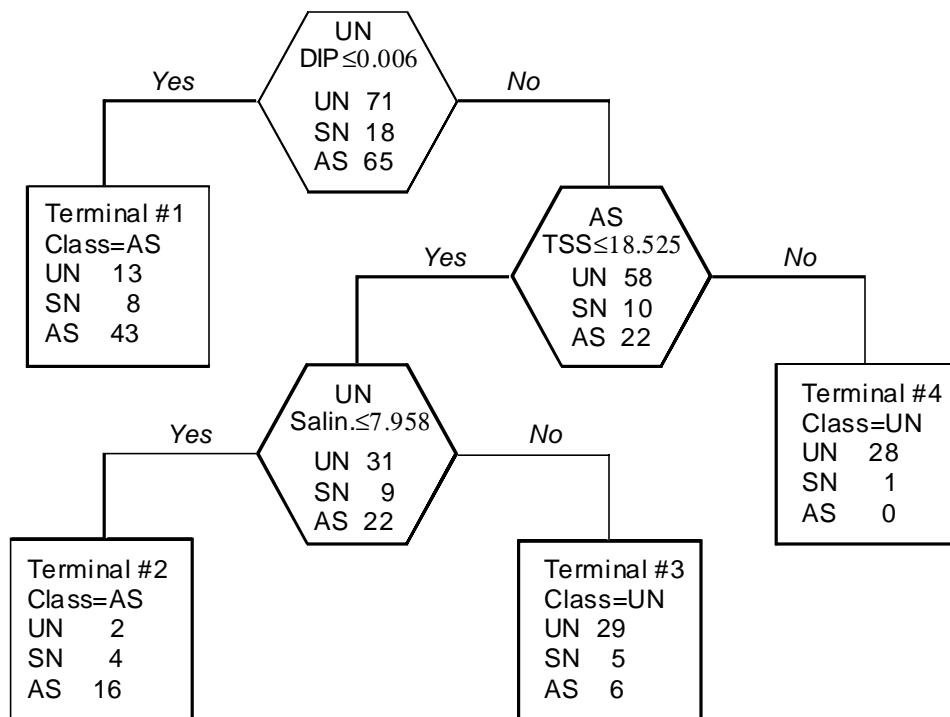


Fig. IV-1. CART Classification tree for Chesapeake Bay and Tributaries. All concentrations are growing season medians. For proper interpretation of the model, it must be recognized that the distribution of all variables may differ among nodes, not just those noted in the splitting rule. Average water quality values for each terminal node are in Table IV-1.

Classification Tree

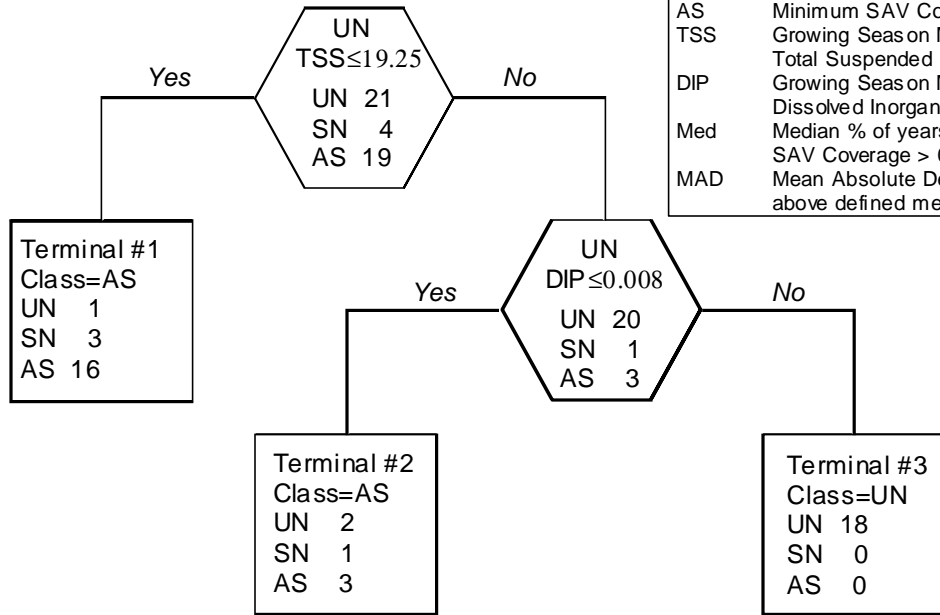
Target Variable: SAV Coverage Class

Candidate Explanatory Variables: TSS, Chla, DIN, DIP, Secchi

Restrictions: Salinity < 5

Definition of Terms:

UN	Median SAV Coverage = 0
SN	Minimum SAV Coverage = 0, Median > 0
AS	Minimum SAV Coverage > 0
TSS	Growing Season Median Total Suspended Solids
DIP	Growing Season Median Dissolved Inorganic Phosphorus
Med	Median % of years with SAV Coverage > 0.
MAD	Mean Absolute Deviation from the above defined median value



Regression Tree

Target Variable: Percent of Years (1986-1997) SAV Coverage > 0.

Candidate Explanatory Variables: TSS, Chla, DIN, DIP, Secchi

Restrictions: Salinity < 5

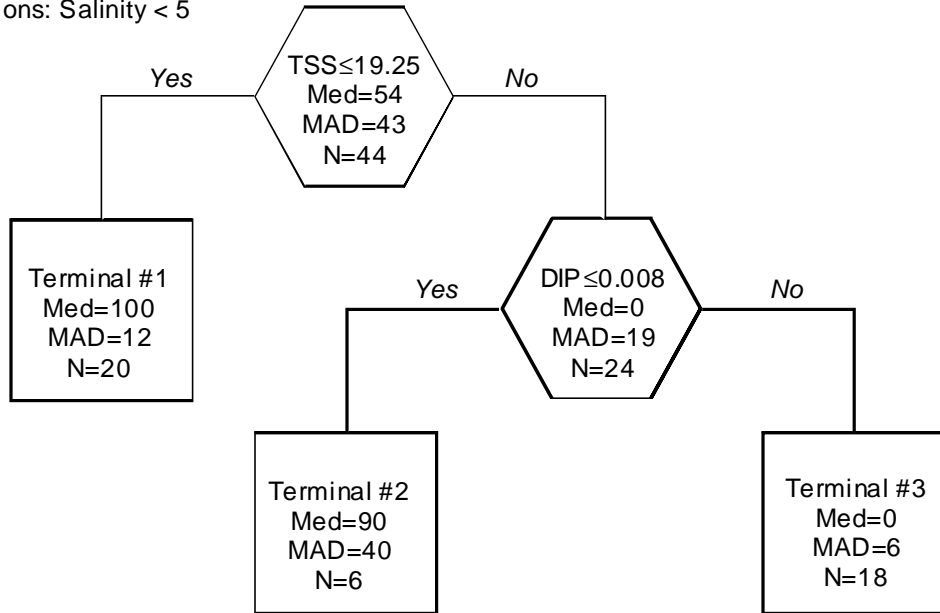


Fig. IV-2. For areas with salinity < 5, equivalent classification (upper) and regression (lower) tree models relating median water quality at nearby Chesapeake Bay Monitoring Program stations to the presence and persistence of SAV in nearby shallow water areas.

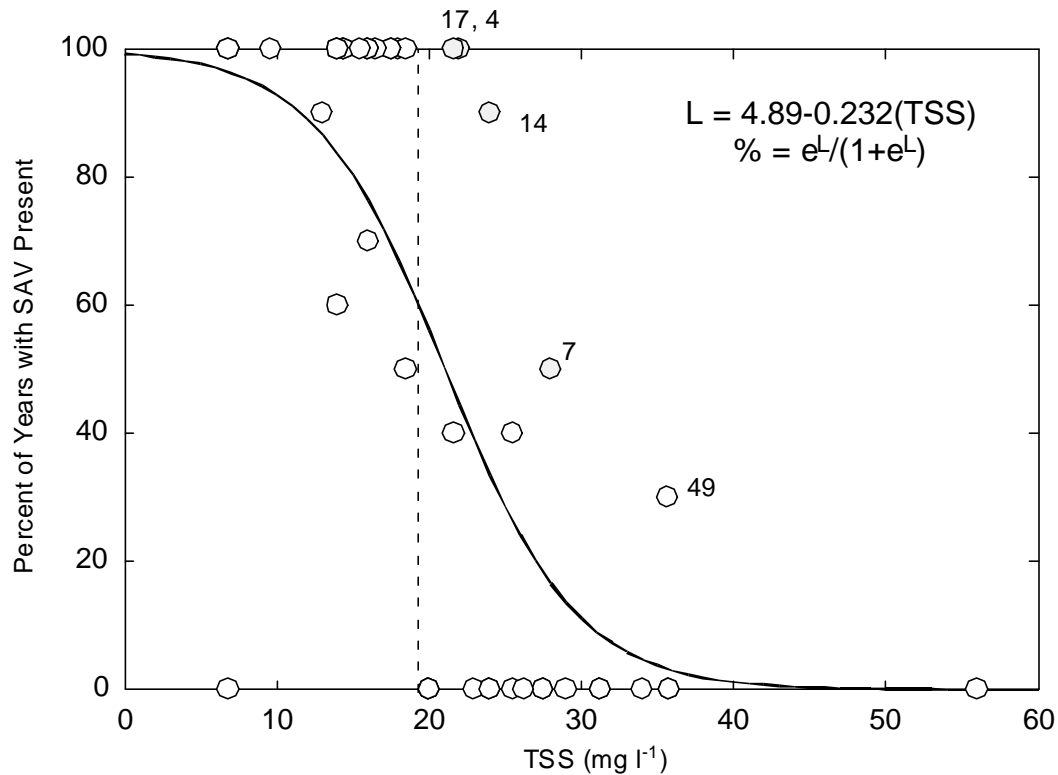


Fig. IV-3. For sites with salinity < 5, a logistic regression relating the percentage of years between 1986 and 1997 in which SAV was present in a quad to the median growing season TSS concentration in a mid-channel water quality monitoring station nearest to the quad. The vertical line indicates the 1st splitting rule for the CART model relating percentage to TSS (Figure 2, lower panel). The value "L" denotes the logit transformed percentage, which is linearly related to TSS. The non-linear backtransformation is shown beneath. Quads with unexpectedly high SAV presence are enumerated and shaded. Quads 4 (Elk River), 17 (Sassafrass River), 14 (Creeks off of Gunpowder River) and 7 (off of Bush River) had very low median DIP (DIP = 0.004 mg l⁻¹). Quad 49 is in the Patuxent River near Benedict and may have supported SAV only in years where water quality was better than suggested by the long term median value.

Classification Tree

Target Variable: SAV Coverage Class

Candidate Explanatory Variables:

TSS, Chl-a, DIP, Secchi

Restrictions: Salinity 5-12 ppt

Definition of Terms:

UN	Median SAV Coverage = 0
SN	Minimum SAV Coverage = 0, Median > 0
AS	Minimum SAV Coverage >0
TSS	Growing Season Median Total Suspended Solids
Chl-a	Growing Season Median Chlorophyll-a

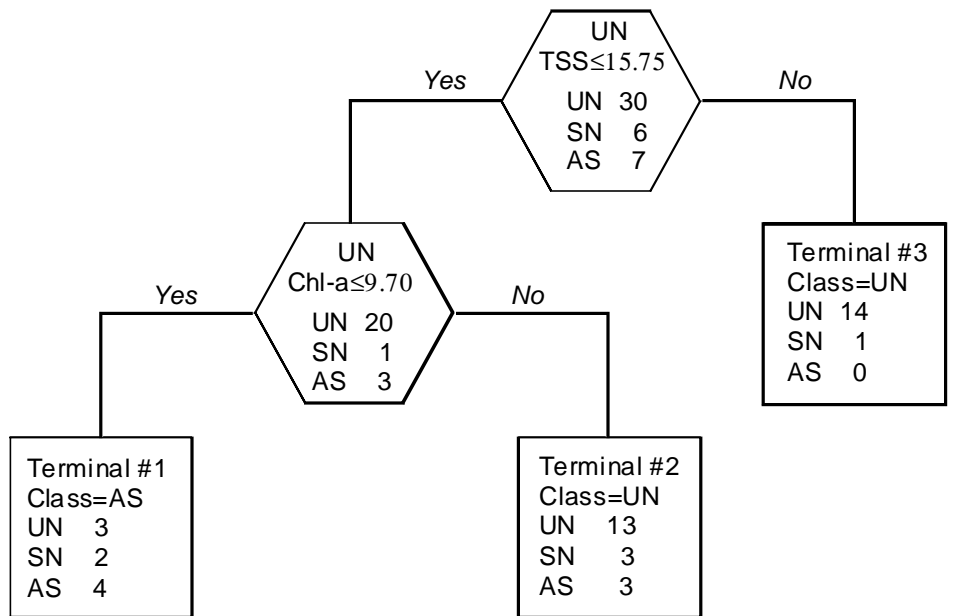


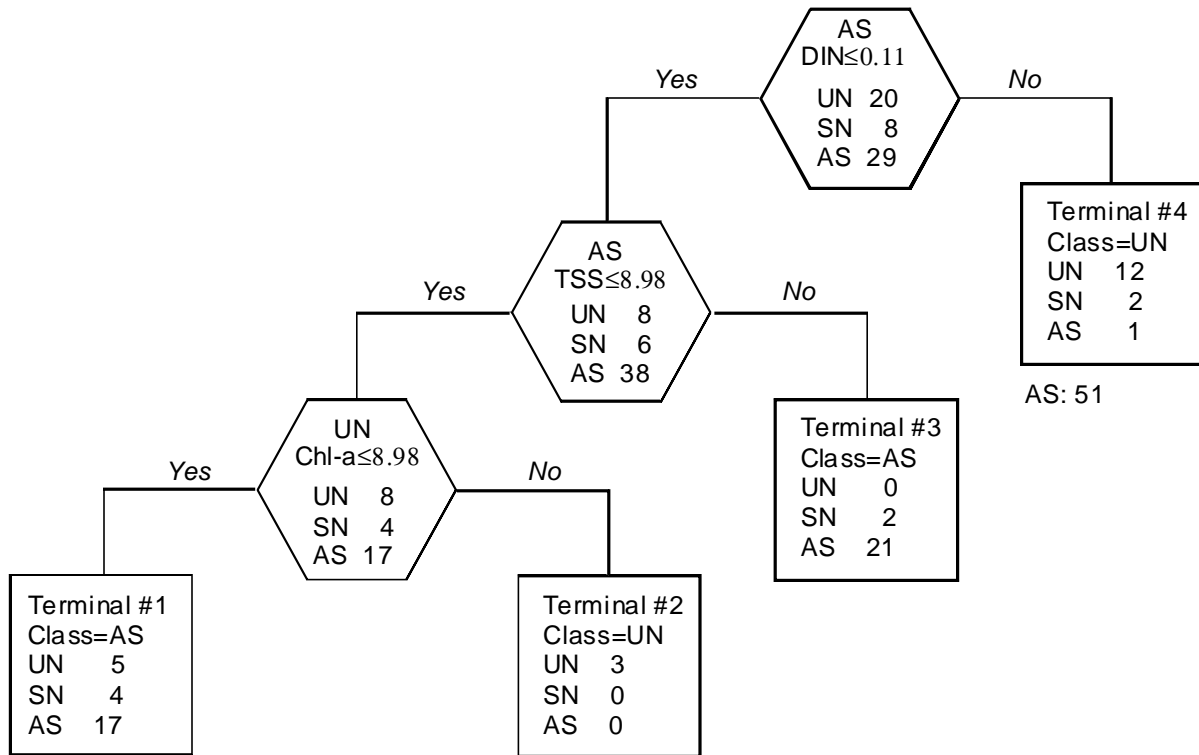
Fig. IV-4. For areas with salinity 5-12 ppt, classification tree models relating median water quality at nearby Chesapeake Bay Monitoring Program stations to the presence and persistence of SAV in nearby shallow water areas. DIN was eliminated from the model because it replaced chlorophyll-a due to correlation, resulting in a non-sensical prediction (i.e. higher DIN, more SAV).

Classification Tree

Target Variable: SAV Coverage Class

Explanatory Variables: TSS, Chlorophyll-a, DIN, DIP, Secchi Depth

Restrictions: Salinity > 12 ppt



UN: 61, 81, 98,
151, 186

Fig. IV-5. CART Classification tree for high salinity (>12 ppt). Exceptional quads are noted by quad number. Quad 51=Little Choptank R., MD; Quad 61=Patuxent R., MD; Quad 81=Point No Point, MD; Quad 98=Smith Pt. MD/VA; Quad 151=Little Creek, VA; Quad 186=Fisherman's Island, VA. Locations and boundaries can be found in Orth et al. (1992 or other years).

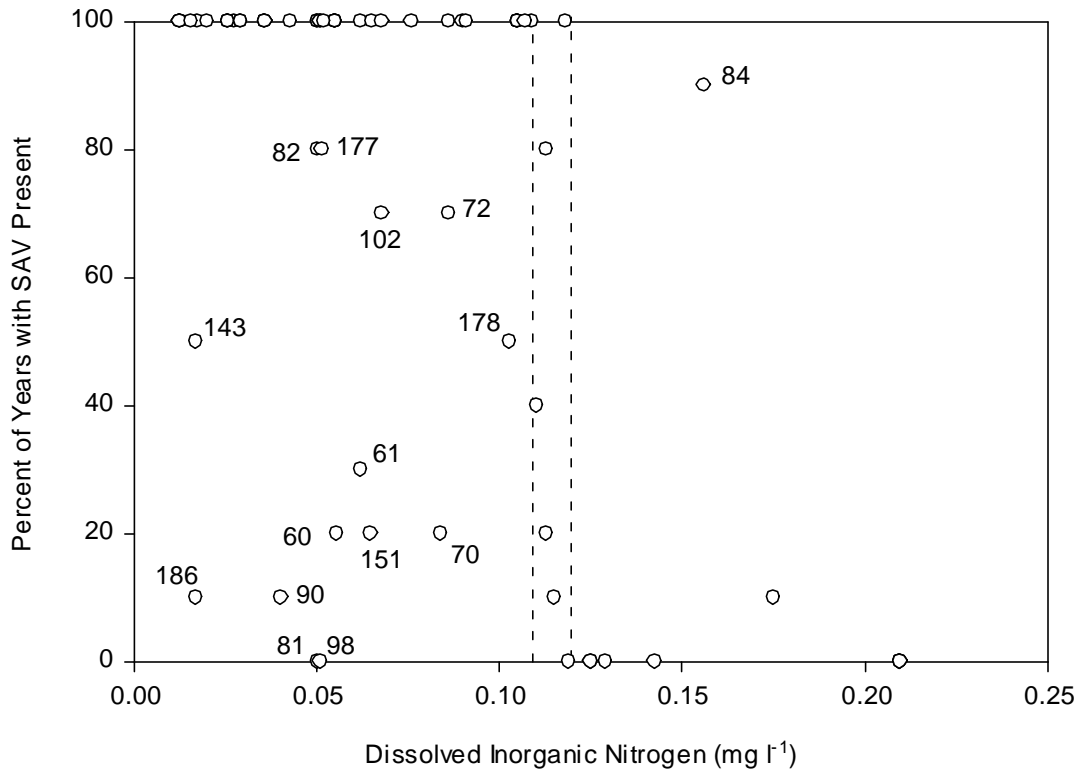


Fig. IV-6. The percentage of years from 1986-1996 in which SAV was present in quads with salinity > 12 ppt related to dissolved inorganic nitrogen (DIN) concentration by a CART model. The two vertical lines indicate the splitting rules identified by CART on DIN. Numbers adjacent to observations indicate quad numbers which may be referred to Table 3.

Chapter V

Controls on Hypoxia in Chesapeake Bay and its Major Tributaries

J. D. Hagy and W. R. Boynton

Abstract

Persistent summertime hypoxia is a major feature of Chesapeake Bay and most, but not all of its major tributaries. Among the affected estuaries, the intensity, extent and duration of hypoxia vary from year to year. To examine the factors affecting the differences among basins and across years for the same basin, the effect of mean depth, total nitrogen loading, total phosphorus loading, and freshwater residence time were evaluated using up to a 10-year record of hypoxia. A unique way of scaling time-space integrals of hypoxia was developed to remove the effect of basin size and permit comparative analysis of hypoxia in 6 distinct but morphologically similar Chesapeake Bay estuaries. A sigmoidal function of mean depth explained a large proportion of the variability in long-term mean levels of hypoxia. Estuaries became substantially more vulnerable to hypoxia as their mean depth increased from 5 to 7 meters. Interannual differences in hypoxia were explained by TN loading rate, but not by TP loading rate or freshwater residence time. This suggests that under present loading regimes, management efforts to reduce hypoxia should focus strongly on reducing TN loading rates. A $10 \text{ g N m}^{-2} \text{ y}^{-1}$ change in TN loading rate, approximately the range observed for most of the systems considered, resulted in a substantial change, 25 on a 0-100 scale, in the expected level of hypoxia. While this change would be significant, this model suggests that likely reductions in TN loading rates due to management actions will not eliminate hypoxia in most cases. This is supported by historical evidence of hypoxia in the deepest channels; however, there is also evidence to suggest that ecosystem feedback responses would enhance any management-driven improvement in oxygen conditions.

Introduction

Persistent summertime hypoxia in sub-pycnocline waters is a common feature in Chesapeake Bay and the sub-estuaries at the seaward ends of its tributary rivers. Such hypoxia, defined here as the depletion of dissolved oxygen to concentrations less than 3 mg l^{-1} for periods of longer than 24 hours, generally forms in these estuaries in late spring to early summer and begins to dissipate in late summer or early fall. It is of particular interest because the habitat loss, loss of benthic and pelagic productivity, and adverse biogeochemical changes associated with hypoxia and especially anoxia (zero oxygen) are among the major impacts of nutrient pollution in estuaries.

Despite the fact that the Chesapeake Bay and its sub-estuaries are all typical temperate, partially-stratified estuaries, they are different in important ways and experience hypoxia to different degrees. In addition, hypoxia in any one estuary tends to vary interannually. With this in mind, we undertook a comparative analysis to examine

several hypotheses regarding factors affecting hypoxia in these estuaries. These hypotheses all derive from the simple idea that hypoxia results when the local respiratory demand of the ecosystem exceeds the local supply of oxygen. Thus, two main factors, water column stratification and oxygen demand, are expected to drive the development of hypoxia. Many factors can contribute to changes in both of these main factors, however. In particular, factors affecting water column stratification include basin morphology including water depth, river discharge rates, tidal circulation, and wind events. Oxygen demand is also a product of many factors, but a major influence is the amount and chemical lability of the organic matter supplied to heterotrophic organisms, especially bacterial decomposers in the lower water column. In the regions of Chesapeake Bay and its sub-estuaries where hypoxia develops, generally the mesohaline zones, the largest component of the organic matter supply is phytoplankton production within the estuary by phytoplankton (Kemp et al. 1998). Thus, the many factors affecting phytoplankton productivity are all implicated in regulating hypoxia. This includes nutrient recycling processes.

This conceptual model for controls on hypoxia illustrates why hypoxia has been and should continue to be an important organizing issue for environmental management in estuaries subject to hypoxia. The ecosystem processes that affect hypoxia include many of the important abiotic and biotic features of estuarine ecosystems, especially those related to primary production and biogeochemical cycling. Moreover, the consequences of hypoxia may exert feedback effects on the lower consumer trophic levels and direct and indirect effects on upper trophic levels through habitat limitation and trophic effects cascading through the ecosystem. Although hypoxia is invisible to the average Bay visitor, breezing across the Chesapeake Bay bridge, and while it is more abstract than fish harvests or acreage of SAV, hypoxia is a very tangible consequence of nutrient enrichment. It is without a doubt a major factor structuring any estuarine ecosystem affected by it. Even if disguised in terms more engaging to public policy makers, decisions regarding nutrient loading reductions should be informed by knowledge of the requirements for reducing the incidence of hypoxia. This study addresses that need by directly examining the relationship between nutrient inputs and the incidence of hypoxia in Chesapeake Bay and 6 of its tributaries.

Methods

We applied a series of algorithms to precisely quantify hypoxia and the factors that were hypothesized to regulate it. Regression models were applied to test and quantify the effect of each factor (explanatory variable) on hypoxia, as well as to examine if interacting effects of several factors were important. The definitions and quantification procedures used are described below.

Hypoxia

Hypoxia can be characterized in three main ways: intensity, or the actual oxygen concentration, spatial extent, and temporal extent. The oxygen concentration at which one considers water to be hypoxic is somewhat arbitrary since some species exhibit

behavioral avoidance at a relatively high threshold, while other species can tolerate hypoxia very well and can even endure brief periods of anoxia. We chose a relatively generous 3 mg l^{-1} as an upper limit. Since the extent of more intense hypoxia (e.g. < 1 or $< 2 \text{ mg l}^{-1}$) often occurs proportionally, this choice preserves more information than a narrower definition. To quantify the amount of hypoxia, we calculated the volume of water on each cruise date with a dissolved oxygen concentration less than 3 mg l^{-1} from a 2-D interpolated profile of dissolved oxygen. Cross-sectional volumes obtained from tabulated data in Cronin and Pritchard (1975) were used to extrapolate the 2-dimensional profiles to three-dimensional volumes. This yields so-called "hypoxic volumes." Hypoxic volumes encompass the intensity and extent of hypoxia. To quantify the duration as well, hypoxic volumes were integrated through a period of one year. All the dissolved oxygen data were obtained from the Chesapeake Bay Water Quality Monitoring Program.

This time-space integral yields a large quantity which, lacking a quantitative benchmark, can be interpreted only as a relative measure indicating interannual variability in the extent of hypoxia. Especially troublesome is that these values cannot be compared among estuaries because they depend on the size of the estuary. To arrive at a simple benchmark, we estimated the maximum value that this time-space integral could attain given two very uniform properties of estuaries. These are: (1) seasonal permanent hypoxia tends to only occur below the pycnocline and (2) hypoxia generally occurs only during summer, usually for a period of about 90-120 days. Furthermore, the typical relationship between depth and volume of estuaries in the Chesapeake Bay region (i.e. the hypsography) indicates that about 25% of the volume of the estuary is below the pycnocline. Thus, our benchmark "maximum likely hypoxia" is quantified as 25% of the volume of the estuary multiplied by 90 days. It is not important that the spatial or temporal assumption be exactly correct. The analysis would not be invalid if hypoxia occurred for more than 90 days or over a greater extent than 25% of the estuarine volume. The important fact is that the size-dependence of the quantity is effectively removed and that the resulting measure has a direct interpretation. In summary, our index of hypoxia, a time-space integral of the hypoxic volume scaled to a benchmark maximum, is a ratio that nominally (but not strictly) varies between zero and one and represents the percentage realization of the likely worst-case scenario for hypoxia. Zero represents zero hypoxia while 1 is the worst-case scenario. Hereafter, "hypoxia" refers to this scaled, time-space integrated measure of hypoxia.

Four factors were evaluated as potential regulators of hypoxia. These factors include the total nitrogen (TN) and total phosphorus (TP) loading rates, the residence time of freshwater (FRT), and the mean depth (\bar{z}) of the estuary. Estimates were averaged over the "water-year" which spans October through September, rather than the calendar year because nutrient and freshwater inputs occurring after hypoxia has abated could not reasonably affect the extent of hypoxia. The methods for calculating these values are described below.

Total Nitrogen and Total Phosphorus Loading Rates.

TN and TP loading rate estimates are routinely estimated by the USGS Chesapeake Bay River Inputs Monitoring Program (RIMP) and by the Chesapeake Bay Watershed Model (US EPA). The RIMP estimates nutrient inputs at the fall lines of 9 major tributary rivers of Chesapeake Bay. These rivers include the Appomattox, James, Mattaponi, Pamunkey, Rappahannock, Potomac, Patuxent, Choptank, and Susquehanna. Daily nutrient concentrations at the fall line are estimated from a less frequent and irregular time series of observations using a 7-parameter log-linear model (Cohn 1989). Because a disproportionate amount of nutrient loading occurs during peak flow events and loads associated with these events are difficult to estimate, there is a significant, but quantified, uncertainty associated with fall line nutrient loading rate estimates.

Below fall line nutrient loading and freshwater input rate estimates were obtained from the Chesapeake Bay Watershed Modeling program. The watershed model combines an HSPF (Hydrologic Simulation Program - FORTRAN) simulation with an extensive database of land use information, nutrient yield information, point source nutrient inputs and other data. The output includes estimates of freshwater flow and nutrient inputs delivered to the head of tide of each of many Chesapeake Bay watershed segments. Two main types of simulations have been run. The first type estimates changes in loading rates as a result of changes in land-use practices under an assumption of constant hydrologic conditions. The second type, which we used, is a simulation of nutrient input rates assuming constant land-use practices but varying hydrologic conditions. These model outputs were selected because, over the short term, hydrologically-driven variability in loads is greater than that caused by land-use changes. All CB Watershed Model runs are extremely computationally intensive, requiring hours of computing time on Cray supercomputers; therefore, we requested and received nutrient loading estimates generated by previously run simulations (P. Wang, personal communication).

Water-year (October-September) means of above and fall line freshwater and nutrient input rate estimates were combined to obtain rates for the whole estuary. The total nutrient input rates were expressed relative to the surface area of the estuary to obtain nutrient input rates comparable across estuaries.

Residence Time of Freshwater Water

The residence time of freshwater (FRT) was estimated using the fraction-of-freshwater approach of Dyer (1973). This approach actually yields the freshwater replacement time, which is equal to the residence time of freshwater when salinity is at steady state. This condition is nearly met on annual time scales, the scale used here. When salinity is at steady state, this approach yields the same residence time estimates as are obtained via the much more detailed box model approach of Hagy (1996). The required inputs for the fraction of freshwater method are the mean salinity within the

estuary (S_{in}) and at the seaward margin of the estuary (S_{out}), the volume of the estuary (V) and the freshwater input rate (Q_f). The fraction of freshwater is calculated as

$$V_f = \left(\frac{S_{out} - S_{in}}{S_{out}} \right) V \quad (1)$$

and the residence time (T) is given by

$$T = \frac{V_f}{Q_f} \quad (2)$$

The mean salinity was calculated from a 2-dimensional interpolated salinity profile, with all salinity data obtained from the Chesapeake Bay Water Quality Monitoring program. The correct extrapolation from a 2-dimensional profile to the 3-dimensional average salinity was determined using tabulated cross-sectional volume data in Cronin and Pritchard (1975).

Volume, Surface Area, and Mean Depth

The volumes and surface areas for each estuary were calculated from data tabulated in Cronin and Pritchard (1975). Therefore, the assumed estuary boundaries were based on exactly the same boundaries delineated therein. The Chesapeake Bay volume and surface area does not include the tributaries or the Tangier Sound region as defined in Cronin and Pritchard (1975). Mean depth was calculated from the ratio of volume to surface area for the region of each estuary covered by the interpolated oxygen and salinity fields, which also corresponds to the region for which tabulated volume and cross-sectional width data were available in Cronin and Pritchard (1975).

Results and Discussion

Hypoxia vs. Mean Depth

There are many reasons that one should expect mean depth to affect the propensity for an estuarine system to develop hypoxia. All are related to the ability of the system to transport oxygen from the water surface to the location of oxygen demand. First, a deeper system has more volume within which respiration can occur relative to the surface area across which oxygen may diffuse to supply the demand. A deeper system most likely also has a larger fraction of aphotic waters that always consume oxygen. Finally, and potentially of greatest importance, a deeper estuary is more likely to have a stratified water column. This is true for at least three reasons. One reason is that mixing caused by wind-driven surface waves is attenuated with depth, increasing the potential for water column stratification in estuaries deep enough that a significant portion of the

water column is beyond the reach of surface mixing. Similarly, turbulent mixing caused by shear stress associated with currents at the sediment-water interface is dissipated with increasing height above the sediment surface, also contributing to greater potential for stratification in deeper water columns. Finally, where two layer circulation is present, a deeper water column has more capacity to dissipate internal shear stress at the pycnocline. Regardless of the mechanism, deeper water columns are more likely to have downward oxygen transport inhibited by water column structure, leading to depletion of oxygen if ecosystem respiration exceeds the oxygen transport rate.

As mean depth increased, hypoxia increased according to a sigmoidal function with 50% hypoxia reached at a mean depth of 5.3 m and 95% reached at a mean depth of 9 m. (Fig. V-1). This function, fitted with non-linear least squares regression, is

$$H = -0.099 + \frac{1.057}{1 + e^{-1\left(\frac{\bar{z}-5.088}{0.787}\right)}} \quad (3)$$

where H is hypoxia and \bar{z} is the mean depth in meters. Model fit is excellent (Fig. V-1) but cannot be quantified using the coefficient of determination (i.e. r^2) because of the non-linearity of the model (Kvalseth 1985). In the James River, which averages about 3 m in depth, hypoxia was essentially absent. Similarly, the Choptank River, which has a mean depth of 4.9 m, has essentially no hypoxia. Because an interpolator has not been developed for the Choptank River, hypoxia was not explicitly calculated for the Choptank River; however, dissolved oxygen was rarely less than 3 mg l⁻¹.

The mean depth of an estuary is clearly an important factor affecting its sensitivity to hypoxia; however, interannual variability makes it clear that other factors are also important. For example, hypoxia in Patuxent River varied between 0.27 and 1.00 during 1986 to 1996. We hypothesized that these interannual differences were related to nitrogen and phosphorus input rates and that the responses to these inputs were modified by the residence time of freshwater.

Hypoxia vs. Total Nitrogen (TN) Loading

Several different models were used to evaluate whether there was an effect of TN loading on hypoxia in the 5 sub-estuaries and Chesapeake Bay, while factoring out the known differences in mean hypoxia among the basins. An analysis of covariance (ANCOVA) model found a significant positive effect ($p < 0.01$) of TN loading on hypoxia. The slope of this relationship indicates that for a 10 g N m⁻² y⁻¹ increase in TN loading, hypoxia increased by 0.25±0.06 (mean ± std err) on the 0 to 1 scale, or 25% (Fig. V-2). Given that interannual variability in TN loading encompassed that range or larger in almost all the basins, this indicates a significant response to TN loading within basins. No among-basin differences in the response of hypoxia to TN loading could be detected statistically. Clearly, such a difference exists, since the James River had no hypoxia in any year. Recognizing this issue, the model was re-run without including the James River observations. The conclusions were largely unchanged. The estimated

response of hypoxia to TN loading was slightly higher, 0.28 ± 0.06 per $10 \text{ g N m}^{-2} \text{ y}^{-1}$. There remained no significant difference in the response to TN loading among basins, however.

The ANCOVA model described above modeled the differences among basins as a categorical or class variable, maximizing the ability of the model to detect differences due to TN loading. There are several shortcomings to this linear modeling approach. First, the model treats each system as a unique system, except with regard to the effect of TN loading rate. The model does not combine the effect of mean depth and TN loading into a single expression. This precludes adding additional estuaries to the model. A second shortcoming is that the linearity of the model does not effectively address the fact that hypoxia cannot be less than zero, nor can it be substantially greater than 100% (slightly greater than 100% is possible). To address both these shortcomings, TN loading was added, as an additional effect within the sigmoidal model developed to relate hypoxia to mean depth. The resulting model is

$$H = -0.29 + \frac{1.25}{1 + e^{-F(\bar{z}, TN)}} \quad (4)$$

where

$$F(\bar{z}, TN) = \frac{1}{1.016} (\bar{z} + 0.065TN - 5.66) \quad (5)$$

and \bar{z} is the mean depth in meters and TN is the total nitrogen loading rate in $\text{g N m}^{-2} \text{ y}^{-1}$. For this model, the effect of an increase or decrease in TN loading rate depends on the both the mean depth of the estuary and the level of TN loading before the change (Fig. V-3). The effect of changes in the TN loading rate is greatest for estuaries with an intermediate mean depth, TN loading rate, and average level of hypoxia. Consistent with the sigmoidal functional form, a smaller slope occurs at either extreme near the asymptotes.

Hypoxia vs. Total Phosphorus (TP) Loading

An ANCOVA model identical to the one described for TN loading was used to evaluate the effect of TP loading on hypoxia in these estuaries. As with TN loading, a positive and statistically significant effect was observed ($p < 0.01$). However, unlike the case of TN loading, there were significant differences among basins in the response to TP. Specifically, there was a relationship between TP and hypoxia for Patuxent River and York River, but not other basins. Because these basins are the only basins for which TP and TN loading rates were very highly correlated ($r = 0.94$ for Patuxent and $r = 0.99$ for York River), this suggests that the correlation between TN loading and TP loading was responsible for the observed response of hypoxia to TP loading in these basins. Additional evidence is provided by the fact that in a multiple regression involving both TN and TP loading rates, the effect of TN is essentially unchanged from the model

without TP and the effect of TP is non-significant. Given the fact that TN and TP loading rates were not universally correlated, it appears possible to conclude that TP loading was not an important factor affecting hypoxia. One is reluctant to discount the potential role for phosphorus as a factor regulating hypoxia because phosphorus availability can be the most limiting nutrient for phytoplankton production in oligohaline regions and even in other areas during periods of nitrogen rich runoff. It remains possible that a reduction in the TN:TP loading ratio might make phosphorus inputs more critical at some time in the future. However, the evidence at present suggests that management efforts to reduce hypoxia should focus strongly on reducing TN loading.

Hypoxia vs. Residence Time

We hypothesized that basins with shorter residence times might have a lower propensity to develop hypoxia given a particular nutrient loading rate. The results indicate that while the larger estuaries with the longest residence times, namely Chesapeake Bay and Potomac River, were the most hypoxic, mean depth was a better predictor of inter-basin differences in hypoxia. There was no evidence refute an assertion that estuaries with short residence times would be less sensitive to hypoxia given a particular nutrient loading regime; however, for these estuaries, residence time differences did not appear to generate inter-basin differences in hypoxia.

References

- Cohn, T. A., L. L. Delong, E. J. Gilroy, R. M. Hirsch, and D. K. Wells. 1989. Estimating constituent loads. Water Resources Research. 28(9): 2353-2363.
- Cronin, W. B. and D. W. Pritchard. 1975. Additional statistics on the dimensions of the Chesapeake Bay and its tributaries: Cross-section widths and segment volumes per meter depth. Reference 75-3. Special Report 42. Chesapeake Bay Institute, Baltimore, MD.
- Dyer, K. R. 1973. Estuaries: A Physical Introduction. New York: John Wiley and Sons.
- Kemp, W. M., E. M. Smith, M. Marvin-DiPasquale, and W. R. Boynton. 1997. Organic carbon balance and net ecosystem metabolism in Chesapeake Bay. Marine Ecology Progress Series. 150: 229-248.
- Kvalseth, T. O. 1985. A cautionary note about r^2 . American Statistician. 39: 279-286.

Table V-1. Mean depth, freshwater residence time, TN loading rates, TP loading rates, and average hypoxia for 6 sub-estuaries of Chesapeake Bay and for the mainstem of Chesapeake Bay. All averages are for the water year, which begins in October.

Basin	Mean Depth (m)	Median Residence Time (days)	Average TN Loading Rate (g N m⁻² y⁻¹)	Average TP Loading Rate (g P m⁻² y⁻¹)	Average Hypoxia Index
Chesapeake Bay (Mainstem)	9.3	116	12.0	0.39	0.92
Potomac	7.2	66	31.8	2.1	0.86
Patuxent	5.9	48	17.1	0.9	0.63
Rappahannock	4.8	53	11.5	1.5	0.37
York	4.3	35	12.5	1.0	0.14
James	3.3	31	19.3	2.8	0.00
Choptank	4.9		4.0	0.3	0.00

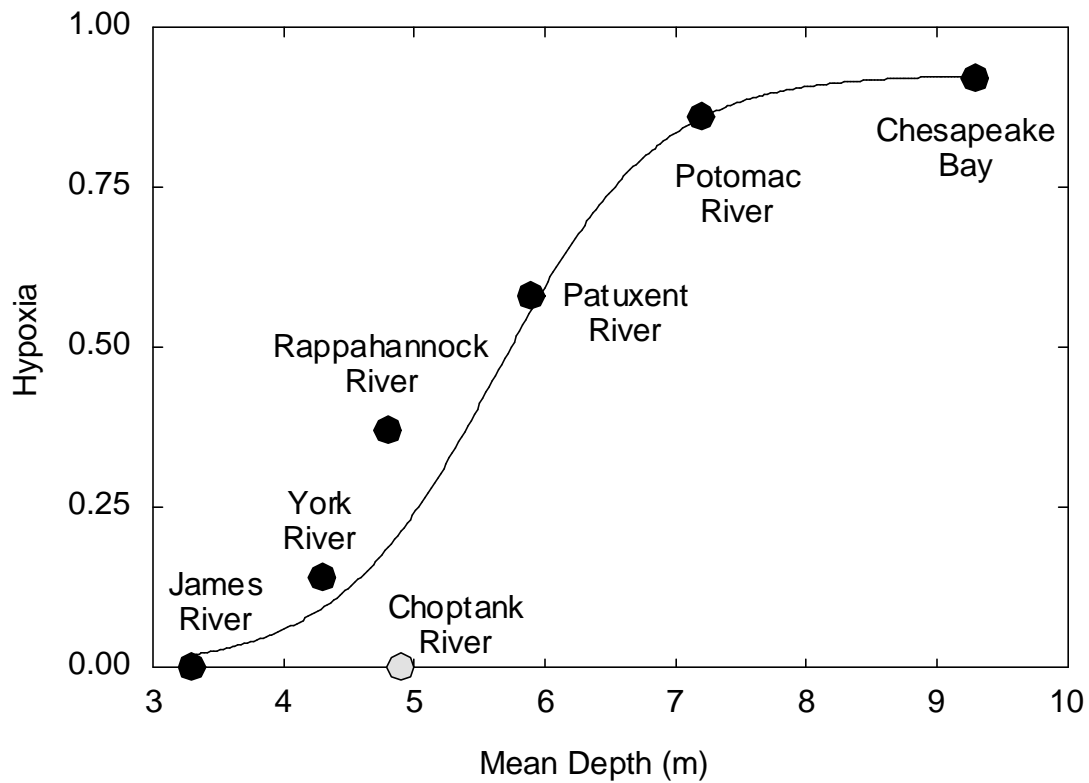


Figure V-1. Long-term mean hypoxia in Chesapeake Bay and selected tributaries as a function of the mean depth of the estuary. Hypoxia was not explicitly calculated for Choptank River, however, the extent of hypoxia in the Choptank River known to be small based on available water quality data.

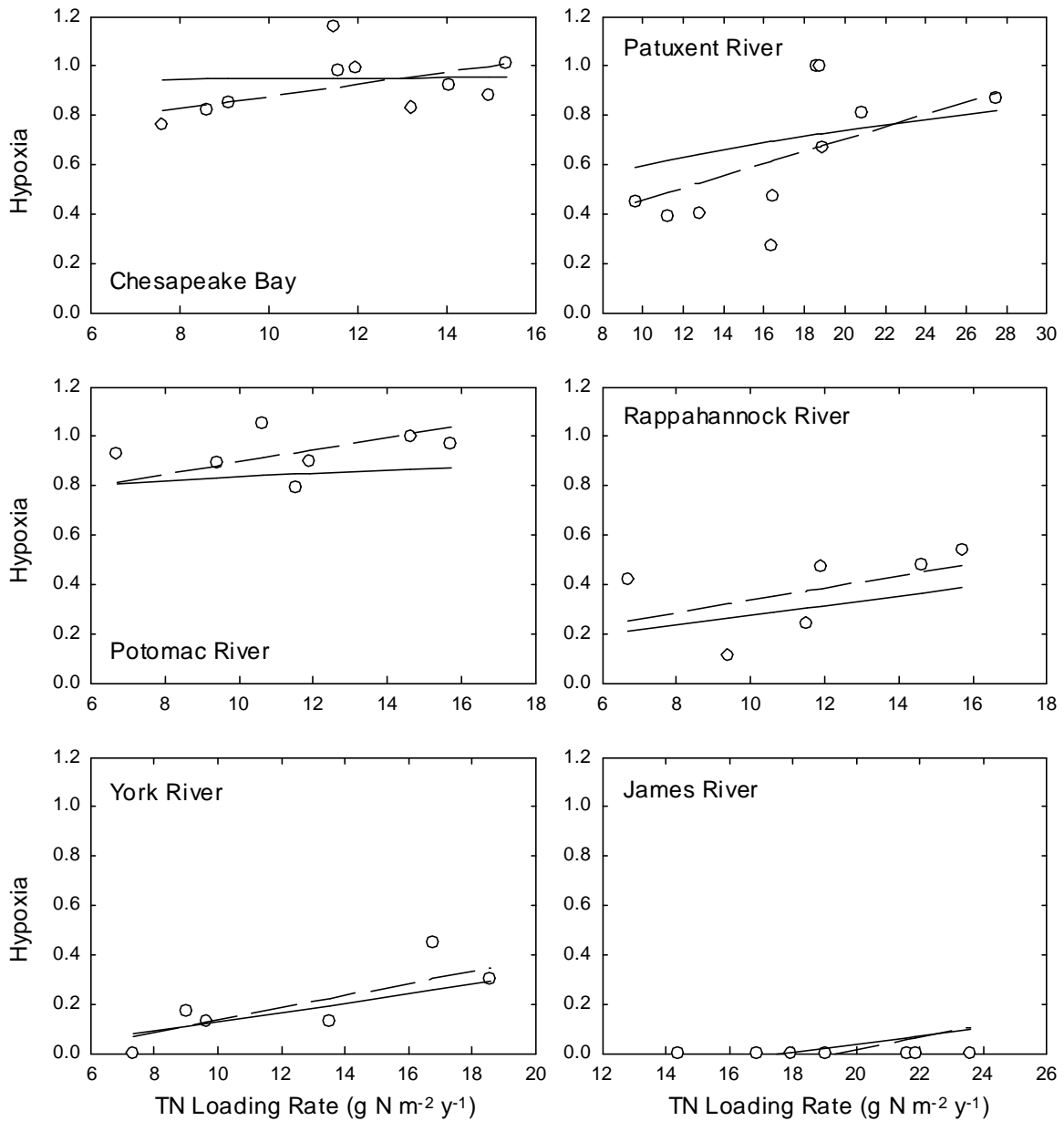


Figure V-2. Observed and predicted hypoxia in Chesapeake Bay and each of 5 tributaries between 1986 and 1996. The solid lines indicate the predictions from the bi-variate sigmoidal model relating hypoxia to TN loading rate and mean depth of the estuary. The dashed lines indicate the predictions of the ANCOVA model relating TN loading to hypoxia with a different Y-intercept for each estuary.

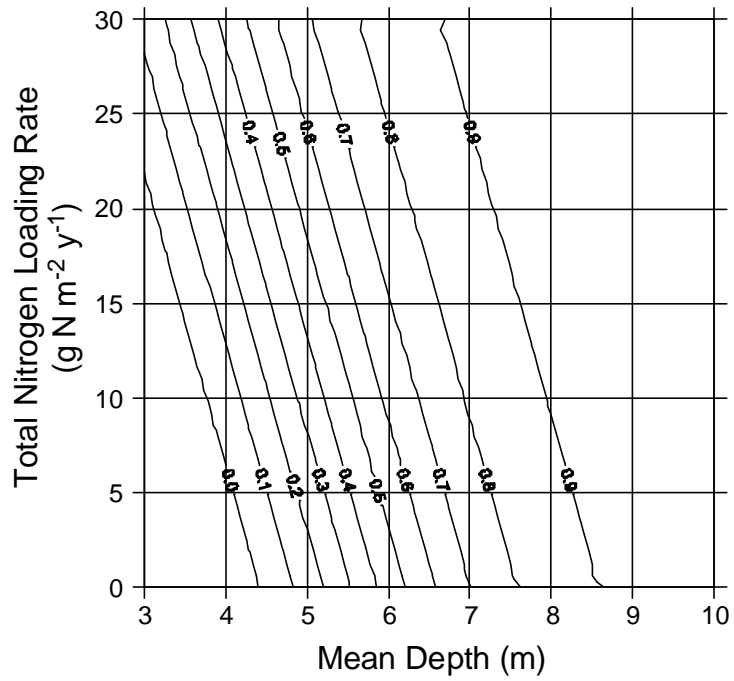


Figure V-3. The predicted effect of total nitrogen loading rates on hypoxia in estuaries of varying depths according to a bi-variate sigmoidal model. The contours refer the the proportional realization of the estimated worse-case scenario for seasonal hypoxia in the estuary.

Chapter VI

Empirical Analysis of Mesozooplankton and Gelatinous Zooplankton Abundance in Maryland Chesapeake Bay and Patuxent River

J. Hagy

Abstract

Mesozooplankton and gelatinous zooplankton abundances were examined at 4 stations in the Maryland portion of the Chesapeake Bay and three stations in Patuxent River to seasonal and interannual patterns of abundance and possible environmental and food-web controls on those patterns. In addition to well known seasonal patterns of abundance, a dramatic increase in some abundances was noted during the 1990s at some stations. Both tree-structured CART models and parametric modeling approaches identified substantial dependence of zooplankton abundances on water temperature and salinity. Recent changes in the joint distribution of salinity and water temperature due to increased rainfall may explain some of the increases in zooplankton abundances that were observed, especially the increase in abundance of *Bosmina longirostris*. In addition, significant effects of ctenophore abundance on *Acartia* spp. abundance during summer at stations where salinity was appropriate for both species provided evidence that, despite some evidence to the contrary, ctenophores were frequently abundant enough to reduce *Acartia* spp. abundance substantially. Chlorophyll-a concentration did not appear reliably as a significant explanatory variable in CART or other models. When it did appear, often lower chlorophyll-a was associated with higher zooplankton abundances. This supports most accounts in the scientific literature that the mesozooplankton are not food limited in Chesapeake Bay most of the time.

Introduction

The crustacean mesozooplankton (e.g. the copepods *Acartia tonsa* and *Eurytemora affinis*) are widely recognized as important links in the transfer of phytoplankton production to upper trophic level organisms such as the striped bass, *Morone saxatilis* (Fig. VI-1). According to the synthesis of Baird and Ulanowicz (1989), mesozooplankton convey a large (50-100%) fraction of the carbon transferred to fish larvae, alewives and blue herring, bay anchovy, weakfish, summer flounder, and striped bass. Menhaden were also noted to depend substantially upon zooplankton, despite their herbivory as adults.

As grazers of phytoplankton, the mesozooplankton also play an important role in maintaining water quality. Because of this central role in the trophic structure of Chesapeake Bay, understanding the notoriously difficult dynamics of the mesozooplankton is an important component of an overall understanding of the Chesapeake Bay ecosystem from the perspective of both the scientist and environmental manager. From the management perspective, zooplankton abundances are a key habitat

quality indicator for their fish predators, making zooplankton monitoring an important component of the Chesapeake Bay Monitoring Program since its inception. More recently, representations of the zooplankton are being added to the Chesapeake Bay Program's biological-physical models. The present study examines a portion of the Chesapeake Bay Monitoring Program mesozooplankton data (4 stations in the Maryland portion of Chesapeake Bay and 3 stations in the Patuxent estuary) with the goal of examining several hypotheses related to factors controlling zooplankton abundance. These abundances vary dramatically on an interannual basis, seasonally, and among stations.

We examined the following specific hypotheses: (1) mesozooplankton abundances are relatively insensitive to changes in algal biomass because they are nutritionally replete most of the time; (2) mesozooplankton abundances are mostly controlled by the abundance of their major predators, which include the ctenophore *Mnemiopsis leidyi*, the scyphomedusan *Chrysaora quinquecirrha*, and the bay anchovy *Anchoa mitchilli*; (3) major perturbations of predator-prey relationships are caused by interannual variations in river flow through its effect on seasonal and spatial salinity and water temperature patterns. We focused on the Maryland Chesapeake Bay and Patuxent River and began with an exploration of the major abundance patterns. Our method of analysis was exploratory data analysis; however, examination of these questions is also well suited to bioenergetic/network analysis, an approach that we plan to undertake in the future.

We did not expect to resolve the questions that we addressed because of the history of contradictory results related to these issues. For example, the scientific literature documents both nutritionally deficient and nutritionally replete zooplankton populations in Chesapeake Bay (White and Roman 1992). Similarly, examples are also present to suggest that gelatinous zooplankton can in some cases control zooplankton populations, while in other cases their population ingestion rates are not sufficient (Purcell 1992; Purcell et al. 1994). Luo and Brandt (1993) concluded that consumption of zooplankton by bay anchovy could account for only a small fraction of zooplankton production, while Wang and Houde (1995) concluded that bay anchovy could have a considerable impact upon zooplankton communities. Most likely, the complex reality is that none of these factors can be eliminated as potential factors driving zooplankton dynamics at any given place or time. These apparent contradictions most likely result from both real spatial and temporal variability in trophic energy flow, the difficulty of estimating the many values required to arrive at such estimates, and perhaps methodological differences. We hope that by evaluating the long-term record of zooplankton abundances collected by the Chesapeake Bay Program, that we will be able to ascertain whether consideration of these ecological mechanisms can meaningfully inform the interpretation of that record for scientific and management purposes.

Methods

This study involves principally an exploratory data analysis using data from the Chesapeake Bay Monitoring Program. The relevant data files were obtained directly

from the Chesapeake Bay Program and were structured within a SAS database using the variable names and definitions recommended by EPA (1997) for the mesozooplankton taxon data files (MDMZTXYY.txt). Specific taxonomic data were extracted from the database for analysis using both NODC codes and life stage (LIFE_STG) designations. In some cases (e.g. *Acartia* species), sub-strings of NODC codes were used to combine abundances into broader taxonomic designations than the database contains. Gelatinous zooplankton biovolume and abundance (counts) data were also downloaded directly from the Chesapeake Bay Program and processed into a SAS database using variable names and definitions recommended by EPA (1997). For the biovolume data, the "Taxon" files and the "Event" files were merged as recommended by EPA (1997) to facilitate calculation of gelatinous zooplankton densities.

Mesozooplankton and gelatinous zooplankton samples were collected concurrently by replicate oblique tows of paired 202 μm plankton nets (bongo nets) equipped with a General Oceanics digital flow meter (EPA 1999). Filtered volumes were calculated from the size of the net opening and the number of turns recorded by the flow meter (EPA 1999). Most filtered volumes were between 10 and 20 m^3 . Gelatinous zooplankton, including sea nettles (*Chrysaora* and *Cyanea*) and ctenophores (*Mnemiopsis* and *Beroe*) were recovered from the plankton nets, counted and settled volumes determined and recorded. One of the paired plankton samples from each tow of the bongo net was used to calculate total mesozooplankton biomass, while the other sample was preserved for later enumeration under a dissecting microscope. A graduated sub-sampling scheme was used to ensure that both abundant and rare forms were enumerated accurately (EPA 1999).

Results and Discussion

Seasonal and Interannual Variability in Water Quality

The Chesapeake Bay stations covered in this study span a salinity range of 3.5-17.4 ppt (Table VI-1). For Patuxent River, mean salinity varied between 0.2 and 12.2 ppt. Salinity at all the stations was lowest in April and highest in October. Annual mean water temperature varied very little among stations within Chesapeake Bay (Table VI-1), but the more saline stations averaged slightly higher temperatures, probably due to the moderating influence of ocean water during winter. Patuxent river stations tended to be slightly warmer than the Chesapeake Bay stations, probably due to a shallower water column, which led to mid-summer water temperatures 2-5°C warmer than in Chesapeake Bay.

Of the 4 stations in Chesapeake Bay, the 3 deeper and more seaward stations, CB3.3C, CB4.3C, and CB5.2 experienced significant hypoxia during mid-summer. In July, all three stations has mean dissolved oxygen concentrations (DO) less than 3.0 mg l^{-1} at 8-9 m depth, less than 2.0 mg l^{-1} at 10 m depth, and less than 1.0 mg l^{-1} at 12-13 m depth. The total depth at these stations was 25, 27, 30 m, respectively. Since survivorship of copepod adults and hatch success of copepod eggs is reduced in waters

below 2 mg l^{-1} (Roman et al. 1993), approximately half to two-thirds of the water column height, but not the volume, was unfavorable for zooplankton at these stations. Of the three stations in Patuxent River, only the lower estuary station (LE 1.1) was subject to hypoxia. The mean July DO concentration was less than 2.0 mg l^{-1} at 6.0 m and less than 1.0 mg l^{-1} at 9.0 m. The total depth at LE1.1 is about 12 m, leaving about half of the water column not favorable to zooplankton.

The March-September average temperature, salinity and chlorophyll-a concentration was calculated for each year and station. Because water quality in locations not accessible to zooplankton is not relevant, observations where dissolved oxygen was less than 2 mg l^{-1} were excluded from the mean. There were no trends in water temperature at any of the stations. The only noticeable feature was that 1991 was warmer than other years at all the stations. Similarly, for chlorophyll-a, there were no significant trends despite substantial variability among years. (Note: the lack of trends was established by the lack of a year effect in an ANCOVA model, not a seasonal Kendall test; however, we are confident based on the graph of the data that any trend that might be established statistically is not ecologically important) For salinity, however, a declining trend was obvious graphically and was substantiated statistically. Mean March-September salinity (in normoxic waters) declined by $0.17\text{-}0.21 \text{ ppt y}^{-1}$ in Chesapeake Bay (except for CB2.2), and by 0.24 and 0.32 ppt y^{-1} at LE1.1 and TF1.7 in Patuxent River, respectively. The decline in salinity over the period of record reflects the prevalence years with high river flow in recent years, particular 1993, 1994 and 1996 (Fig. VI-2). River flow in 1993 was characterized by high flow very early in the year and very low river flow during summer. In 1994, a generous spring run-off period preceded more normal flow conditions later in the year. In 1996, higher than normal river flow occurred in nearly every month, while flood events were not as strong as in 1993 and 1994. Lacking trends in water temperature or chlorophyll-a, the downward trend in salinity may be an important cause of changes in zooplankton abundance and species composition observed over the past decade.

Seasonal Patterns of Mesozooplankton Abundance

Strikingly similar seasonal zooplankton dynamics were observed across the stations evaluated (Fig. VI-3; Chesapeake Bay: CB2.2, CB3.3C, CB4.3C, CB5.2; Patuxent River: TF1.5, TF1.7, LE1.1). All stations except TF1.5 (upper Patuxent) included a substantial spring abundance peak, followed by a late spring/early summer decline, followed by a late summer-fall increase. With the exception of the lowest salinity stations, the spring abundance peak was much larger than the summer abundance peak. At the low salinity station in Chesapeake Bay (CB2.2), the spring zooplankton pulse occurred in March, while the highest spring zooplankton abundances elsewhere occurred in April. All stations exhibited a spring-time increase in the abundance of *Eurytemora affinis* relative to *Acartia* spp., which increased in abundance later in the year. This was most pronounced at the lower salinity stations and at all stations in Patuxent River. At CB4.3C and CB5.2, *E. affinis* was never especially abundant. *E. affinis* and *Acartia* spp. accounted for the vast majority of the mesozooplankton

abundance. An important exception is TF1.5 in Patuxent River, which has significant abundances of *Bosmina* spp. during early summer, especially in recent years.

Chesapeake Bay - CB2.2. Maximum spring zooplankton abundance occurred March (13019 m⁻³), with the population consisting nearly exclusively of *Eurytemora affinis* copepodites (9192 m⁻³) and adults (3252 m⁻³). The April assemblage was similar, but with lower abundance. In May, a mixture of low salinity species appeared along with *E. affinis* (2283 m⁻³), including *Daphnia* (1446 m⁻³) and *Bosmina longirostris* (946 m⁻³). *Acartia* spp. adults were most abundance from June through September, the lower salinity species largely dropping out by August. In September, out of a total abundance of 11656 m⁻³, no species other than *Acartia* spp. adults and copepodites numbered more than 300 m⁻³.

Chesapeake Bay - CB3.3C. *Acartia* spp. dominated the mesozooplankton in January and February, but by March, *E. affinis* adults and copepodites accounted for 30% of 20665 m⁻³. The zooplankton assemblage virtually exploded April, increasing numbers nearly 5-fold from March. *E. affinis* copepodites accounted for 63%, while the adults accounted for 25%. The remainder consisted of *Acartia* spp. The zooplankton decreased in numbers in May to only 14% of the April abundance with the nearly sudden disappearance of *E. affinis*. *Acartia* spp. decreased in abundance as well, but not as dramatically as *E. affinis*. In June, *E. affinis* disappeared completely, while *Acartia* spp. remained nearly as abundant. From July through the end of the year, *Acartia* spp. accounted for most individuals. Barnacle nauplii and polychaete larvae appeared in modest numbers in November and persisted into January.

Chesapeake Bay - CB4.3C. *Acartia tonsa* adults and nauplii dominated the mesozooplankton assemblage throughout the year. Only in April did *E. affinis* appear in significant numbers, with adults and copepodites contributing 32% of individuals. *A. hudsonica* adults accounted for 20%. Lower abundances in both May and June presaged a large *Acartia* spp. resurgence in July, accounting for 97% of individuals. *Acartia* spp. was the only abundant taxa through rest of the year, with the exception a small population of *Oithona colcarva* in September and barnacle nauplii and polychaete larvae in December.

Chesapeake Bay - CB5.2. This most seaward station was also the most dominated by *Acartia* spp.. *A. hudsonica* appeared significantly in February through April. *E. affinis* appeared only in April, accounting for 24% of individuals. Barnacle nauplii were present (>300 m⁻³) in January, March, April and December, while *O. colcarva* was present from August through October.

Patuxent River - TF1.5. There was no spring pulse of zooplankton abundance at TF1.5. Rather, abundances gradually increased through winter and early spring, dominated by *E. affinis* through April. Only small populations of *Bosmina longirostris* in February through April preceded the explosive increase of this taxa in May to 89065 m⁻³. This population explosion nearly eliminated *E. affinis* from the assemblage. A mix of freshwater species combined with *Bosmina* in May and April. April *Bosmina*

abundances increased further, to 98339 m⁻³. In July, *Acartia spp.* reappeared in large numbers (19674 m⁻³, or 67%) and remained abundant along with *Bosmina* through October. In November and December, *E. affinis* returned.

Patuxent River - TF1.7. Massive populations of *E. affinis* (169301 m⁻³ or 96% in April) dominated the mesozooplankton at TF1.7 from January through April. In May, this population abruptly collapsed, with total mesozooplankton abundance dropping to only 7% of April abundance. *Acartia spp.* dominated the smaller populations until November, when *E. affinis* appeared again. Modestly abundant *Bosmina* populations appeared April, May and November.

Patuxent River - LE1.1. A mixture of *E. affinis* and *Acartia spp.* was present at LE1.1 from February to July, when *Acartia spp.* became the exclusive dominant. Barnacle nauplii were more abundant at this station than at any other, with significant abundance from March through May and 8948 m⁻³ in at the peak in April. Both barnacle nauplii and polychaete larvae were present in November and December.

Interannual Variability in Zooplankton Abundances

The most obvious pattern of interannual variability is the dramatic increase in zooplankton abundance through the 1990's at several stations in both Patuxent River and Chesapeake Bay. The increase was most dramatic at station TF1.5 in Patuxent River where the increase was almost exclusively caused by an increase in members of the genus *Bosmina*, essentially a freshwater taxa (Fig VI-4). From maximum densities of 3-6,000 m⁻³ in late spring in 1986 and 1987, *Bosmina* densities increased to regularly May peaks near or in excess of 100,000 m⁻³. In June 1996, the *Bosmina* density was nearly 1,000,000 m⁻³. At other stations in Patuxent River, there was not as obvious a trend (Fig VI-4), although total abundances appeared to edge higher due to increasing *Eurytemora* abundances at LE1.1 and increases in both *Eurytemora* and *Acartia* at TF1.7. Mesozooplankton abundances at TF1.5 declined in 1997 and 1998 relative to 1996 highs, but remained higher than earlier in the decade. Compared to all other stations and species, the *Bosmina* abundances at TF1.5 from 1993-1998 were very high. The significance of this increase may be tempered only by the fact that *Bosmina longirostris*, the most abundant species of *Bosmina* is much smaller (about 2.3 µg/indiv) than adult copepods (10-15 µg/indiv), and only 50% of the size of most copepodites.

A dramatic increase in zooplankton abundances was also observed during the 1990's at CB2.2 and CB3.3C in Chesapeake Bay. However, the increase was not driven by *Bosmina* abundance. At station CB2.2, varying but persistent increases in both *Eurytemora* and *Acartia* abundances accounted for an overall increase in total density from 1987 to 1998. In 1998, *Acartia spp.* dominated the assemblage, while *Eurytemora* and *Bosmina* abundances both declined. In contrast, at CB3.3C, *Acartia* abundance varied around a stationary mean, while *Eurytemora* increased the zooplankton increase through the 1990's was accounted for by both *Eurytemora affinis* and *Acartia tonsa*, except in 1996, when *Bosmina* replaced *A. tonsa* at CB2.2 (Fig. VI-2A).

At stations CB4.3C and CB5.2, where *Acartia* dominated the mesozooplankton in most years, there was no substantial increase in zooplankton abundance. Only in 1997 was there a substantial increase in zooplankton abundance, driven by *Eurytemora*, which had been increasing in abundance in higher flow years (1993 and 1994). A pulse of *Eurytemora* abundance was also observed in 1993 and 1994 at station CB5.2, but this merely stalled what had been a steady decline in *Acartia* and total mesozooplankton abundance.

Given the fact that zooplankton densities are notoriously variable, the presence of a clear pattern of increasing zooplankton abundance may provide an opportunity for insight and probably indicates that a real change has taken place in at least one aspect of the ecosystem. Moreover, the fact that abundance increased only at lower salinity stations could offer additional evidence regarding the mechanism causing the increase.

Effect of Water Temperature and Salinity

Water temperature and salinity were found to have a significant effect on the species composition of the zooplankton community, but not on the total zooplankton abundance. The effect of temperature and salinity on *Acartia* spp., *Eurytemora affinis*, and *Bosmina* spp. abundance was evaluated graphically (Fig. VI-5) and via tree-structured (CART) regression models, which optimally partitioned the temperature-salinity plane into regions that predict median density for a given taxa (Fig. VI-6). Logistic regression was used to evaluate the proportion of total abundance contributed by each taxon as a function of water temperature and salinity (Fig. VI-7). *Eurytemora affinis* was most abundant when salinity was between 4.7 and 15 ppt and water temperature was between 5.2 and 11.3 °C. *Acartia* spp. was most abundant at salinity greater than 11.6 ppt. High *Acartia* densities were maintained at lower salinity when water temperature was also higher. A tree-structured regression model for *Bosmina* (not shown) found that the median *Bosmina* abundance was 7 m⁻³ or less when salinity >1.4 ppt and 164 m⁻³ or less when salinity > 0.311. Fig VI-4 shows median abundances as a function of salinity and temperature. Since the CART models were constructed using log-transformed abundances, confidence intervals based on the mean average deviation from the median are asymmetric. At this very low salinity, *Bosmina* was only abundant when water temperature was >15 °C. Finally, if the salinity was zero, the median abundance within this temperature range was 6561 (confidence interval: 650, 66171), while for non-zero salinity, the same was 1258 (247, 6400). Logistic regression models (Fig. VI-7) showed via continuous functions the fraction of total abundance contributed by each taxon. Logistic regression models use the LOGIT transformation to obtain a linear relationship between a proportion and the explanatory variables. Subsequent back-transformation of the LOGIT yields the predicted proportion. The LOGIT for each species is expressed by the following linear function:

LOGIT (<i>Acartia</i> spp.)	= -7.610 + 0.230T + 0.475S - 0.004TS
LOGIT (<i>Eurytemora affinis</i>)	= 5.786 - 0.319T - 0.362S + 0.009TS
LOGIT (<i>Bosmina</i> spp.)	= -3.461 + 0.186T - 0.672S - 0.096TS

where T=water temperature, S=salinity, and TS=the product of T and S. Both water temperature and salinity are for waters with dissolved oxygen greater than 2 mg l⁻¹. The back transformation function is

$$P = \frac{e^{LOGIT}}{1 + e^{LOGIT}}$$

These functions, however, do not predict likely abundances since total abundance varies substantially. For example, the maximum proportion of *Eurytemora affinis* is obtained at very low salinity and temperature, even though the maximum abundance of *E. affinis* occurred, as shown by the CART model, at an intermediate water temperature and salinity.

These temperature-salinity models are important because of the decrease in salinity that has occurred in recent years. For example, at TF1.5 in the upper Patuxent River, water temperatures typically increase from 20 to 25 during May to June. At this water temperature, neither *Eurytemora affinis* nor *Acartia* spp. is in ideal habitat. However, non-zero salinity first appears typically at TF1.5 in May, usually eliminating *Bosmina* as well. Thus, even a small decrease in salinity, with no change in water temperature, would create an ideal habitat for *Bosmina* in waters that, incidentally, have very high phytoplankton production and abundances. Under a low flow condition, the upper Patuxent would support *Acartia* once salinity increased to some extent.

A similar situation exists at station CB3.3C. Annual mean salinity at this station is 13.9 ppt. Higher salinity is typically present in January and February, decreasing as the spring freshet arrives. The ideal water temperatures for *Eurytemora affinis* are present during March and April, when the spring zooplankton maximum occurs. However, in a dryer than normal winter and spring, salinity will be at the upper end of the ideal range for *E. affinis* and the low end of the range for *Acartia* spp. With higher river flow, optimal conditions are created for *E. affinis* during spring. At stations CB4.3C and CB5.2, salinity is usually much more favorable for *Acartia* spp. than for *E. affinis*. However, under the extreme conditions of 1993, 1994 and 1996, average salinity decreased sufficiently, *E. affinis* abundances increased in the those years, and *Acartia* spp. abundances declined very slightly.

Curiously, *E. affinis* remained abundant in 1995, 1997 and 1998 despite a return to more normal or lower river flow conditions in 1995 and 1997. This may indicate that resting eggs left by these organisms may contribute to higher abundance in years following years with high abundance. Alternatively, it may indicate that flow-dependent effects, primarily on salinity, may not be the only factor generating increasing zooplankton abundance. Changes in predation by gelatinous zooplankton or planktivorous fishes are potential factors worth examination, the former of which is discussed below.

Effect of Gelatinous Zooplankton on Zooplankton Abundance

The ctenophore *Mnemiopsis leidyi* and the sea nettle *Chrysaora quinquecirrha* dominate the gelatinous zooplankton in Chesapeake Bay. In addition, the ctenophore *Beroe ovata* and winter jellyfish *Cyanea capillata* are also present. Both *Mnemiopsis* and *Chrysaora* can be very abundant during summer, especially in the mesohaline Bay, but abundances are highly variable. Both are voracious predators that feed on zooplankton. In addition, *Chrysaora* is known to feed on fish eggs and larvae and *Mnemiopsis*. To evaluate the factors influencing gelatinous zooplankton abundances, we examined the abundances of the gelatinous zooplankton, identifying interannual differences in their abundance, evaluating the relationship of abundance to water temperature and salinity, and looking for evidence that either taxa has a measurable effect on mesozooplankton abundances. Additionally, we attempted to develop empirical models to predict when *Mnemiopsis* and *Chrysaora* were abundant.

Fig. VI-8 shows the distribution of ctenophores and sea nettles relative to average water temperature and salinity (excluding waters where dissolved oxygen is less than 2 mg l⁻¹). Ctenophores were largely abundant only when water temperature was greater than 17°C and salinity was greater than 5 ppt. Sea nettles were also typically abundant only in waters 17 °C and warmer. Their salinity range was relatively narrow at low temperatures, but broadened at higher water temperatures to include a salinity range down to about 5 ppt, but extending only up to 18 ppt. Despite this apparently clear pattern, gelatinous zooplankton abundances were highly variable at any temperature and salinity, largely thwarting the ability to develop a clear empirical model. This variability may result from the small volume of water typically filtered by the plankton net (10-20 m³) relative to the expected abundances. Although appropriate for mesozooplankton, the less abundant and more patchily distributed gelatinous plankton, especially sea nettles generally require a larger sample to obtain a good estimate of abundance.

Annual mean gelatinous zooplankton abundances exhibited the same dramatic long term increase as did the mesozooplankton. However, the stations that had the most pronounced trends in mesozooplankton abundance (e.g. CB2.2 and TF1.5) did not have strong trends in ctenophore abundance. Stations CB4.3C and CB5.2, which had stable or slightly declining abundances of *Acartia*-dominated mesozooplankton, showed strong increasing trends in ctenophores. The cause of this increase is not clear since statistical analysis, including CART analysis, could not predict *Mnemiopsis* abundance even given salinity, *Chrysaora* abundances, and zooplankton abundances as potential explanatory variables. The inability to relate *Mnemiopsis* and *Chrysaora* abundance may simply reflect the problem, noted above, that *Chrysaora* was poorly sampled due to inadequate sample size. For example, in the high flow years of 1993, 1994 and 1996, when *Chrysaora* were known to be reduced in number in the middle Chesapeake Bay, *Mnemiopsis* abundance was particularly high at CB4.3C and CB5.2. Interestingly, zooplankton abundances were not a good predictor of *Mnemiopsis* abundance, even though, as will be discussed below, the opposite is not true: *Mnemiopsis* abundance does predict zooplankton abundance via a CART model. This apparent contradiction can be explained by the fact that in a CART regression model, extreme values of a target

variable tend to inflate the variance within model "nodes." Thus, the extremely high variance of ctenophore biomass contributes to poor model fit. In contrast, since extreme values of explanatory variables are generally not optimal splitting values, this same variance does not cause a problem when *Mnemiopsis* biovolume is used as an explanatory variable.

Two types of models, both a CART model and an analysis of covariance model were able to effectively show an effect of *Mnemiopsis* biovolume on mesozooplankton abundance. However, both models were limited in scope to June-August, to predicting *Acartia* spp. abundance, not total zooplankton abundance, and to waters where the salinity was greater than 10 ppt. Essentially, these limitations require that water temperature and salinity be appropriate for both species for a statistical relationship to emerge. The CART model (Table VI-2) shows that, with variability, very normal changes in *Mnemiopsis* abundance had an enormous impact of *Acartia* spp. abundance during summer. As with the temperature-salinity models, this model was constructed on log-transformed abundances, giving asymmetric confidence intervals. An analysis of covariance (ANCOVA) model predicted *Acartia* spp. abundance during the same summer period as a function of ctenophore biovolume, when salinity > 10 ppt. This model gives one equation for each station, but a common slope predicting the response of *Acartia* spp. abundance to ctenophore biovolume. Although the model had a high degree of statistical confidence for the effect of ctenophore biovolume, this was substantially aided by large sample size, not excellent statistical fit. Thus, the precision of the CART model and the ANCOVA model may be comparable even though the ANCOVA model yields a continuous function. The CART model offers the advantage of fewer model assumptions. There was no relationship between gelatinous zooplankton and either *Eurytemora affinis* or *Bosmina* spp. abundance because these species rarely co-occurred due to their different salinity and water temperature preferences.

References

- EPA. 1997. The 1997 Users Guide to Chesapeake Bay Program Biological and Living Resources Monitoring Data. Chesapeake Bay Program, Annapolis, MD.
- EPA. 1999. Maryland Chesapeake Bay Program Mesozooplankton Surveys Data Dictionary. US EPA Chesapeake Bay Program, Annapolis, MD.
- Luo, J. and S. B. Brandt. 1993. Bay anchovy *Anchoa mitchilli* production and consumption in mid-Chesapeake Bay based on a bioenergetics model and acoustic measures of fish abundance. *Marine Ecology Progress Series*. 98: 223-236.
- Purcell, J. E., J. R. White, and M. R. Roman. 1994. Predation by gelatinous zooplankton and resource limitation as potential controls of *Acartia tonsa* copepod populations in Chesapeake Bay. *Limnology and Oceanography*. 39(2): 263-278.
- White, J. R. and M. R. Roman. 1992. Egg production by the calanoid copepod *Acartia tonsa* in the mesohaline Chesapeake Bay: the importance of food resources and temperature. *Marine Ecology Progress Series*. 86: 239-249.
- Wang, S. and E. D. Houde. 1995. Distribution, relative abundance, biomass and production of bay anchovy *Anchoa mitchilli* in the Chesapeake Bay. *Marine Ecology Progress Series*. 121: 27-38.

Table VI-1. Mean salinity and water temperature over the entire water column, averaged by month for 1984-1996 (Chesapeake Bay stations) and 1986-1997 (Patuxent River station). April and October salinity reflect annual minima and maxima, respectively, while April and July water temperatures reflect temperature during critical times of the year for zooplankton.

Station	Salinity (ppt)			Water Temperature (°C)		
	April	October	Annual Mean	April	July	Annual Mean
CB2.2	2.00	5.68	3.52	10.83	26.46	14.16
CB3.3C	11.81	15.68	13.86	9.15	24.03	14.18
CB4.3C	14.02	17.60	15.87	9.36	24.34	14.26
CB5.2	15.67	19.01	17.44	9.92	24.89	14.72
TF1.5	0.00	0.59	0.22	13.38	28.37	15.19
TF1.7	1.97	6.74	4.25	14.13	29.28	16.08
LE1.1	10.29	14.30	12.22	11.69	26.75	14.88

Table VI-2. Terminal Nodes of a CART regression model relating June-August *Acartia* spp. abundances to ctenophore biovolumes in waters of salinity > 10 ppt.

Model Node	Ctenophore Biovolume (ml / 100 m ³)	Median <i>Acartia</i> Abundance (# m ⁻³)	Confidence Interval
1	< 344	10027	(3881, 25900)
2	344-2971	3032	(558, 16481)
3	>2971	787	(176, 3519)

Table VI-3. ANCOVA model equations for each station where salinity > 10 ppt expressing the decline in *Acartia* spp. abundance with increasing ctenophore biovolume. The slope with respect to ctenophore biovolume was $-4.3(10^{-4}) \pm 9.8(10^{-5})$, $p < 0.01$. Salinity < 10 ppt at stations TF1.7 and CB2.2

Station	Model Equation	<i>Acartia</i> abundance (# m ⁻³), Ctenophore Biovolume = 0 ml / 100 m ³	<i>Acartia</i> abundance (# m ⁻³), Ctenophore Biovolume = 2000 ml / 100 m ³
CB3.3C	$\ln(D) = 8.85 - 0.00043(V)$	6974	2951
CB4.3C	$\ln(D) = 8.81 - 0.00043(V)$	6701	2835
CB5.2	$\ln(D) = 8.76 - 0.00043(V)$	6374	2697
LE1.1	$\ln(D) = 9.03 - 0.00043(V)$	8350	3533

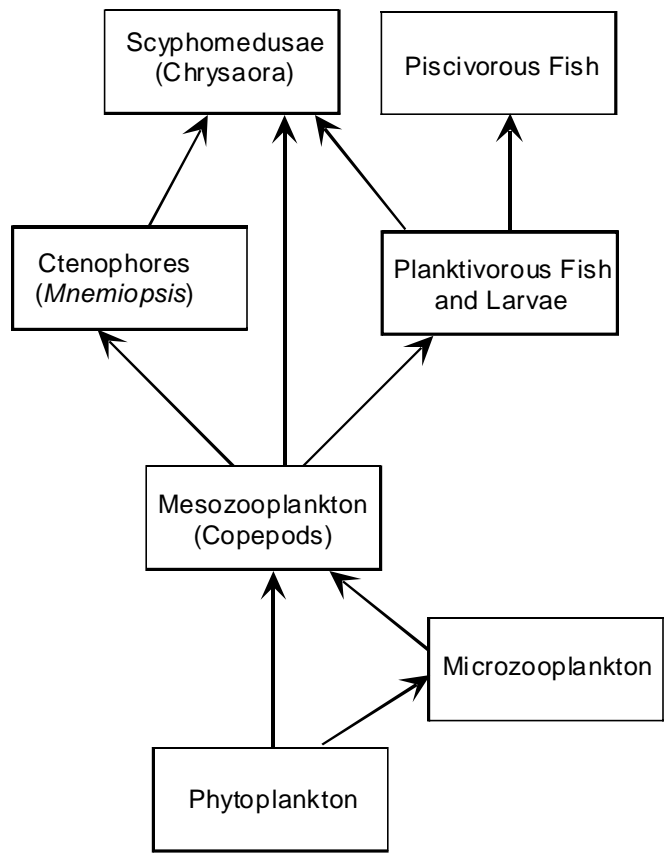


Fig. VI-1. Major trophic relationships relevant to mesozooplankton illustrating, for mesozooplankton, the potential for resource limitation, predatory control, and release from predation due to trophic cascade effects. The microzooplankton are illustrated as a facultative intermediate step in the trophic structure due their known role in trophic transfer of organic carbon to mesozooplankton.

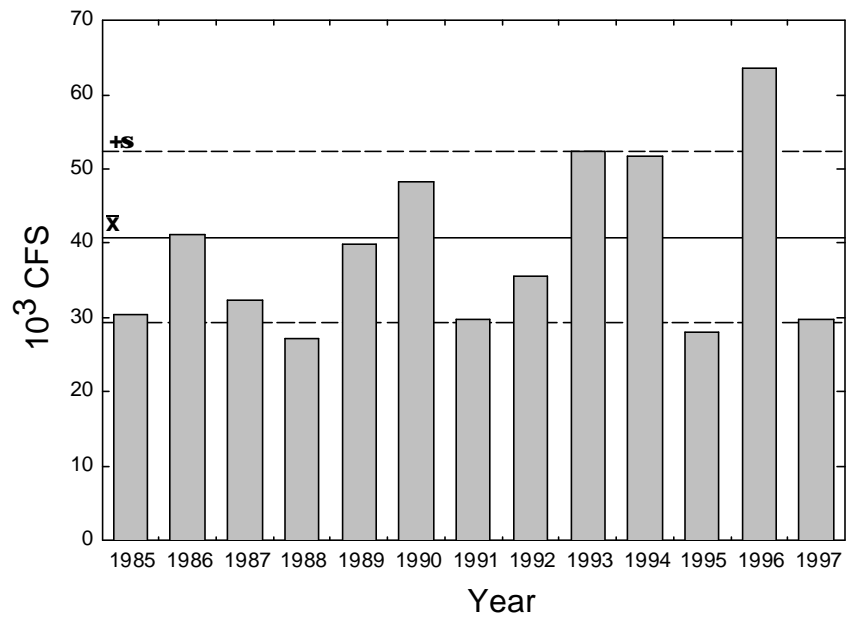


Fig. VI-2. Annual mean Susquehanna River discharge at Conowingo, MD from 1984-1997 with the 1984-1997 mean and standard deviation as reference lines.

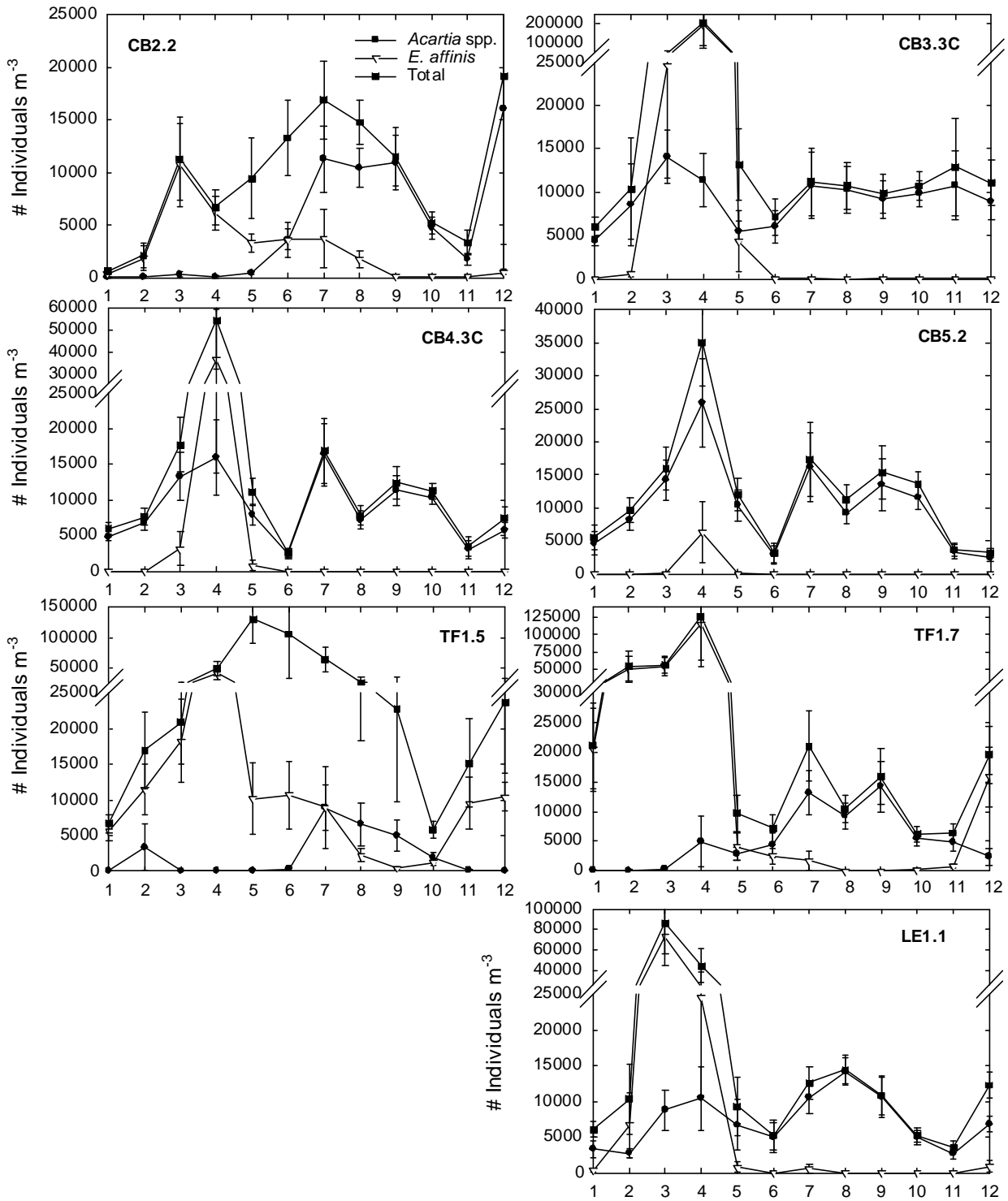


Fig. VI-3. Monthly means and standard errors for abundances of *Acartia* spp. and *Eurytemora affinis* adults and copepodites and total zooplankton abundance at 4 stations in the Maryland Chesapeake Bay and 3 stations in Patuxent River.

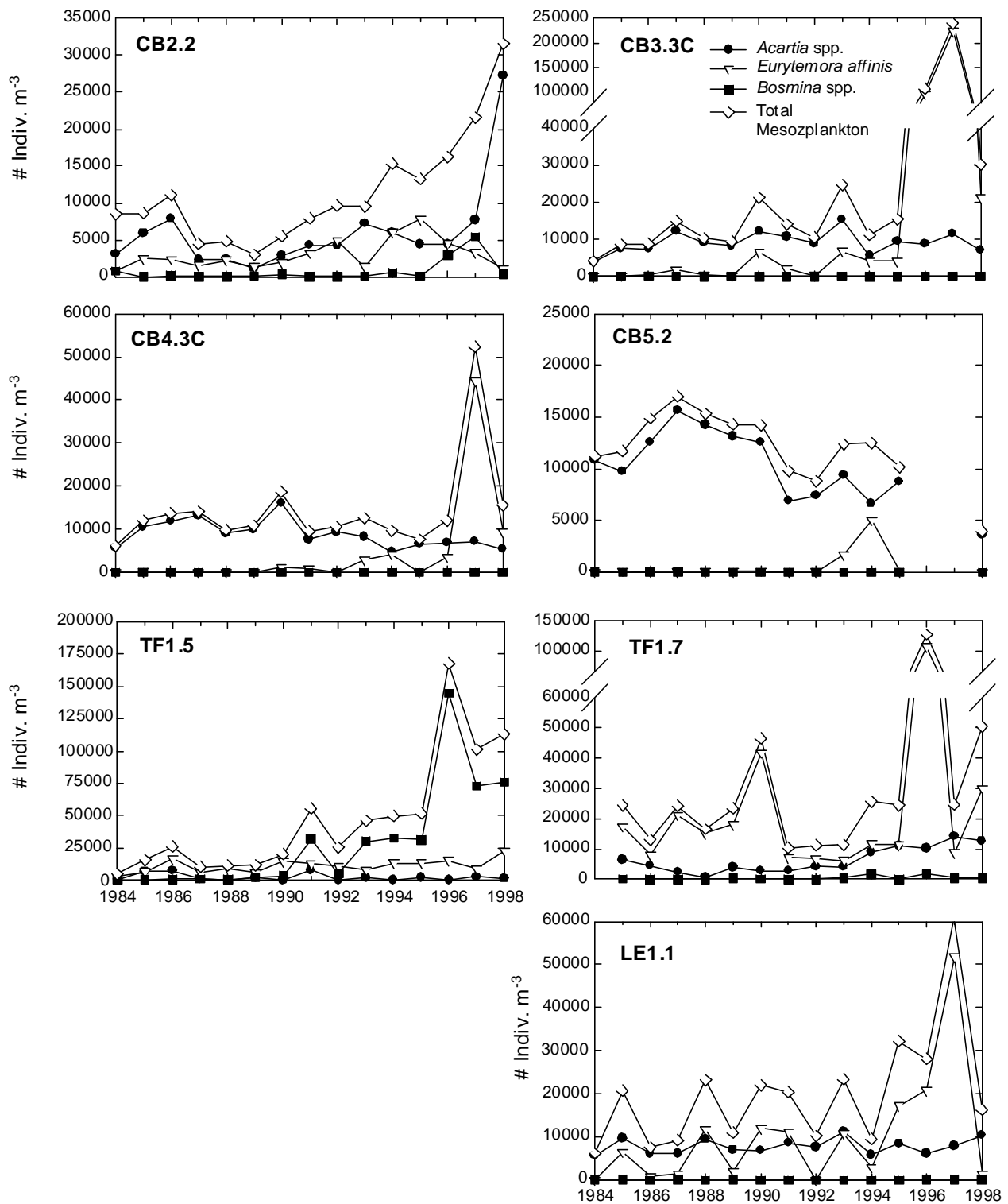


Fig. VI-4. Annual mean abundances of *Acartia* spp. and *Eurytemora affinis* adults and copepodites, *Bosmina* spp. and total mesozooplankton at 4 stations in the Maryland Chesapeake Bay and 3 stations in Patuxent River from 1984-1998.

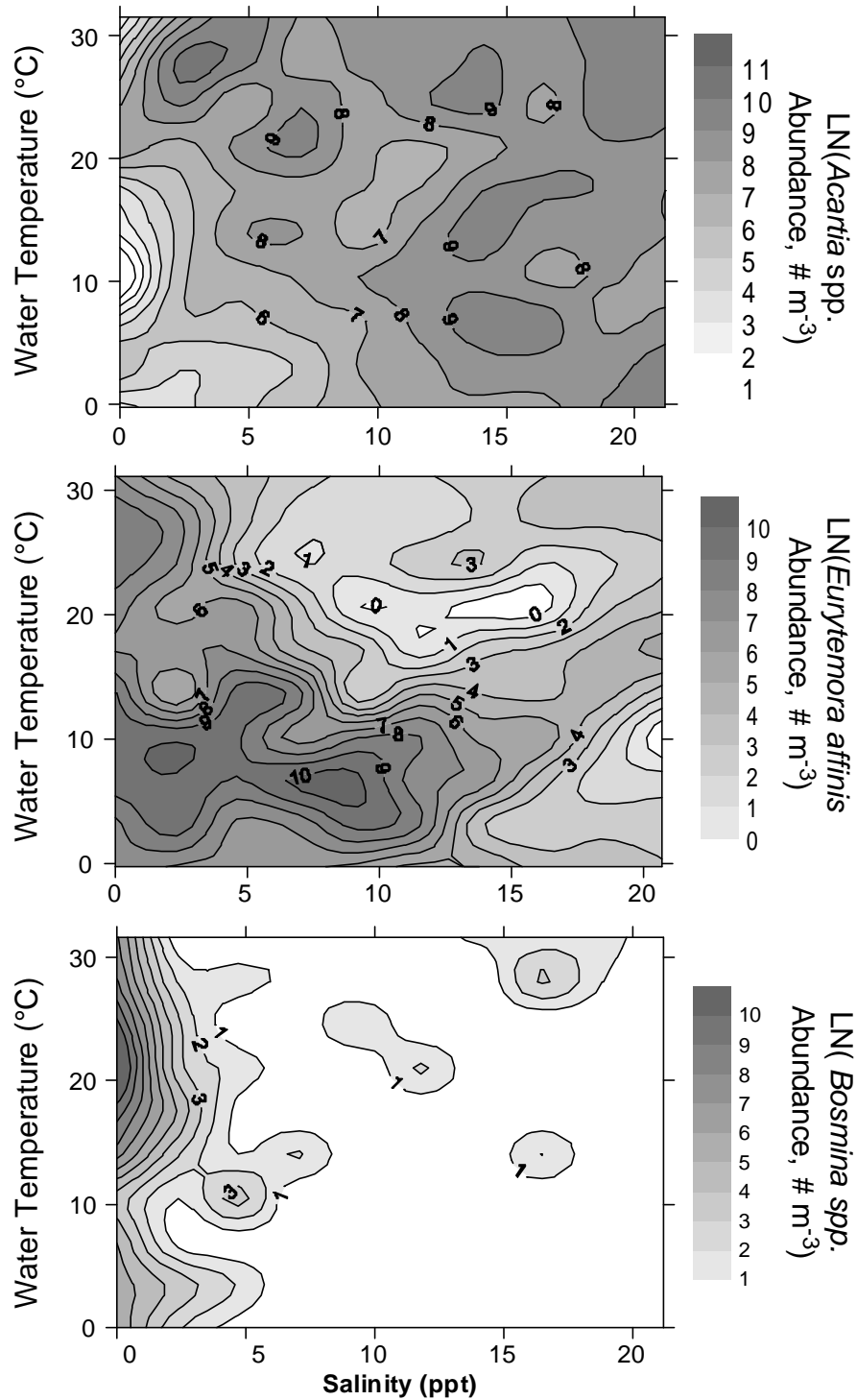
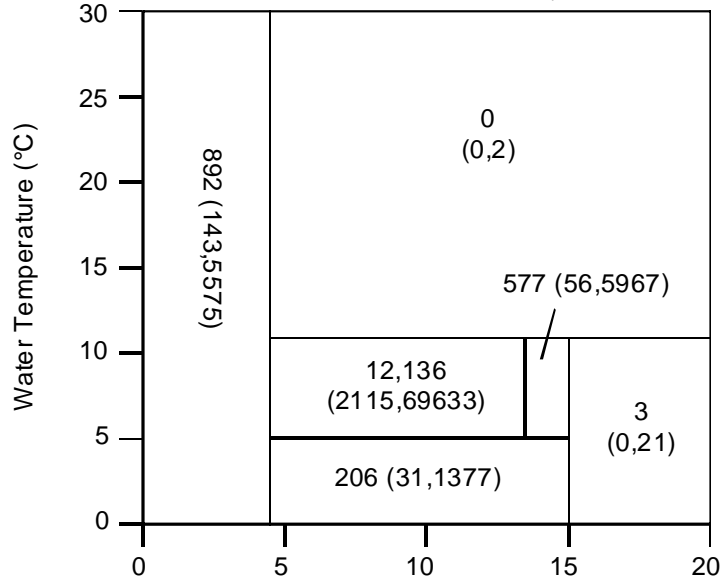


Fig. VI-5. Contour plots showing the distribution of *Acartia* spp., *Eurytemora affinis*, and *Bosmina* spp. abundance over a range of water temperature and salinity in Maryland Chesapeake Bay and Patuxent River. Contours were generated by kriging more than 1000 observations of mesozooplankton abundance.

Eurytemora affinis

Overall Median=0, Units: #m⁻³



***Acartia* spp.**

Overall Median=3278 m⁻³

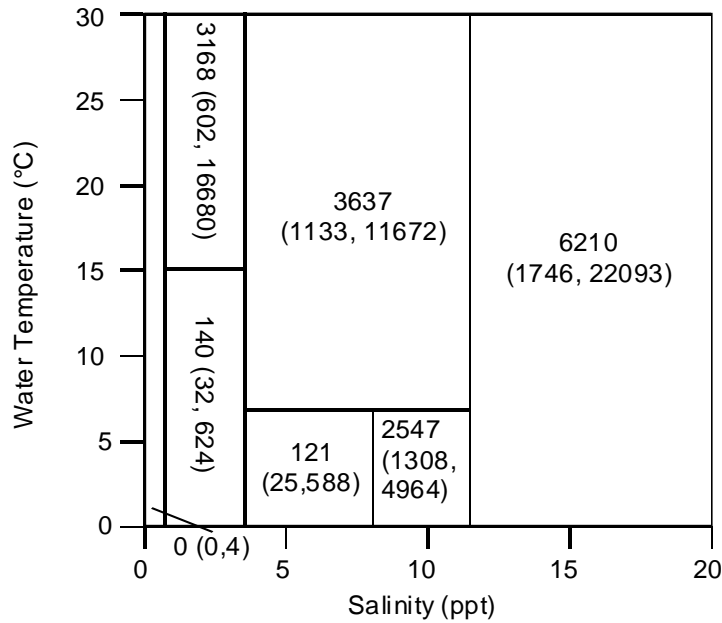


Fig. VI-6. Tree-structured regression models predicting median abundances of *Acartia* spp. and *Eurytemora affinis* adults and copepodites in Maryland Chesapeake Bay and Patuxent River. Confidence limits are based on the mean average deviation and are asymmetrical because they are back-transformations of natural-log values.

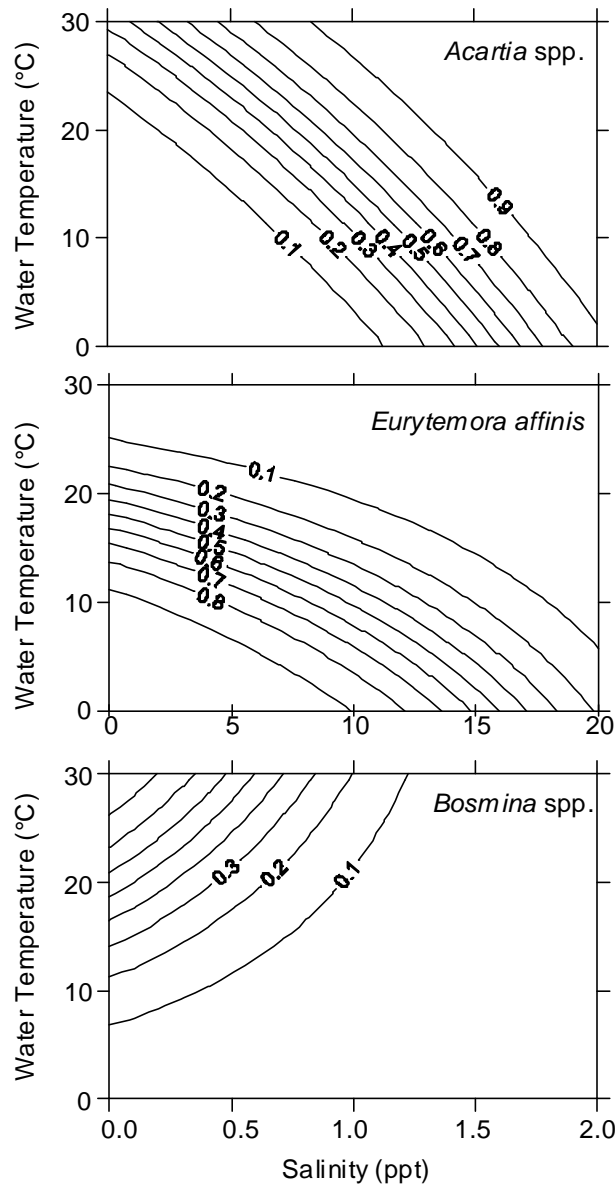


Fig. VI-7. Contour plots showing the proportion of the total mesozooplankton abundance contributed by *Acartia* spp., *Eurytemora affinis*, or *Bosmina* spp. predicted as a function of water temperature and salinity by a bivariate logistic regression model. Observations were from the Maryland Chesapeake Bay and Patuxent River. Note that the salinity scale for *Bosmina* spp. only extends from 0-2 ppt.

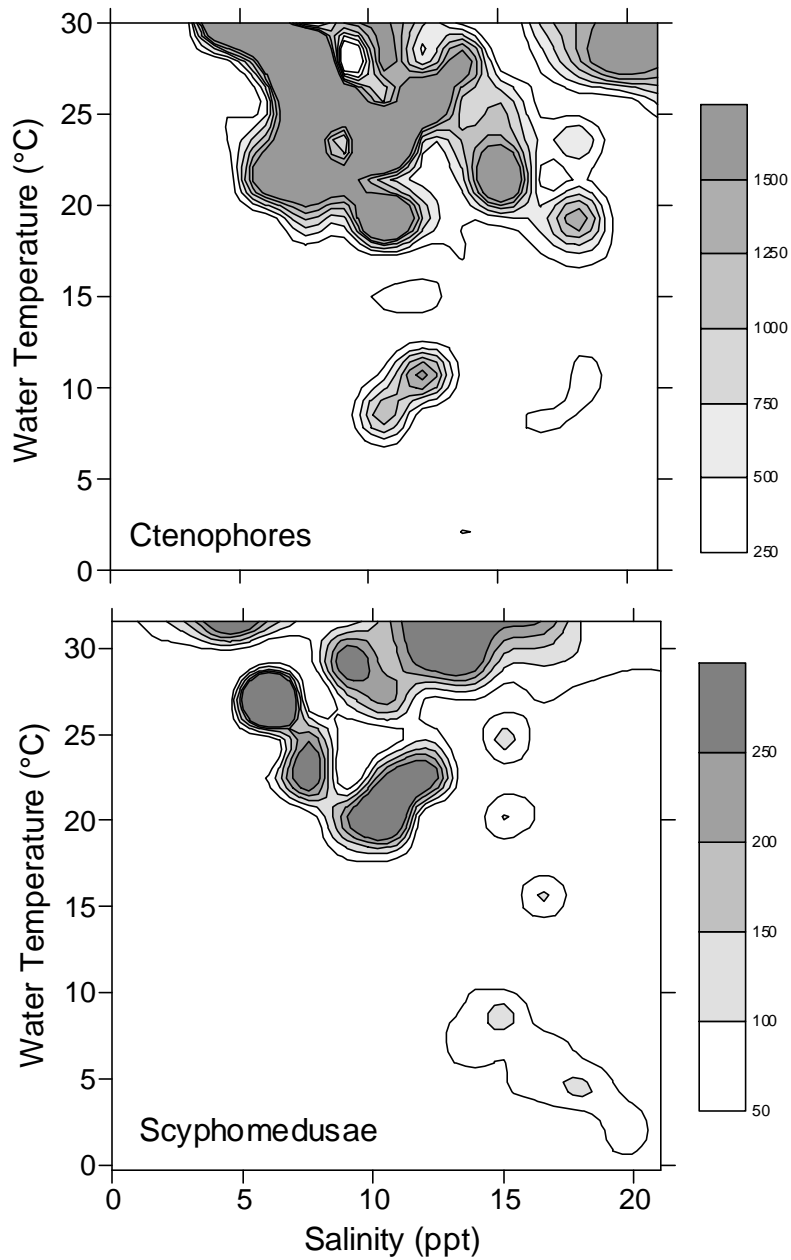


Fig. VI-8. Contour plots showing the biovolume of ctenophores (*Mnemiopsis leidyi* and *Beroe ovata*) and Scyphomedusae (*Chrysaora quinquecirrha* and *Cyanea capillata*) as a function of average salinity and water temperature in oxic water columns ($\text{DO} > 2. \text{ mg l}^{-1}$) in Patuxent River and the Maryland Chesapeake Bay.

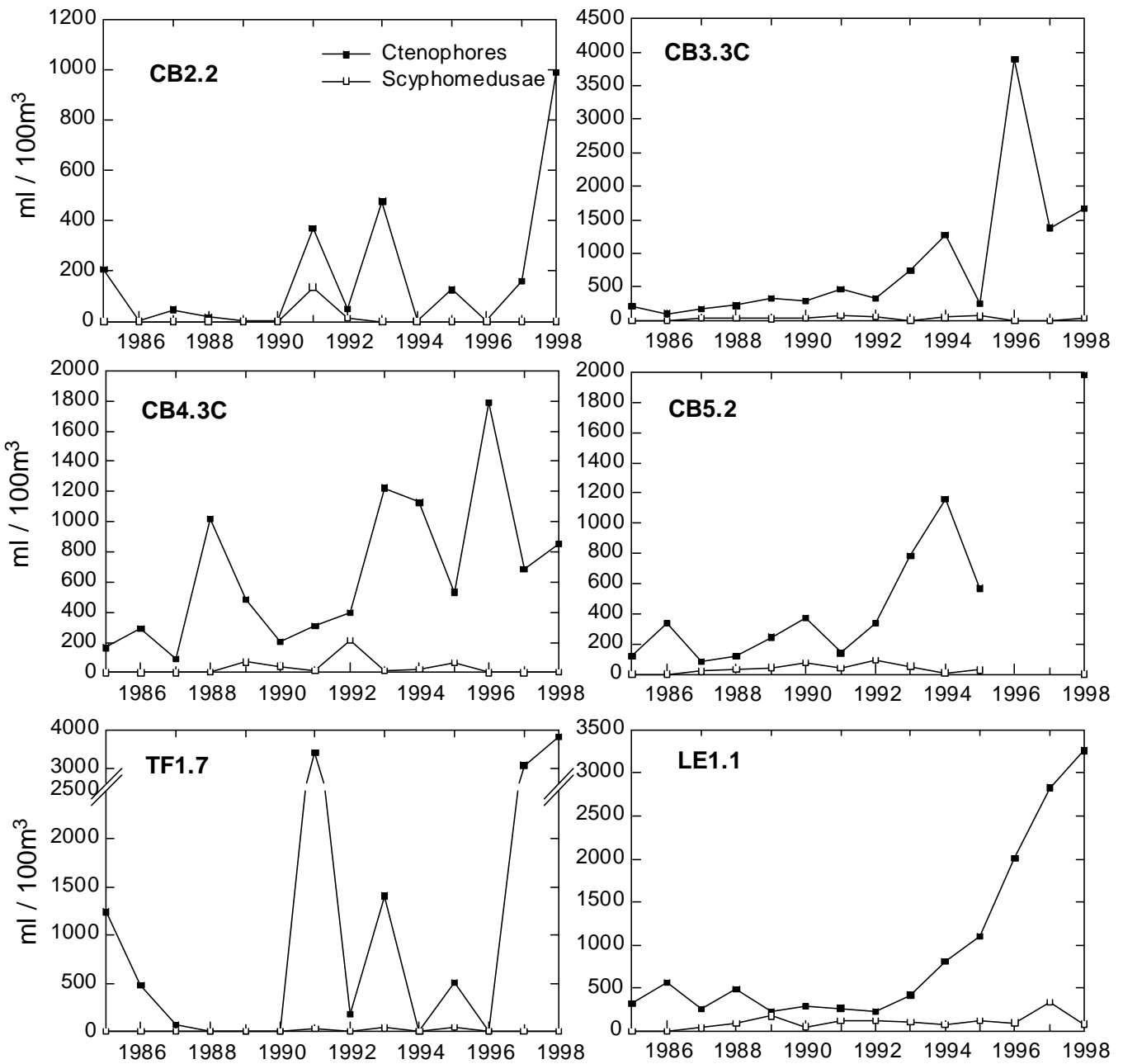


Fig. VI-9. Annual mean gelatinous zooplankton biovolume at four stations in Chesapeake Bay (CB2.2, CB3.3C, CB4.3C, CB5.2) and two stations in Patuxent River (TF1.7, LE1.1). Annual mean gelatinous zooplankton abundances at TF1.5 were all zero.

**University of Maryland
Center for Environmental Science**

This report is cited in the following way:
Kemp, MW., R. Bartleson, S. Blumenshine, J.D. Hagey, and W.R. Boynton. 2000. Ecosystem Models of the Chesapeake Bay Relating Nutrient Loadings, Environmental Conditions, and Living Resources Technical Report. January, 2000. Chesapeake Bay Program Office, Annapolis, MD. <http://www.chesapeakebay.net/modsc.htm> -
Publications Tab. Date Retrieved: *retrieval date*